LAPIN AMK
Lapland University of Applied Sciences

Modification of Creality FDM printers for improved quality and non-planar printing methods

Kreutzinger Michael

Thesis

Mechanical Engineering
Bachelor

2023

LAPIN AMK
Lapland University of Applied Sciences

Mechanical engineering
Bachelor's degree

Author(s)	Michael Kreutzinger	**Year**	2023
Supervisor(s)	Ari Pikkarainen, D.Sc. (tech.)		
Commissioned by	Antti Niemelä		
Title	Modification of Creality FDM printers for improved quality and non-planar printing methods		
Number of pages	99 + 16		

In the context of this work, it was investigated how non-planar printing could be realised with existing standard FDM 3D printers. On the one hand, the approach of printing only the top layer non-planar and thus obtaining a high-quality surface was investigated. For this purpose, a Linux-based slicer was tested which prints the main part of the model in planar and then, limited by the print head geometry, traces the surface contour.

A further approach was conical slicing, in which a model was first warped along the Z axis, then sliced and finally the G-code transformed back. This slicing method was tested by converting a Creality Ender 3, in which a fourth, rotatable axis with a 45° nozzle was integrated. Both the motherboard and the corresponding software were replaced and extended by a further axis and finally tested.

In order to test the effect of a conversion from a V-roller system to a linear rail system, a Creality CR10 Max was converted. The focus was on improving the accuracy as well as the wear and tear and the printing speed in the long term. In addition, the existing Bowden kit was replaced with a direct drive extruder to investigate its effect on stringing.

Keywords 3D-printer modification, non-planar printing, tilted nozzle, rotatable nozzle, direct drive

FOREWORD

First of all, I would like to thank my supervisor, Antti Niemelä, who played a key role in both technical questions and the acquisition of the installed components.

I would also like to thank my supervisor Ari Pikkarainen, who always had answers to organisational and procedural questions.

I would also like to thank Jouni Kanto, who assisted in the production of the turned parts and established contact with the neighbouring vocational school, which was commissioned to CNC-manufacture a component.

Finally, I would like to thank Lapin UAS, which provided the necessary laboratories, workshops and tools, as well as the funding for this work.

SYMBOLS AND ABBREVIATIONS USED

2D	2 Dimensions
3D	3 Dimensions
AC	Alternating Current
CAD	Computer aided Design
CLAS	Curved Layer adaptive Slicing
CNC	Computer Numeric Control
DC	Direct Current
DDE	Direct Drive Extruder
DWS	Duet Web Server
EOL	End-Of-Line
FDM	Fused Deposit Modeling
G-Code	Geometric Code
MCU	Motor Control Unit
PLA	Polylactic Acid
PTFE	Polytetrafluoroethylene
RR	RepRap
RRF	RepRap Firmware
SD	Secure Digital
STL	Standart Triangulation Language
TMC	Trinamic motion control
UAS	University of Applied Sciences
VIN	Voltage input
Wi-Fi	Wireless Fidelity
WSL	Windows Subsystem for Linux

1 INTRODUCTION

Accuracy and printing time are essential aspects of 3D printing process and can vary depending on the type of print, manufacturer, and model. Furthermore, the components used, and their durability play a decisive role in ensuring good print quality in the long term.

Since exactly these bullet points have deteriorated over time with the FDM 3D-printer CR10 Max from Creality, placed in the 3D-printing laboratory in the Lapland University of Applied Sciences (Lapland UAS) in Kosmos, Kemi, it is now to be modified in such a way that an acceptable level of quality can be achieved again. For this very reason, this printer will be modified so that the old drive system with V-rollers will be replaced with the more accurate and reliable linear rail system. The existing Bowden setup consisting of the main gear and a separate hotend shall be replaced with a direct drive kit and should therefore prevent stringing.

Newly developed printing methods aim to save even more time but require a certain amount of know-how as well as the corresponding hardware and software. One of these methods describes non-planar printing, which saves both time and material, especially due to the possibility of printing without a support structure.

In order to implement this innovative technology into the university laboratory, a Creality Ender 3 will be converted to non-planar printing operation with the stock nozzle, so only software changes are made at first. As this is a very new field, accurate and in-depth research is necessary to gather sufficient information. For this purpose, information, insights, and ideas are going to be derived from works with similar goals. In later stages, the standard nozzle will be replaced by a rotatable 45-degree axis, thus enabling angle-independent printing. For this, however, essential elements of the slicer software and its basic process of slicing have to be changed.

1.1 Motivation

The 3D printing laboratory at Lapland UAS offers students a great opportunity to expand their skillset in the field of 3D printing. However, as machines wear out over time, they need to be maintained and overhauled. To further improve the print quality, a Creality CR10 Max and an Ender 3 are modified for this purpose. In addition, this offers the possibility to teach different drive types and print head variants as well as their advantages and disadvantages during lectures. Furthermore, various FDM printing processes can be communicated and illustrated and also show what a possible future in this sector could look like.

1.2 Objectives

The primary focus of this study is on enhancing 3D printers through modifications and acquiring knowledge in the field of non-planar printing processes, with these objectives being pursued independently of each other.

The key aims of the study are twofold. Firstly, to achieve a higher quality of prints by introducing a more precise process for all three movement axes. Secondly, to minimize the potential for errors, such as blockages, by switching to a direct drive system. This will involve adapting purchased components for installation without any further modifications, as well as changing the printer's firmware and calibrating it to the new hardware components.

In terms of non-planar printing, the initial goal is to explore the feasibility of this process using an original 3D printer and a standard nozzle, while identifying any potential issues. Subsequently, the use of a rotatable nozzle will provide deeper insights into this topic. In order to utilize this 3D printing method, the slicer software will also need to be modified to prevent any potential collisions.

1.3 Scope

The scope of this project is focused on modifying the 3D printers, Creality CR10 Max and Ender 3, to improve their print quality by installing newly purchased components. The modifications will require firmware changes to accommodate the new parts and the creation of a custom mounting for the direct drive head and the linear rail block. Additionally, new wiring will be required due to repositioning of the direct printhead. The slicing operation will also need to be adapted for non-planar printing.

The project will be constrained by the need to return the printers to an operational state within the timeframe of the project. Purchased parts must be readily available and deliverable in a timely manner. The laboratory's occupancy schedule may impact processing time, and the project costs must be justified and kept within a certain range. The workshop and tools available are limited to a specific period of time.

The project exclusions include printer maintenance, developing a new printing method, reinventing the printer design, and writing completely new code lines for the firmware or slicer software.

2 LITERATURE REVIEW

2.1 3D printing

3D printing, also known as additive manufacturing, is a process of creating physical objects from digital designs. The printer builds the object layer-by-layer using various materials such as plastics, metals, ceramics, and even biological materials like cells and tissues. There are different processes, the most frequently used method is the Fused Deposit Modeling (FDM) process, also known as fused filament fabrication (FFF). Other processes are stereolithography (SLA), in which a laser hardens the liquid layer by layer to form a solid object, and selective laser sintering (SLS), in which a laser powder material, which can be made of plastic or metal, is also fused layer by layer and is therefore the only variant that does not require a support structure. The technologies just mentioned and other representatives are shown in Figure 1. (Ahmed et al. 2020, 2995–2996.)

3D printing has numerous advantages over traditional manufacturing methods, including the ability to produce complex geometries and customized designs quickly and cost-effectively. It has therefore applications in a wide range of industries, from healthcare and aerospace to automotive and fashion. (Peko, Špar & Basic 2016, 2995.)

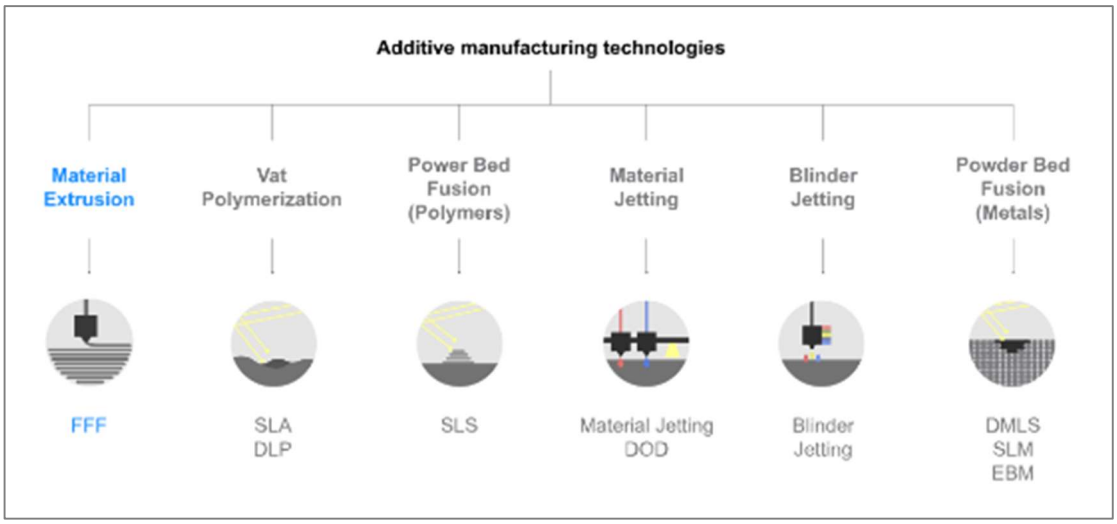

Figure 1. Additive manufacturing technologies (Introduction to Fused Filament Fabrication (FFF) 3D printing technology, 3)

2.1.1 What is FDM printing

Fused deposition modeling (FDM) is an additive manufacturing technique where thermoplastics are melted and deposited in layers through a heated nozzle, meanwhile the cold end also called extruder, feeds the material from the spool, and therefore controls the flow rate. If several of these layers are placed on top of each other, a solid is created. depending on the geometry of the model, a support construction may be necessary, as a so-called support angle of around 45° cannot be exceeded. The individual components will be described in more detail in chapter 2.1.2. However, this process can be seen in Figure 2. (Peko, Špar & Basic 2016, 115–116.)

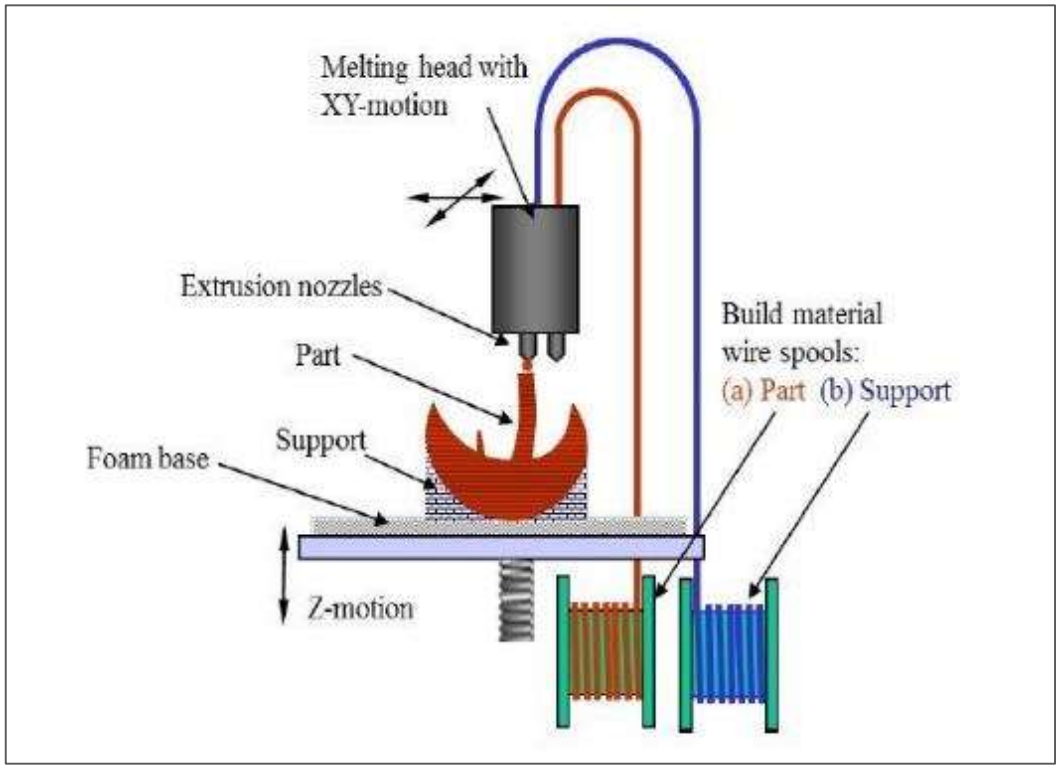

Figure 2. Schematic diagram of an FDM (Peko, Špar & Basic 2016, 115)

The motion system can be achieved in a variety of ways, including Cartesian machines that use the position given by three linear coordinates (X, Y, and Z) and polar coordinate systems that use linear and angular values to describe a physical position (Ahmed et al. 2020, 2998). Furthermore, FDM filaments are the cheapest 3D printing materials, which makes them very popular for private use. (Introduction to Fused Filament Fabrication (FFF) 3D printing technology, 5.)

2.1.2 Printer components

In principle, FDM printers are constructed in the same way, but the design can certainly differ. Figure 3 shows the Ender 3 model from Creality and its components. The biggest difference is the framework, which is responsible for providing structural support and stability to the entire printing mechanism. It holds all the other components of the printer in place, such as the motors, the print bed, the extruder, and the control board. The frame needs to be sturdy and rigid to ensure accurate and precise printing, and to prevent any unwanted vibrations or movements during the printing process. (Kalpesh et al. 2021, 236.)

The motherboard acts as the central processing unit, controlling and coordinating all the printer's functions. It interprets the commands sent from the printer's software and sends signals to the various components, such as the motors, heaters, and sensors, to execute the desired actions. The motherboard also monitors the printer's status and provides real-time feedback to the software, enabling it to adjust settings and parameters as necessary. (Alexandra 2021.)

The display screen and control unit serve as the user interface, allowing the user to interact with the printer and control its various functions. The display screen shows important information about the printing process, such as the status of the print job, the temperature of the extruder and build platform, and any error messages that may occur. The control unit allows the user to adjust settings such as print speed, temperature, and layer height, and also provides access to the printer's menu system for performing maintenance tasks and other operations. (Richter 2023.)

The print bed’s main job is to provide a stable and level base for the print to adhere to. It needs to be able to withstand high temperatures, as the plastic material is melted and deposited onto it during the printing process. Additionally, the printer bed may have a surface treatment applied to improve the adhesion of the plastic, such as a textured coating or adhesive sheet. The bed is usually heated to minimise warping and ensures that the plastic remains stuck to the bed until the print is complete. (Leapfrog 3D Printers 2019.)

The power supply is responsible for converting the electrical power from an AC source into the 24V or 12V DC power required by the printer's components. It also helps to regulate the temperature of the printer's heated bed and extruder. (Kalpesh et al. 2021, 235–236.)

The hotend is responsible for melting the filament, which is then extruded through the nozzle to create the 3D object. The nozzle size can vary and determines the thickness of the extruded plastic. The temperature of the hotend is precisely controlled to ensure the correct melting point of the filament and the nozzle is moved exactly by the printer's motors to create the desired shape of the object. (Carolo 2020.)

The extruder is responsible for feeding the filament into the hotend and melting it, before forcing it out through the nozzle to create the 3D object. It consists of a motor, gears, and a drive mechanism that grips and feeds the filament. The hotend and the extruder can be placed separately or in one unit, the so-called direct drive, which is discussed in more detail in chapter 2.4. (Carolo 2020.)

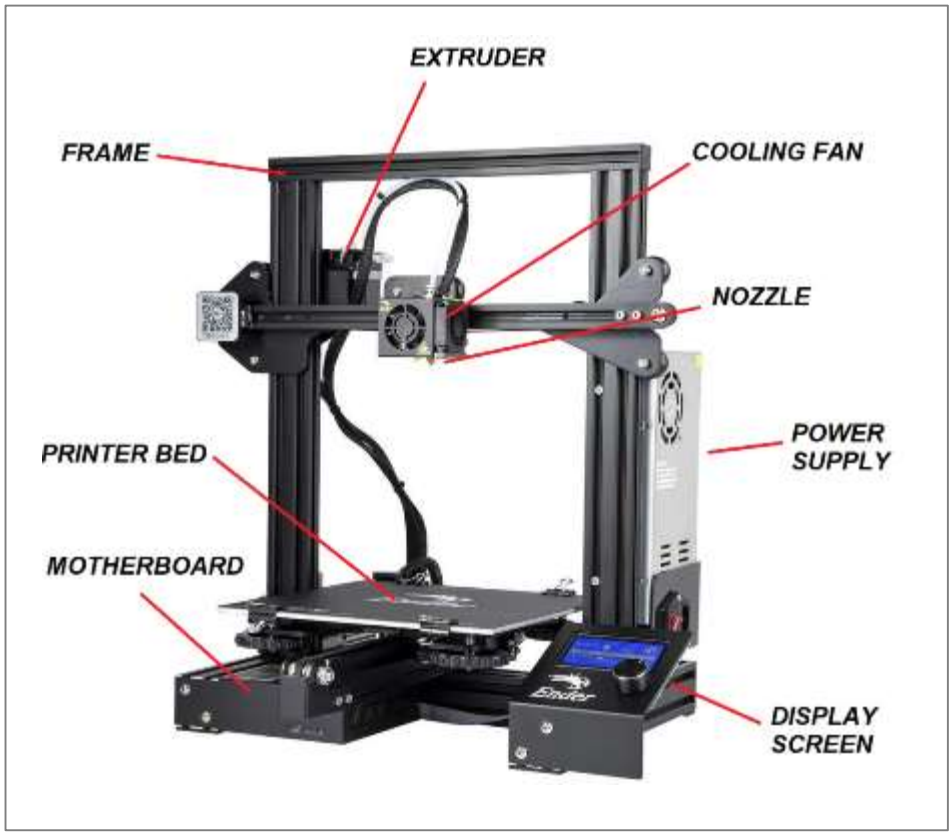

Figure 3. Components of the Creality Ender 3 FDM printer (Inther Software Development 2020)

2.1.3 Pre- and postprocessing

The 3D printing process can be broken down into several steps, starting with the creation of a 3D model in a CAD software or by downloading a pre-existing model in an STL file format. Before printing, the 3D model needs to be prepared for printing, which involves several pre-processing steps such as scaling and orienting. Investing time and effort into pre-processing can lead to better print quality and fewer errors during printing. Additionally, advanced pre-processing software can optimize the model's geometry for printing, reducing print time and material usage. Therefore, it is worth investing in pre-processing to ensure the best possible outcome from a 3D print. (Introduction to Fused Filament Fabrication (FFF) 3D printing technology, 5.)

Once the model is prepared, it needs to be sliced using a slicer software, which converts the 3D model into a set of 2D layers and other commands, which will be explained in chapter 2.1.4 in further detail. After slicing, the printer needs to be set up with the appropriate materials and parameters, and the print can be started. During the printing process, the printer extrudes material to create the 3D object. Once the print is complete, post-processing steps such as removing support structures, sanding, and painting may be necessary to achieve the desired finish. These process steps can be seen in Figure 4. (Nayyeri, Zareinia & Bougherara 2022, 2786–2787)

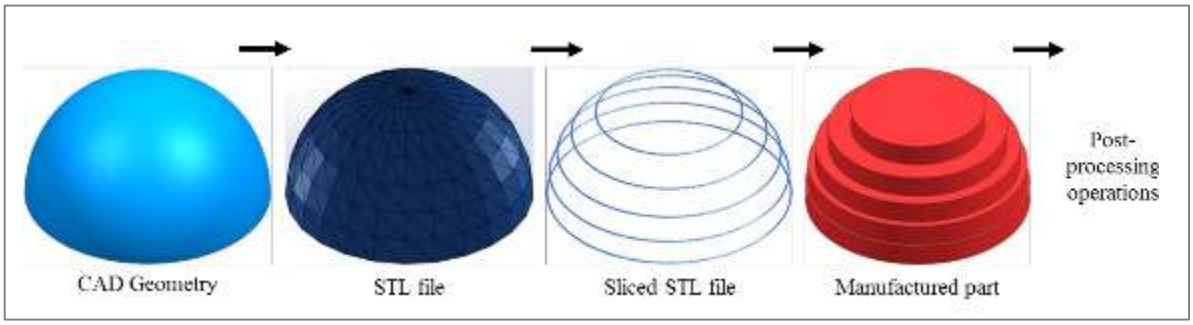

Figure 4. 3D-printing process steps (S. Bedi 2016)

2.1.4 Slicing process

The slicing process is a crucial step in preparing a 3D model for printing. It involves taking the 3D model and converting it into a series of thin, horizontal layers and generating a set of instructions for the printer to follow. The software is used to perform this process, which allows the user to customize various printing settings such as layer height, infill density, and print speed. These settings can have a significant impact on the final quality of the printed object, as well as the time it takes to print. (Mwema, Fredrick, Madaraka Akinlabi & Esther Titilayo, 10–13.)

One important aspect of the slicing process is the creation of support structures. These are temporary structures that are printed alongside the object to help support any overhanging or bridging parts of the model. Without support structures, the printed object may droop or collapse during printing. The slicing software automatically generates support structures based on the geometry of the model and the printer settings which can be seen in Figure 5, where the red and yellow area is the actual model, and the blue is only the support structure. (Mwema et al., 12.)

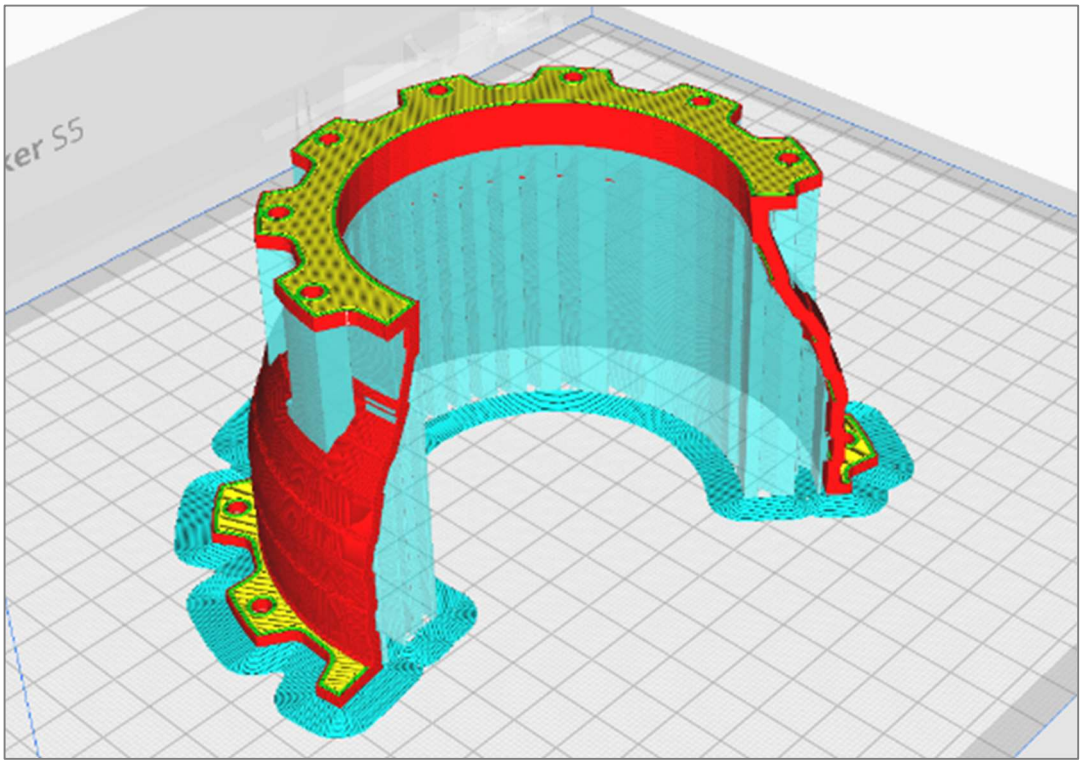

Figure 5. Sliced part in the Ultimaker Cura slicer software

2.2 Firmware of FDM printers

The firmware controls the operation of the printer's hardware, including the motion control system, temperature control, and user interface. It is typically stored on a non-volatile memory chip on the printer's control board. The firmware receives commands from the printer's software, such as the G-code generated by the slicing software, and translates them into low-level commands that are executed by the printer's hardware. (Braam 2017.)

One of the most critical functions of the firmware is to control the motion of the printer's axes, which are typically driven by stepper motors. The firmware must accurately interpret the G-code instructions to move the motors in the correct direction and at the correct speed, taking into account factors such as acceleration, jerk, and backlash. The firmware must also be able to handle error conditions such as motor stalls and communication failures, and respond appropriately to user input, such as pausing or cancelling a print. In addition to motion control, the firmware also handles temperature control, regulating the temperature of the printer's extruder and heated bed. The firmware must monitor the temperature sensors and adjust the power output of the heating elements to maintain the desired temperature within a tight tolerance. (Florian 2023.)

The user interface is another important function of the firmware, allowing the user to interact with the printer via a screen and buttons or a web-based interface. The firmware must be able to display information such as the print progress, temperature, and status messages, and respond to user input to start or stop prints, adjust settings, or perform maintenance tasks. Finally, the firmware may also include additional features such as automatic bed levelling, filament runout detection, and power loss recovery. These features require additional sensors and hardware, and the firmware must be able to interpret the data from these sensors and respond appropriately. (Florian 2023.)

2.2.1 How to import, change and adjust firmware

There are several ways to import or update the firmware of a printer to the latest version. Most manufacturers, such as Prusa and Creality, use the option of updating via the SD card. Another possibility is to use an internet connection, whereby both ethernet and a Wi-Fi connection can be used, such as with Ultimaker. Lastly, this is also possible directly via a connection between the mainboard and a PC or laptop, although this is practically not the case with standard devices and only takes place with conversions. (Dwamena 2023.)

When converting a 3D printer, geometric hardware differences occur which have to be compensated for by means of software adaptation. This can usually be changed in the configuration file of the firmware. All data such as the control value for the end stop sensors, as well as the bed levelling sensor and its Z-axis offset are stored in this file. Such data is usually accessed via a so-called web server by means of an internal connection, in which the corresponding values can be changed with a programme such as the text editor. In addition to the stored parameters, entire processes are also stored, such as a retraction for the Z-axis in idle mode, the G0 command, through which fine-tuning for the print can be made with the necessary know-how, which is no longer possible with slicer software alone. (Dwamena 2023.)

For special applications, such as an additional axis, a separate firmware must be created in which an additional output for the associated stepper motor is stored. There are special configurators on the internet for this purpose, with which the corresponding parameters can be set and stored. (Florian 2023.)

2.2.2 Motor control

The movements of a 3D printer are typically achieved using stepper motors, which work by moving in small steps or increments, rather than continuously rotating like a DC motor. The electromagnets are arranged in a ring as part of the stator assembly, which is the stationary part of the motor and receive the necessary current to rotate the rotor. The printer's control board therefore sends electrical signals to the coils, which move the motor by a specific amount with each signal received. The number of steps per revolution is determined by the number of teeth on the motor's rotor and the number of electromagnets in the motor's stator, which can be seen in Figure 6. (Jess Koeniguer 2023)

By precisely controlling the number of steps, the printer can move the print head and with high accuracy and repeatability, which is essential for creating high-quality 3D prints. The motor control system also includes a range of safety features to prevent damage to the printer and ensure safe operation, such as thermal overload protection and limit switches that prevent the printer from moving beyond its mechanical limits. (Tarun Agarwal 2020.)

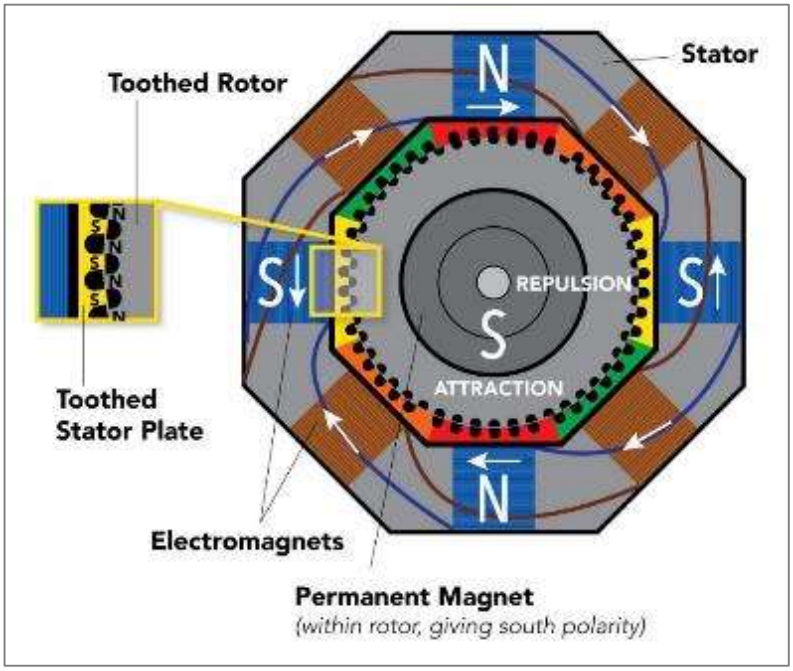

Figure 6. Diagram of a Stepper Motor (Jess Koeniguer 2023)

2.2.3 Sensor technology

Sensors play a key role in the 3D printing process, as it helps to ensure accuracy and reliability. There are several types of sensors that are commonly used in 3D printers, including temperature sensors, filament sensors, bed-leveling sensors as well as many other, more individual ones. (Kalpesh et al. 2021, 235.)

Temperature sensors, also called thermistors, are used to monitor the temperature of the hotend and the heated bed. These sensors provide feedback to the firmware, which can then adjust the temperature of the heating elements to maintain a consistent temperature throughout the printing process. These are either PTCs or NTCs, in which the electrical resistance increases with rising temperature in the case of the former or decreases in the case of the latter. The temperature can be inferred from this ratio. (Carrier 2016.)

Filament sensors are used to monitor when the filament has run out or become jammed (Futek 2023). When the sensor detects a problem or empty filament roll, it can pause the printing process to stop. These are usually positioned in front of the extruder wheels and are again mechanical buttons that convert information into an electrical signal, in rare cases, however, load cells are also installed. (Kalpesh et al. 2021, 235.).

Bed-leveling sensors can detect slight variations in the height of the bed and adjust the nozzle height accordingly. There are three different types of sensors, the first ones are inductive sensors where an electromagnetic induction is used to detect metal objects. Other materials are not possible with this type. Furthermore, there are capacitive sensors which use an electric field to detect objects. They work by emitting an electric field, the field changes and the voltage induced by it changes. Non-metallic materials are also possible here, but temperature and humidity have an influence on the measurement result. Lastly, there are the physical hall effect sensors, which scan the surface using a plastic stylus. A magnet is attached to the upper end of this pen, which acts as a limit switch. This method is independent of environmental conditions, but takes longer to scan and cannot be used for every print head. (Learn Circuit Rocks 2021.)

2.3 Motion systems

There are two different types of motion control systems used in standard FDM printers. On the one hand, there are linear rails and on the other hand roller systems that run in a V-profile, which mainly differ due to their difference in mounting, which can be seen in Figure 7. (Kywoo 2021.)

Linear rails use precision metal rails and bearings to guide the movement of the printer's hotend or build plate along a fixed path. The rails ensure smooth and accurate movement, as the bearings are held in place by a rigid structure that prevents any unwanted wobbling or deviations. Linear rails are typically more expensive than V-roller systems, but they provide higher precision and accuracy, making them a popular choice for high-end 3D printers. (Kywoo 2021.)

On the other hand, V-roller systems use wheels that roll along V-shaped rails to guide the movement of the printer's hotend or build plate. V-rollers are usually made of plastic or nylon and are cheaper to manufacture than linear rails. However, V-rollers are typically less precise and accurate than linear rails, as the wheels can introduce small amounts of play and wiggle room into the system. This play can lead to slight inaccuracies in the print's final dimensions, which can be especially noticeable in larger prints. (Birail Motors 2021.)

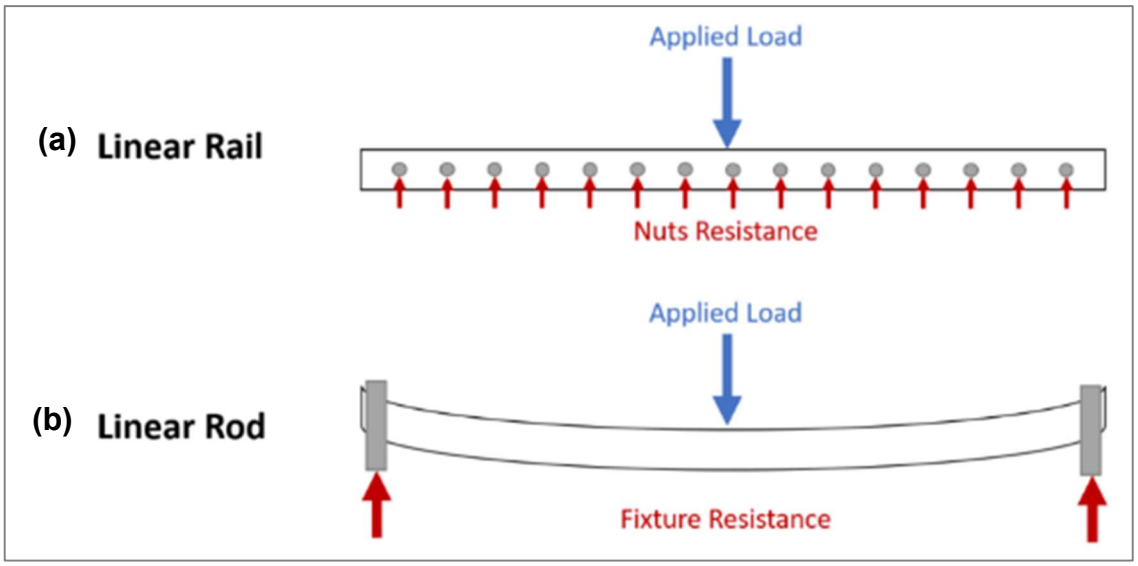

Figure 7. Load absorption of linear rails and linear rod (Birail Motors 2021)

2.4 Feeder- system

Direct drive and Bowden setups are two different types of feeder systems used in 3D printing. As already mentioned in chapter 2.1.2, the feeder system is responsible for guiding the filament from the spool to the extruder, which melts the filament and deposits it layer by layer to create the 3D print. (Marlatt 2022.)

In a direct drive setup, the feeder system is directly attached to the extruder. The feeder motor is located on the print head, which means that the filament is guided through a shorter distance and the system is generally more compact (Figure 8a). This results in more precise control over the filament and allows for better printing especially for flexible or soft materials. Direct drive systems can also handle higher print speeds due to the shorter distance the filament has to travel, but requires corresponding profile rails, since the additional weight must be supported by the frame. However, due to the larger print head, print volume is lost, as the hotend with nozzle is usually located lower. (Bruère, Lion, Holtmannspötter & Johlitz 2022, 446–447.)

On the other hand, a Bowden setup has the feeder motor located remotely from the extruder, and the filament is guided through a long tube or Bowden tube (Figure 8b). This setup is generally used in printers that prioritize speed over precision, such as those used for producing prototypes or models. The long distance the filament has to travel in the tube can result in greater friction, which can lead to under extrusion or jamming. The higher number of components also increases the possibility of errors, which in turn makes maintenance more difficult and access to the individual sections that the filament passes through more complicated. However, the Bowden setup also allows for more flexibility in terms of the print head design and can accommodate larger print volumes. (Bruère, Lion, Holtmannspötter & Johlitz 2022, 446.)

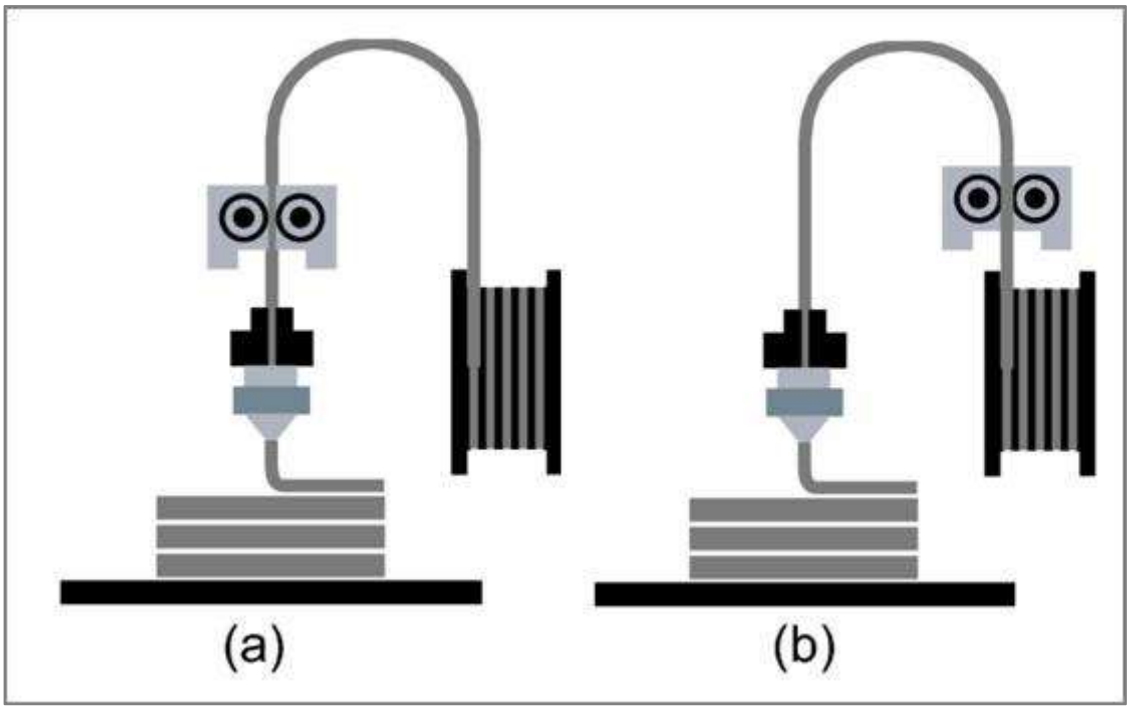

Figure 8. FDM printer with a Direct and b Bowden extruder (Bruère, Lion, Holtmannspötter & Johlitz 2022, 446)

2.5 Planar printing issues

Planar FDM printing has been a popular technique for creating three-dimensional objects layer by layer. However, this method is limited to printing objects in a flat or planar orientation, which often leads to the so-called staircase effect with flat surfaces, where the individual layers become more visible in the form of steps. Non-planar printing, on the other hand, allows for the creation of objects with complex and curved geometries that cannot be achieved with planar printing alone. (Etienne et al., 81:4)

In addition to the printability of components, the surface quality also plays a major role. As already shown initially in Figure 4 from chapter 2.1.3, the model loses accuracy and surface quality first through the conversion to a mesh and then through slicing, which is particularly the case with very flat sloping and non-planar surfaces. Figure 9 shows the problems that can arise at various points on an object. For these very reasons, non-planar printing is a very attractive alternative to solve problems, save material and time, and increase the print quality. (Nayyeri, Zareinia & Bougherara 2022, 2789.)

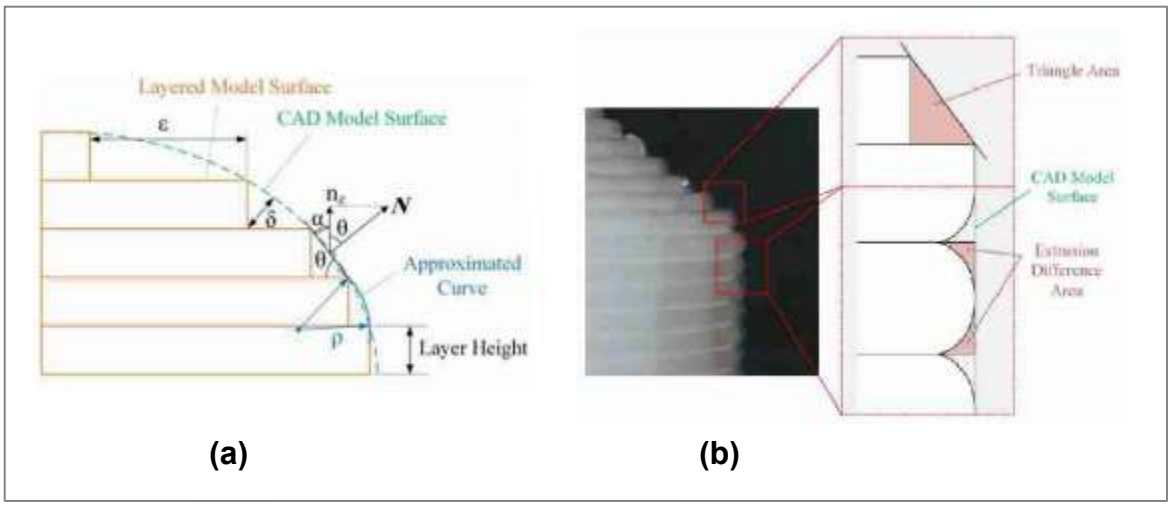

Figure 9. Surface inaccuracies of layered models (adapted from Nayyeri, Zareinia & Bougherara 2022, 2790)

This type of 3D printing can be basically divided into curved slicing for 3-axis printers or multi-axis prints. In the former, only the model is no longer divided into horizontal layers as in the normal FDM process, but a pathing is created by simultaneously moving all three directional axes. This topic, its difficulties as well as

advantages and disadvantages will be discussed in more detail in the following chapter 2.5.2. In contrast, non-planar printing with multiple axes is used, in which rotational axes are added in addition to the usual axes of motion. In most cases, these are 4- or 5-axis machines that operate in a similar way to the CNC machines used in the metalworking industry. However, there are also special applications where, for example, the pressure plate can be tilted in order to change the relative angle to the nozzle. These processes will also be discussed in more detail in the next section 2.5.5. (O'connell 2021.)

2.5.1 Planar Adaptive Slicing

There are different approaches to this. On the one hand, there is the possibility of adaptive slicing, where the software automatically adjusts the layer thickness of non-uniform surfaces to reduce the stair-step effect. This feature can be optimized through the software's user interface and is activated by default. The algorithm is particularly useful for rounded or non-planar surfaces. In Figure 10, two models are compared: one sliced straight and the other using adaptive slicing. When the 3D model is divided into two parts, the layers in the lower part are planar and do not require adjustments, but the top surface in the upper part is non-planar and benefits from the adaptive slicing algorithm. This method is not necessarily Non-planar, but it drastically increases the quality of Non-planar surfaces. (Ömer & Mehmet 2021, 479.)

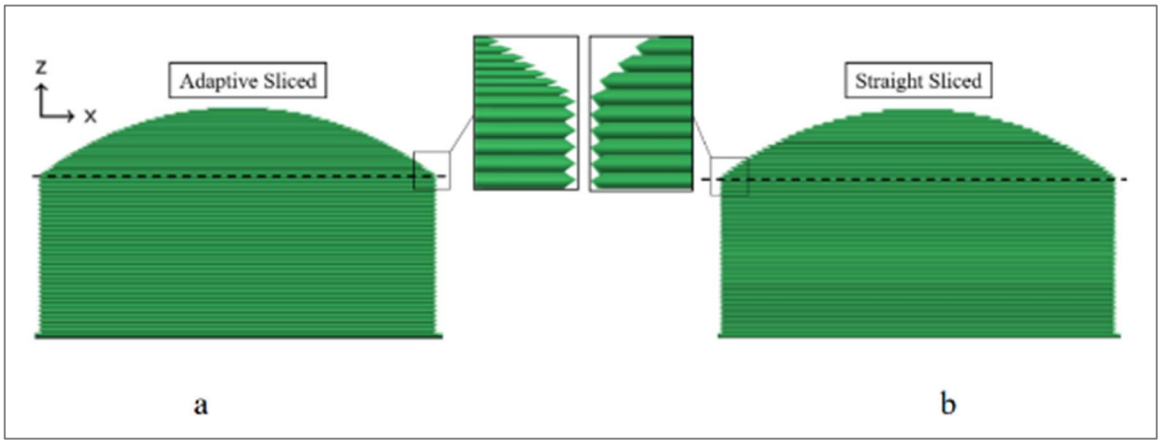

Figure 10. Comparison of adaptive slicing (a) and straight (constant layer thickness) slicing (b) (Ömer & Mehmet 2021, 479), 479)

2.5.2 Non-planar top layer slicing

In the non-planar top- or shell slicing method, the majority of the print is first sliced into layers, as in standard FDM printing. Only a defined number of top layers are then placed over the old step-like layers and must be printed simultaneously using all three axes, thus creating a smooth and high-quality non-planar final layer, which can be seen in Figure 11. (Ömer & Mehmet 2021, 479.)

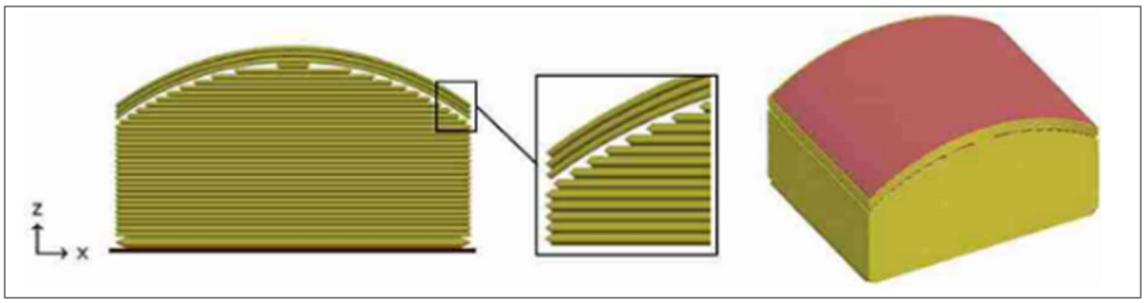

Figure 11. Non-planar top layer slicing Ömer & Mehmet 2021, 479

On the one hand, this improves the print quality enormously, especially for very flat surfaces, but it also brings new challenges that must be overcome in order to achieve an acceptable result. Especially in areas with very steep convex surfaces, there is not only a risk of collision with the print head, which will be discussed in more detail in Chapter 0, but also so-called underfilling (Figure 12a) can occur. In this case, the layers cannot be placed close enough to each other due to the difference in height, but can be avoided by using different filling patterns (Figure 12b). (Ahlers 2018, 54–55.)

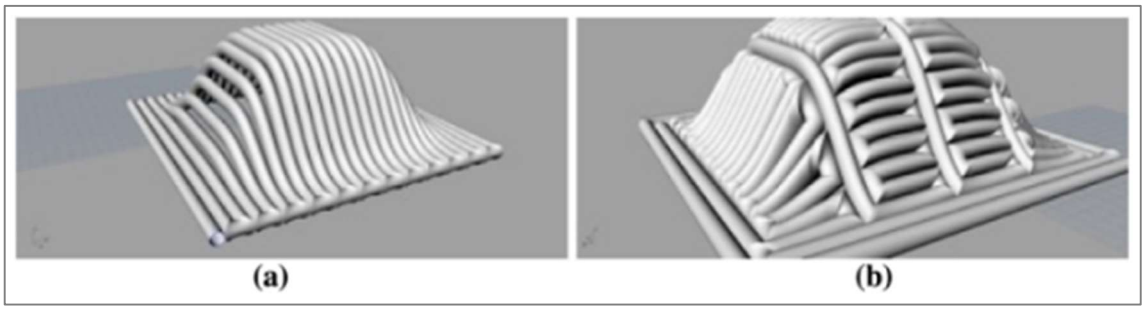

Figure 12. Filament gaps on a radical surface curvature (a), alternative path strategy using smaller segments to minimise the gaps (b) (Lim et al. 2016, 13)

2.5.3 Curved layer adaptive slicing (CLAS)

This slicing method combines planar adaptive slicing with the non-planar traversing method, which attempts to fill the cross-section of any object by adjusting the layer thickness but keeping the number of layers constant. The actual result of slicing a wing like part with curved slicing in side view is shown in Figure 13, with the model outline to be matched in orange and the slices in green/blue. Figure 13a shows a planar slice made from a wing-like profile, whereas Figure 13b shows the curved slice with the top surface perfectly aligned with the top curve. The layers are shaped to accurately follow the object surface whenever possible, with the slice thicknesses allowed to vary between a certain range and the maximum slope constrained to a specific value depending on the geometry of the printing head. To achieve this, a mapping is optimized to deform the surfaces along the vertical direction only, locally compressing or stretching the initial solid and changing surface slopes. (Etienne et al., 81:4-81:5.)

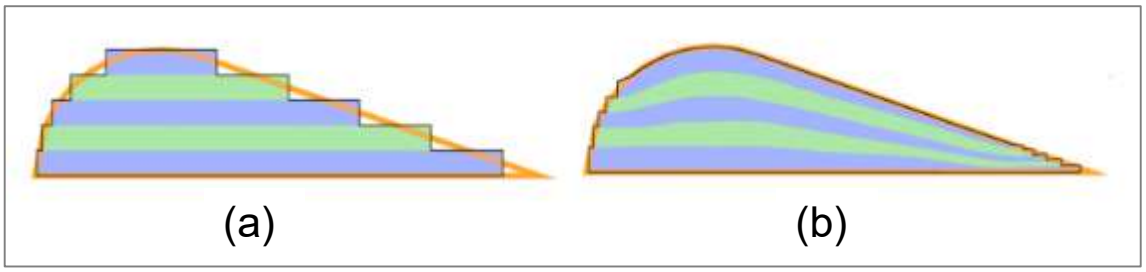

Figure 13. Comparison planar slice (a) and curved slice (b) (Etienne et al., 81:4)

On steep surfaces, it is difficult to precisely extrude a lot of material with a straight nozzle, so this process is difficult to implement with standard FDM printers. Therefore, for such complex prints, multi-axis printers are usually used, where, in addition to the usual 3 axes, either the print head or the print bed can also tilt around one or two axes, in order to always guarantee a right angle between the nozzle axis and the surface. Nevertheless, this technology plays an important role, especially with regard to topologically optimized components, and could thus bring about a kind of revolution in the field of CAD design (Liu et al. 2018, 2458).

2.5.4 Non-planar printing limitations

However, there are limitations which are imposed by the dimensions of the print head and the nozzle. The outer angle of the nozzle, the distance from the nozzle tip to the hotend, and the position of the cooling fans are decisive geometries. They determine the maximum angle a slanted or rounded surface may have without colliding with the printhead, which can be seen. (Ömer & Mehmet 2021, 481.)

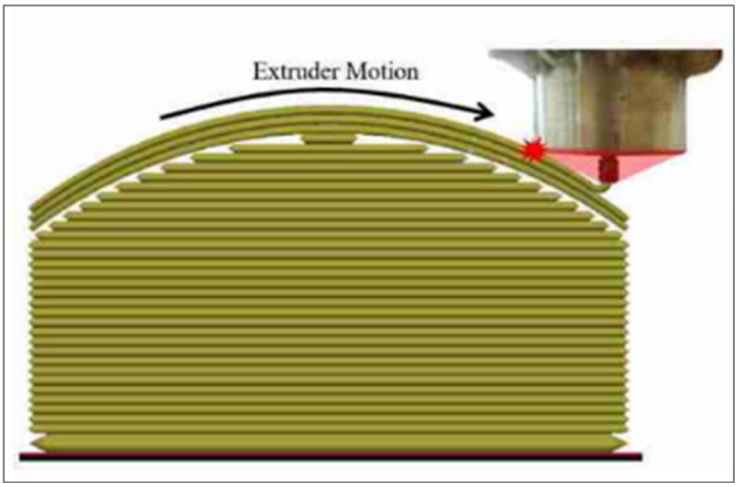

Figure 14. Collision of the printhead with a non-planar surface (Ömer & Mehmet 2021, 481)

Another problem here is the extrusion itself, since in planar printing the nozzle opening is guided parallel to the print surface. This is not possible with this process and, depending on the direction of printing, can lead to compression or expansion of the extruded material and thus to poor printing results, which can also be seen in Figure 13. (Nisja, Cao & Gao 2021, 7.)

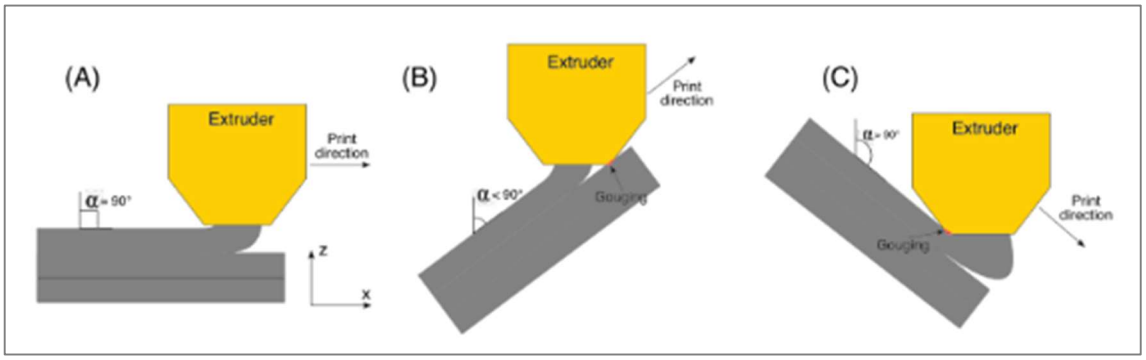

Figure 15. Printing issues for non-planar models with standard nozzle (Nisja, Cao & Gao 2021, 6)

2.5.5 Non-planar printing with a rotatable 45° axis

As already mentioned in Chapter 2.1.4, a support structure is required for angles of 45° and above, which requires both material and printing time. For this reason, a special type of slicing and printing was developed in which the print head is printed with a fourth axis rotating around the z axis with a 45° angle nozzle. In this process, the layers are printed conically from the centre of the object outward at an angle of 45°, as shown in Figure 16. Since at this angle the individual layers overlap slightly horizontally, overhangs of up to 100° are possible without a support structure. This not only saves support material, but also drastically improves the surface quality of sloped surfaces, since the angled nozzle creates a right angle between the nozzle axis and the surface more quickly. (Wüthrich, Gubser, Elspass & Jaeger 2021, 1.)

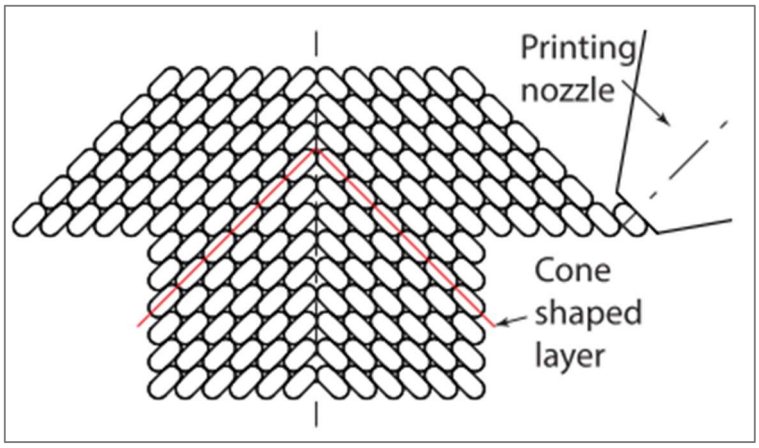

Figure 16. Printing strategy with cone shaped layers. (Wüthrich, Gubser, Elspass & Jaeger 2021, 2)

However, this process requires a special slicing procedure, as otherwise the print head would collide with the component in the area of the centre axis during the printing process. First, the object is stretched in the direction of the z-axis, but the larger the radius from a certain point to the centre axis, the more it is stretched. In the next step, the warped object is divided into planar layers in a normal slicer. The slice settings that have already been determined take into account the layer thickness, the amount of extrusion for flat angles and other things. After the part has been sliced, it is transformed back into the old shape, whereby the previously sliced planar layers are now transformed into 45° conical layers and thus made printable for the inclined nozzle. This transformation takes place in a separate

python script, in which the slicer is also integrated. This process with its individual steps is illustrated from the original .stl part to the active print in. (Wüthrich, Gubser, Elspass & Jaeger 2021, 3–5.)

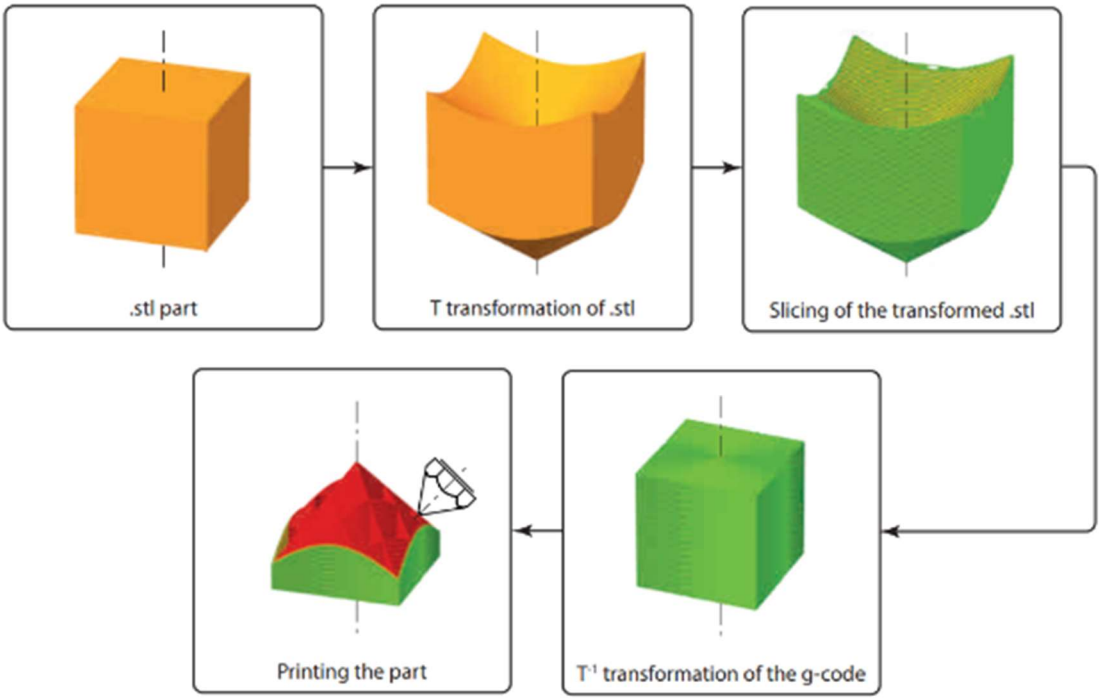

Figure 17. Workflow of the slicing process (Wüthrich, Gubser, Elspass & Jaeger 2021, 5)

Not needing a support structure is a great advantage over other printing methods, but this is also limited with this method. Only overhangs in one radial direction can be created per print, as only one cone can be directed either outwards Figure 18a or inwards Figure 18b. This considerably limits the possibilities for printable objects, which can be divided into individual segments and printed sequentially, but which require extra preparation time. In addition, the fineness of the STL mesh plays a significant role in warping, as the reverse transformation can be very unclean with very coarse mesh structures and this can lead to problems. (Wüthrich, Gubser, Elspass & Jaeger 2021, 2–3.)

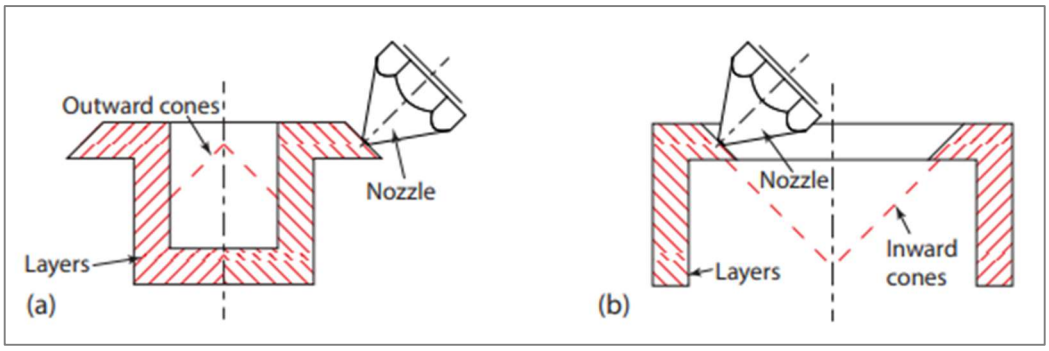

Figure 18. Outward cone print (a) and inward cone print (b) (Wüthrich, Gubser, Elspass & Jaeger 2021, 3)

3 CREALITY CR-10 MAX LINEAR RAIL MODIFICATION

As mentioned in the introduction, the Creality CR-10 Max has been modified to improve print quality and reliability. For this purpose, the old V-rollers were replaced by linear rails. These were ordered from Tiny Machines 3D in Houston in the form of two upgrade kits, the "Linear Rail Upgrade for Creality CR-10 Max" for the X Axis and Y axis.

Figure 19. Linear rail for the X and Y axis of the CR-10 Max (Tiny Machines 3D 2023)

They include a single rail for the X axis with one carriage, and two rails with two carriages each for the Y axis. Such rails can also be specially configured by other manufacturers such as HIWIN. As can be seen in Figure 19, a carriage with the designation MGN12H has been used, where MGN stands for the series, 12 for the size of the carriage and H for the accuracy class. The connection dimensions correspond to a distance of 20mm for the four M3 holes, both horizontally and vertically to each other. The required T-nuts and screws are enclosed, individually packaged and labelled, with which the rails are mounted directly to the frame profiles. However, no instructions were included.

3.1 X-axis

Since not only the linear rails were installed as part of this project, but also the old Bowden extruder kit was replaced with a direct drive extruder, these two conversions overlap in the area of the X axis. For this reason, the hotend section was not only dismantled, but also completely disassembled, which would not be necessary for just the conversion of the rails.

3.1.1 Disassembly

In the first step, the filament was retracted from the hotend while the printer was still switched on, so as to avoid problems later when removing the connection tube. The printer had then been switched off and unplugged from the mains to prevent possible damage to the printer or injury. After that, the hotend cover with the fans attached to it could be removed, giving access to the rest of the hotend section.

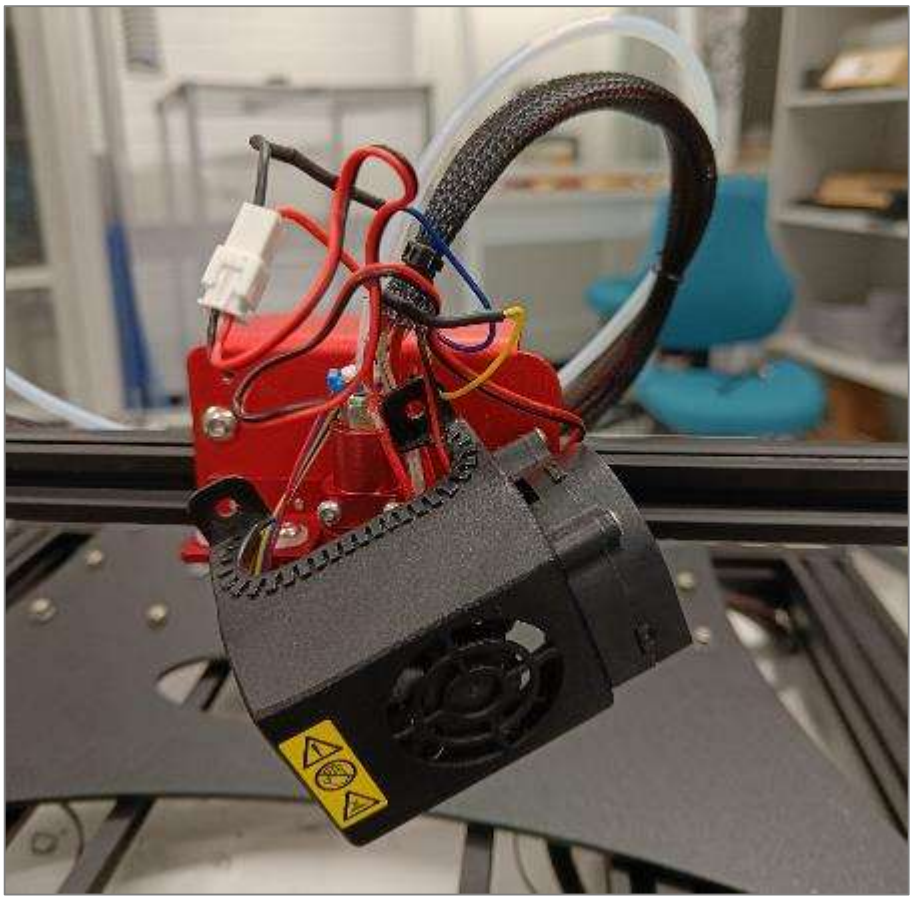

Figure 20. Removal of the hotend cover

Since the fans were still wired at this point, it helped to lower the Z axis to bring the X axis close to the printing bed, as this allows the components that were still connected to be placed down easily. This prevented damage to components that would have been hanging on the cable and could tear out otherwise. In the next step, the entire assembly, which was attached via the heatsink, was removed by two screws next to the cooling rips and were also placed on the pressure plate. The fan shroud, the wiring and the heatsink in the background can be seen Figure 20.

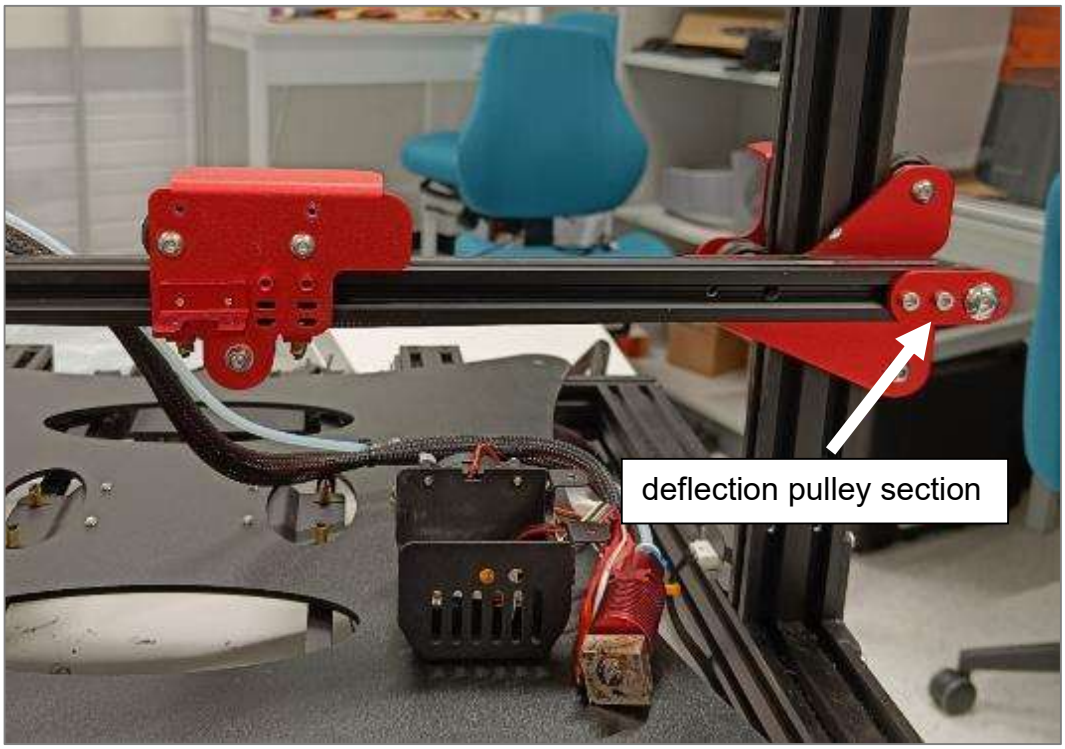

Figure 21. Removal of the hotend section

The drive belt could be unhooked on the lower rear side of the carriage and simply placed in the groove of the aluminium profile. By unscrewing the lower central screw, which at the same time holds the V-roller, the entire carriage could be removed from the rail. The belt tensioner with the deflection pulley had to be removed from the right-hand side. To accomplish this, the belt on the deflection pulley had to be laid to the side and the tensioner loosened via the two smaller hexagon socket bolts and pushed out to the side of the profile. The belt tensioner and the two small screws are located on the right side in Figure 21.

3.1.2 Installations

Now that the entire profile of the x-axis had been cleared, the linear rail could be mounted on it. A screw with a T-nut on the back of the rail had been pre-mounted in every second to third hole in the rail. To insert the rail from the side, a 3D printed part, supplied by the kit has been used by plugging it onto the aluminium profile. It had a conical inlet via which the T nuts were slipped into the groove of the profile. This structure with aluminium profile, linear rail and push-on part can be seen in Figure 22.

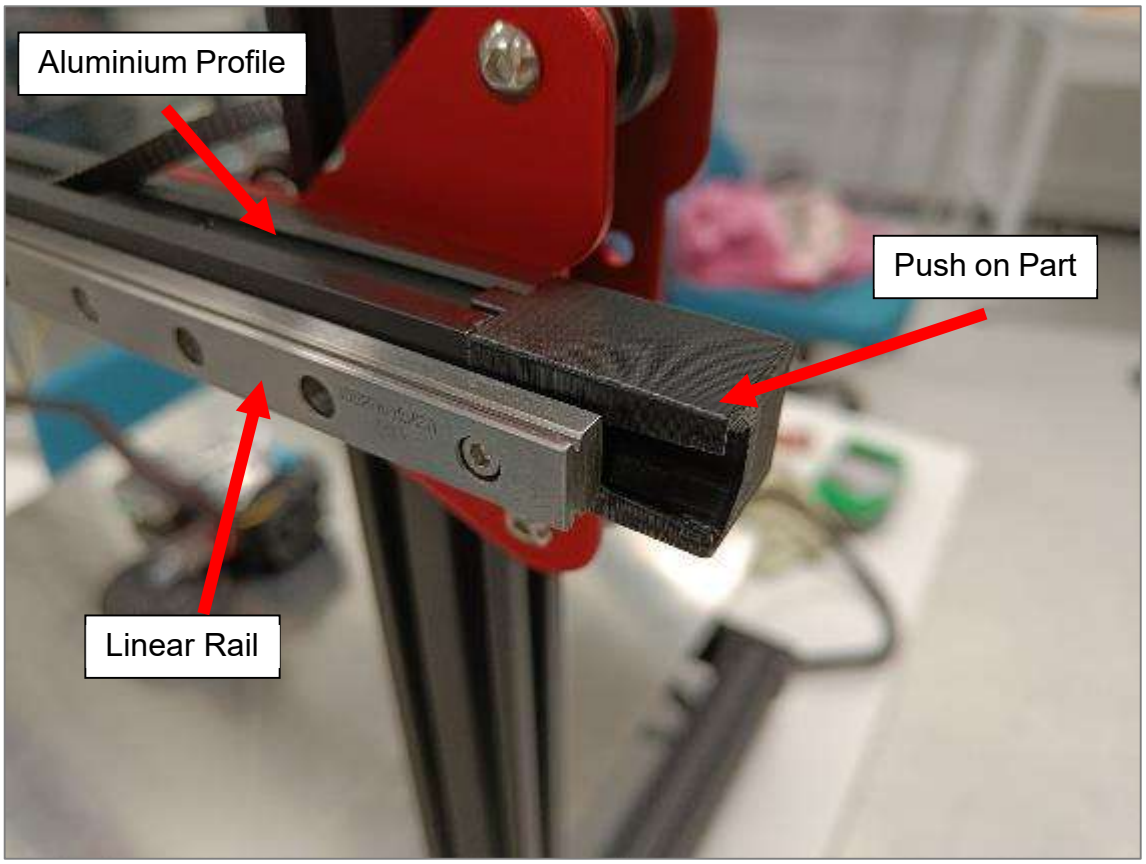

Figure 22. Installation of the linear rail on the aluminium profile

After the rail had been slid on, the slip guide part could be removed again. In order to fix the rail straight to the profile, two 3D printed guides were provided, with which the rail could be centred and held in position for mounting. All the screws were tightened, and the mounting aids were removed.

3.1.3 Adaption

The end stop switch of the X-axis was covered by the rail and had to be repositioned. The screws of the housing held the motor on the opposite side of the red plate and the distance was thus determined, so a recess had to be made especially for the sensor alone. For this purpose, the old housing was measured and reconstructed in the CAD software Solid Works. The recess for the switch was then moved outwards by the width of the linear rail and was then 3D printed. The difference between the old and the new design is in Figure 23 evident, where in the left picture the old housing is shown and on the right picture the new one.

Since the switch holder originally had a thread, but this was not possible with the FDM process, a hole with a diameter of Ø2.8mm was created for the M3 screws. This meant that the screw cut the thread itself into the material, which does not allow for high loads, but in this application this was negligible. The respective STL file is available for download under the following link:

`https://www.thingiverse.com/thing:5986958`

Due to the change in sensor position, design changes had to be made to the carriage. However, this topic will be discussed in more detail in chapter 3.3.3**Error! Bookmark not defined.**.

Figure 23. CR10 Max X axis motor and sensor housing old (left) and new (right)

3.2 Y-axis

3.2.1 Disassembly

To convert the Y-axis, the pressure bed had to be removed first. The four adjustment bolts at the four corners underneath the bed had to be removed, these are marked in Figure 24. Then the entire pressure plate, including the heating unit, could be folded backwards, and placed behind the printer upside down. It was very important to not damage the wiring and the soldering points of the heating unit. The completion of this step is shown in Figure 25.

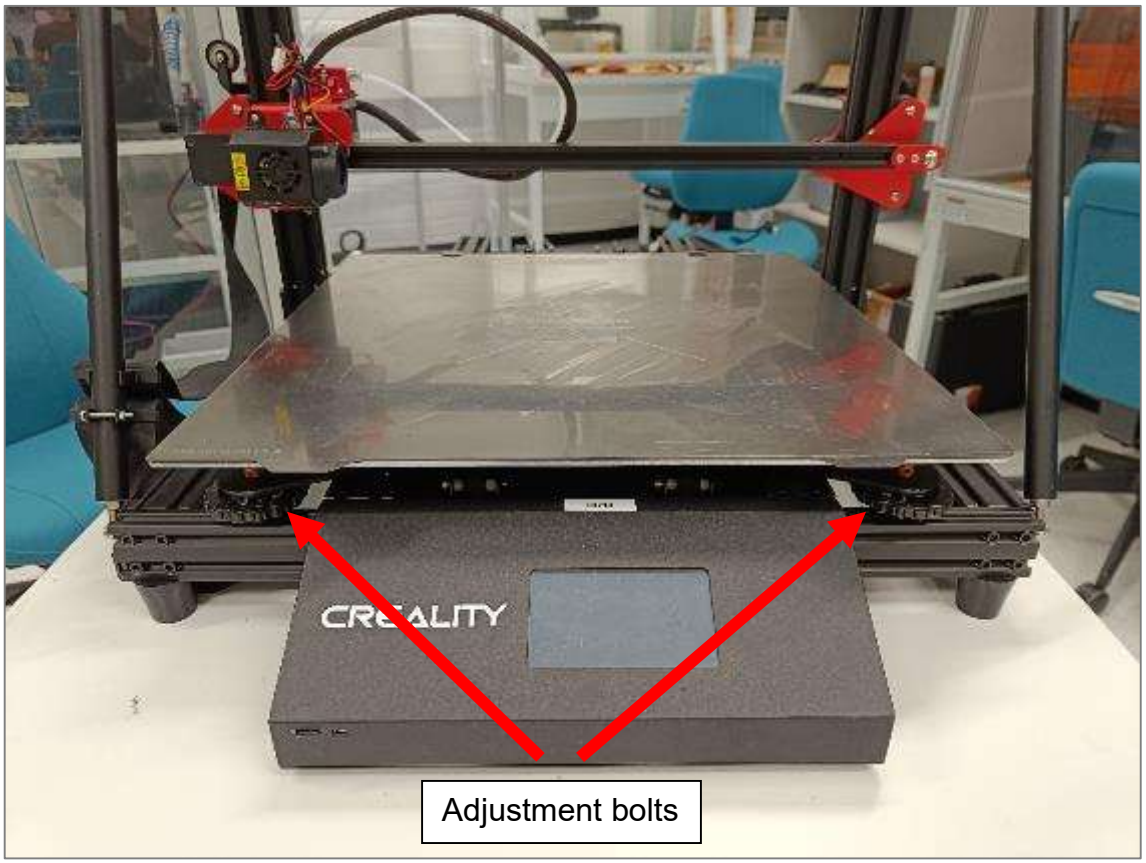

Figure 24. CR10 Max initial situation

In the next step, the two straps were unhooked via the release of the carriage plate by pushing them outwards from their slot. Then the six V-rollers on each side could be unscrewed and be removed from the aluminium profile in which they roll. This allows the entire carriage plate to be removed and put aside. The bolts and strap mountings mentioned are evident in Figure 25.

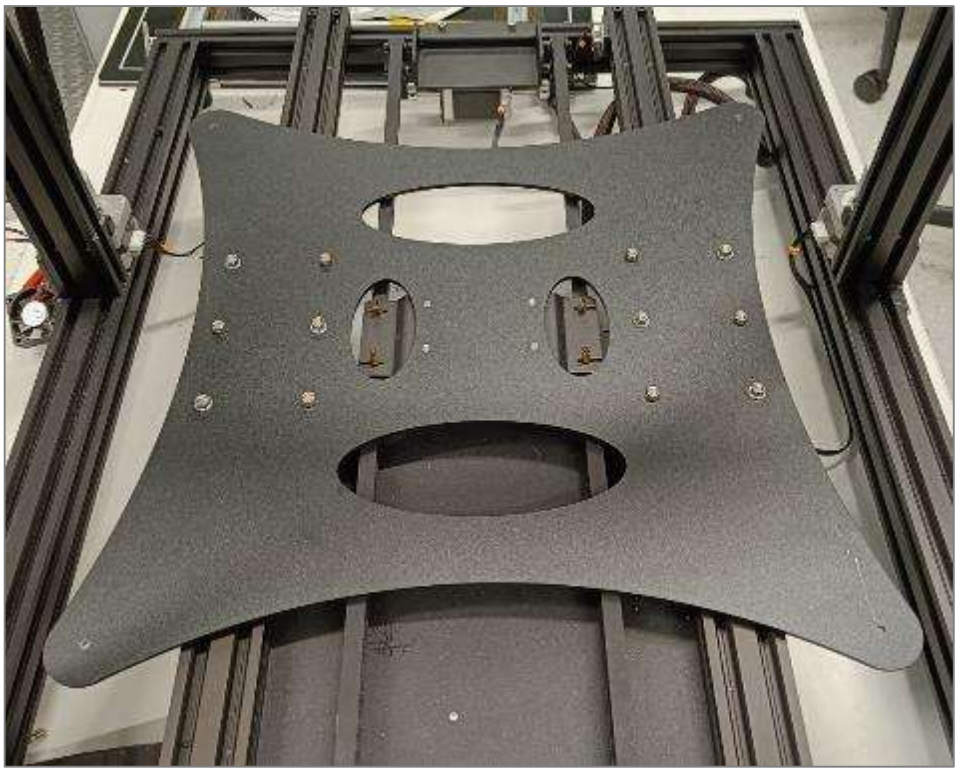

Figure 25. CR10 Max Y axis carriage

3.2.2 Installation

As in chapter 3.1.2, the screws with T nuts were mounted on the linear rail in advance, as the 3D printed part supplied could also be used here, as with the X axis. The plastic caps of the aluminium profiles on the back of the printer had to be removed first. The push on part had been attached and the rail and screws pushed all the way in towards the front. At this point, it was important that the carriages were already on the rail, as they could no longer be inserted from the side later on. The mounting guides which were included in the delivery were also attached here in order to align the rails and the screws were tightened.

The next step was to mount the brackets for the carriage plate. An aluminium plate and a small plate with a vertical thread had to be screwed together at first. This was possible via the fifth screw, which was not connected to the carriage itself. These plates were then mounted on the carriage so that the vertical inlet faced inwards towards the rail. This resulted in the same geometric distance between the two rails in which the V-rollers were mounted. This meant that the two outer holes of the three old holes could be used to screw the plate to the carriages. The orientation of these brackets is shown in Figure 26.

Figure 26. CR10 Max Y axis linear rail carriage

Now the carriage plate could be refitted on the new carriages and the straps re-inserted into the slots via the recesses. The plate had to be held firmly and the belt was pulled into position with a pair of pliers. Then the screws with the hand-adjustable nuts could be put back in place and finally the print bed could be put back on and tightened.

Figure 27 now shows the last step, where the rails have been degreased after assembly to avoid contamination. New lubricant was applied to the side outlets of the carriage with the syringe provided to ensure smooth operation. As these inlets were only accessible from the underside of the printer, a second person was needed to assist. The same was done with the carriage of the X-axis.

Figure 27. Lubrication of the carriage

3.2.3 Adaption

Since the limit switch on the back of the printer was also covered by the rail of the Y-axis, this also had to be repositioned. In this case, however, it was not sufficient to point the sensor further outwards, as it would otherwise have come into contact with the adjustment screws and loosened them permanently. Therefore, the switch had to be mounted on the underside of the aluminium profile, where it is triggered by the lower inclination of the slide. For this purpose, a bracket had to be printed, which was mounted with one of the remaining T-nuts. This part is available for download at the following link:

`https://www.thingiverse.com/thing:5987334`

When mounting the limit switch, care had to be taken that it was triggered in the same position as in the old position, as otherwise the defined print space would have shifted, and the printer could have collided with the frame during print bed levelling or large prints. This corresponded to a distance of approx. 80mm to the

rearmost edge of the printer, whereby the bracket of the cable hose also had to be repositioned as it sat at the same height. The arrangement and positioning of the individual components can be seen in Figure 28.

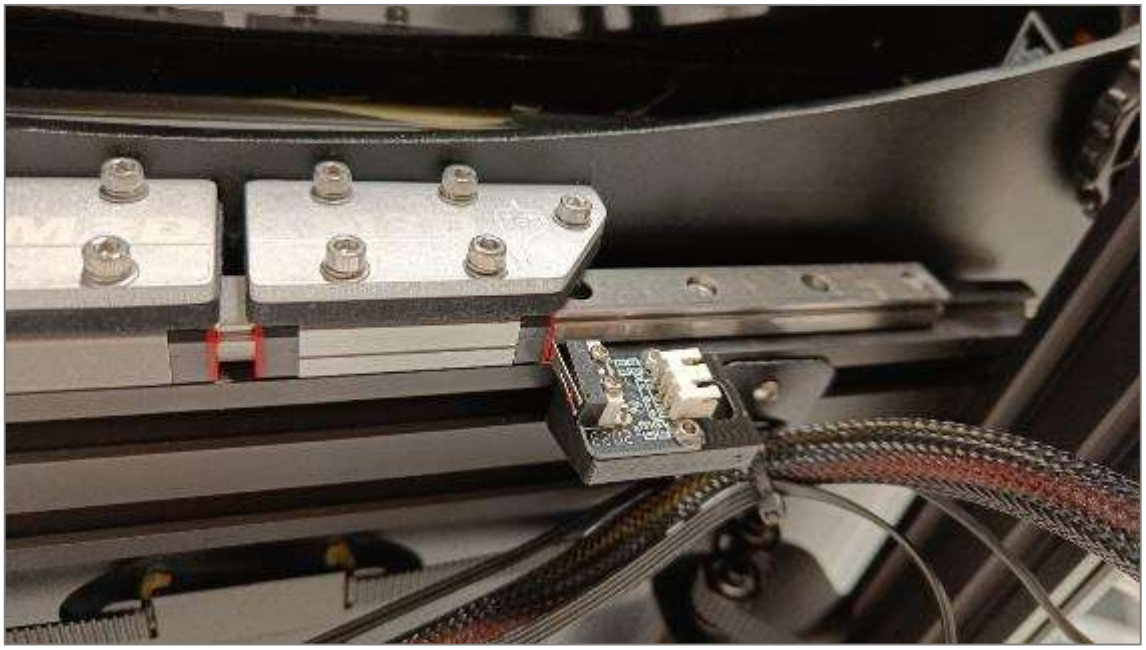

Figure 28. CR10 Max - Y axis end switch mounting

3.3 Creality CR-10 Max Direct Drive extruder (DDE) installation

For the conversion to a direct drive extruder system, the brand MircoSwiss was chosen, as they are well established and also offer special solutions for Creality 3D printers. In the context of this project, the model M2601 was chosen, which is specially designed for the CR10 series.

3.3.1 Disassembly

As already explained in Chapter 3.1, the trolley has already been dismantled and disassembled as part of this project. First, the cover of the hotend was removed and then the heat sink was unscrewed to which the hotend and the PETG pipe were attached. The individual components could be separated from each other, as they were later reassembled on the frame of the direct drive extruder.

The extruder unit of the Bowden kit had to be removed. To do this, the screw of the spring tensioner had to be detached, after which the spring itself could be dismounted. Then the remaining two screws that fixed the extruder and tensioner

unit to the plateau were loosened and removed, as was the filament sensor, which also had to be repositioned as well. The individual components are labelled in Figure 29.

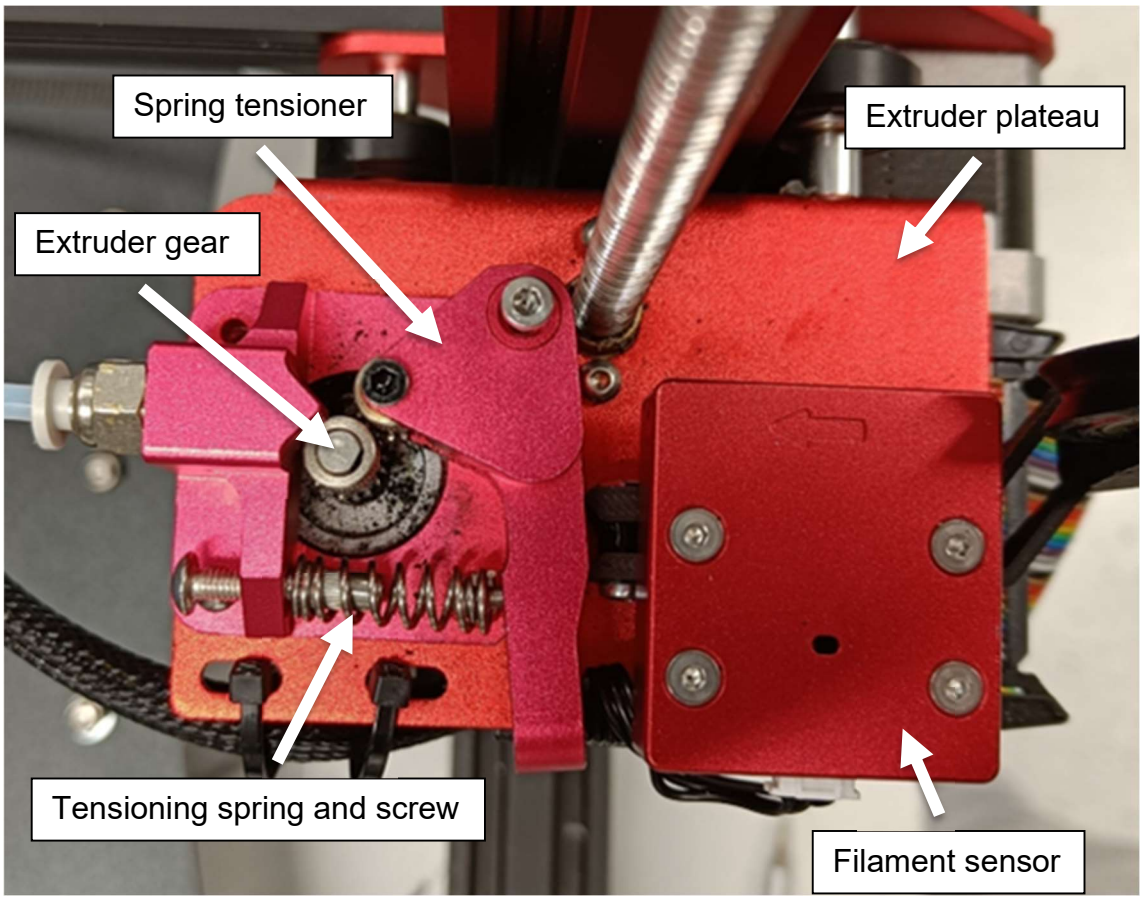

Figure 29. CR10 Max Bowden kit extruder section

3.3.2 Installation

Since the linear rail conversion kit is not compatible with that of the DDE, an adapter plate had to be made before installation. For this purpose, the dimensions of the new carriage and those of the DDE plate were taken and a corresponding intermediate piece was designed using SolidWorks. This was then 3D printed with the PETG filament, which has a high mechanical load capacity and should therefore prevent deformation due to the increased weight of the DDE. The assembly of the mentioned parts can be seen in Figure 30. The corresponding part is freely available for download under the following link:

https://www.thingiverse.com/thing:5991399

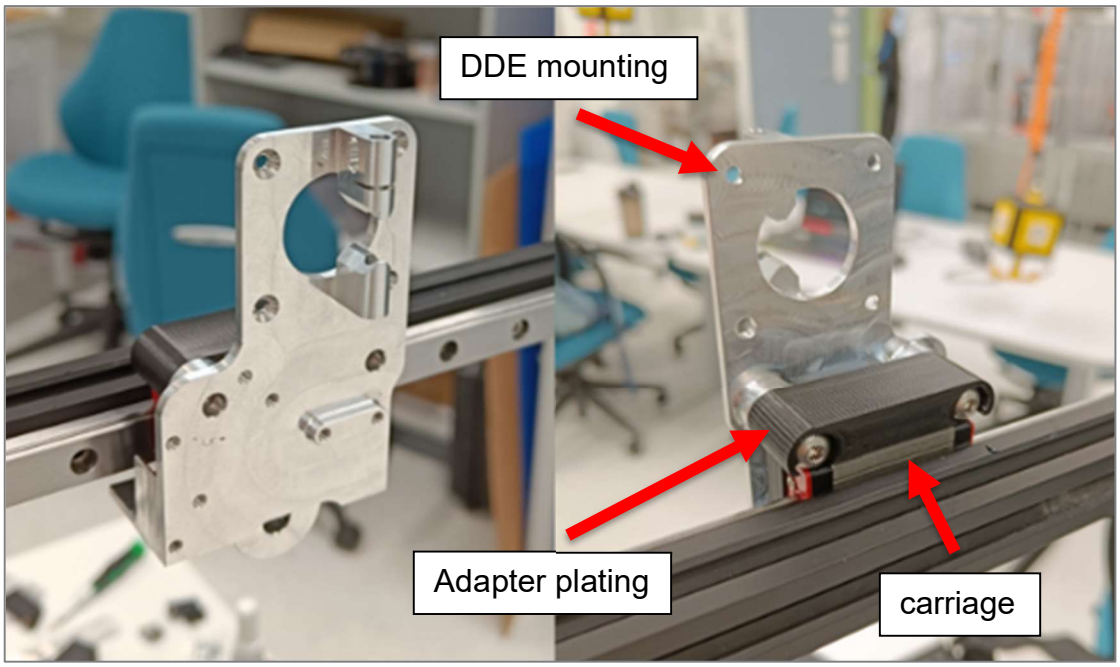

Figure 30. DDE mounting front view (left) and rear view (right)

After the first trial fitting, the mounting plate was removed again and fitted with the previously dismantled components according to the MicroSwiss instructions. First, the extruder was inserted from the rear through the round opening and fastened with the four screws, and the new tensioner supplied by MicroSwiss was mounted on the front next to the extruder wheel. The mentioned parts are marked in Figure 31. Mounted DDE. The old thermistor and heating rod were then inserted into the new hotend, fastened, and then screwed to the heartbreak and heatsink. This sub-assembly was also screwed onto the plate and connected with a small, pointed PTFE tube, which should ensure a fault-free connection. In the next step, the heating element had to be reconnected and heated up, whereupon screws could potentially loosen due to thermal expansion and have to be tightened again. After checking, the DDE unit could finally be attached to the carrier.

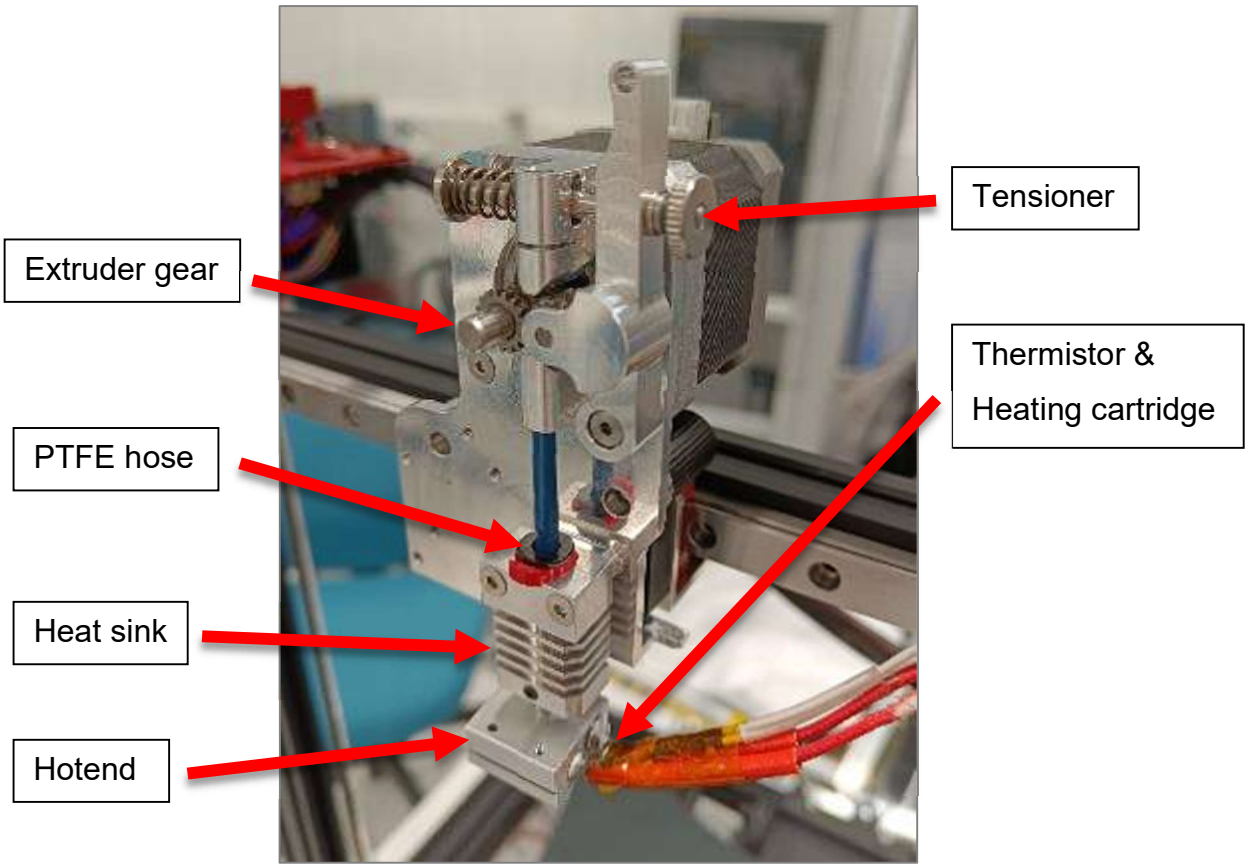

Figure 31. Mounted DDE

As the MicroSwiss kit is not fully compatible with the Max variant of the CR10 series, the old fan shroud could no longer be used, as the pick-up points were different here. For this reason, the cover of a Creality Ender 3 was initially installed, which had the corresponding hole positions. However, since the BL-Touch sensor, which is required for Z axis and bed calibration, would also have needed a new mount, the Ender 3 cover was replaced with a self-printed complete solution, which was available on the internet as a free download under the following link:

https://www.thingiverse.com/thing:4689712

Both the two fans and the sensor could be mounted directly on this cover, which also improved the aesthetic aspect. This meant that the layer fan of the CR10 Max could no longer be used but had to be replaced by the one of an Ender 3, which had a thickness of 10mm instead of 20mm. The complete assembly can be seen in Figure 32

.

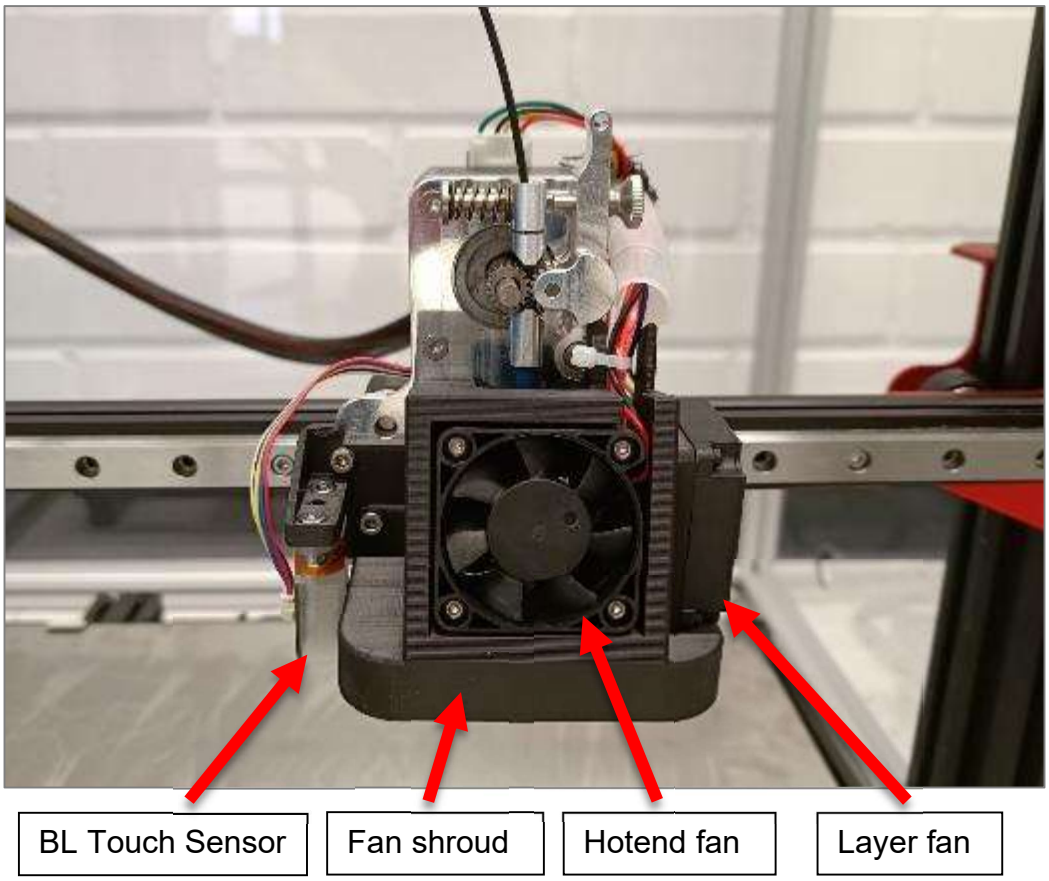

Figure 32. DDE fan shroud with BL Touch mounting

3.3.3 Adaption

Since, as shown in Figure 30, an adapter had to be fitted between the carriage and the DDE, this caused the belt attachment to move away from the centre plane of the aluminium profile by the same amount, which meant that the belt no longer ran straight. This is especially a problem when the printing head approaches the end of the X axis with the idler roller, as the offset pulls the belt off the idler roller and causes it to become slack. The old belt mount had to be cut away with an angle grinder so that a supplied L-profile could be screwed between the adapter and the carriage, which has the same mount. Since this piece was screwed directly to the carriage, the distance to the centre of the profile, where the belt is running, corresponded to the correct value, which can be seen in Figure 33.

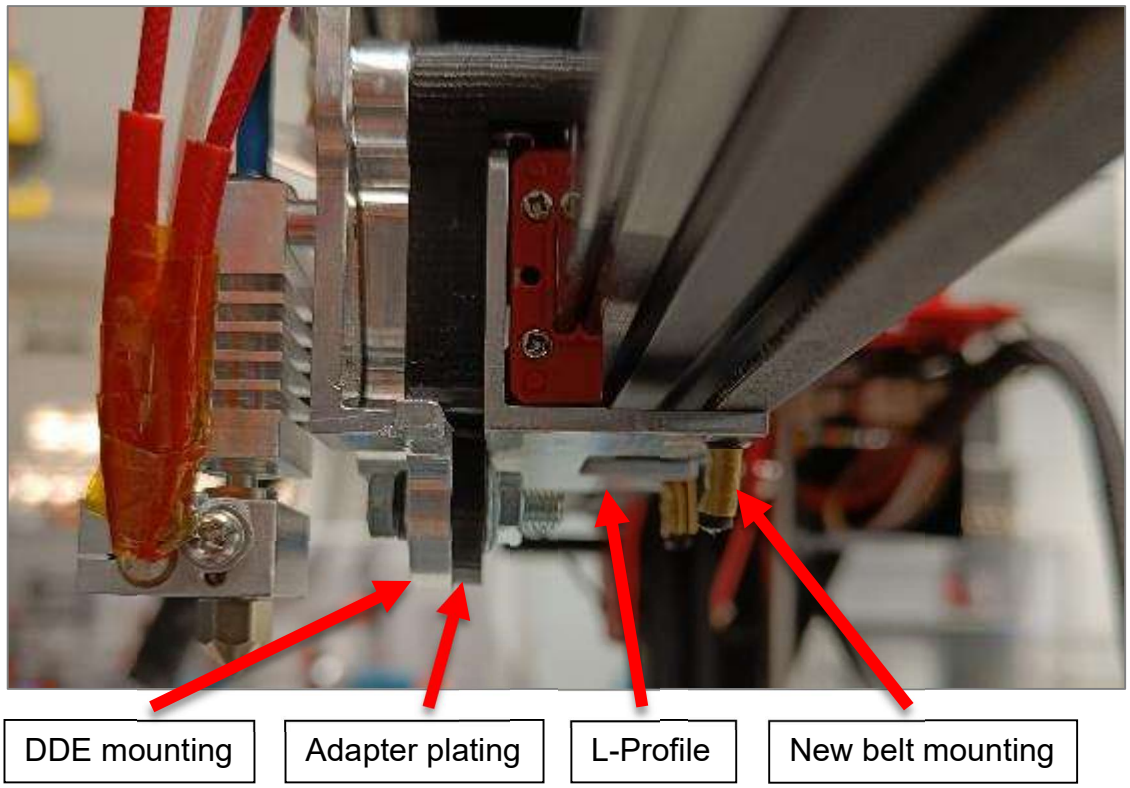

Figure 33. New belt mounting for the DDE

3.4 Printing results

It should be noted that the visual differences in print quality before and after the conversion are not fully visible, which is due to the printing speed. After the modifications, constant results could be achieved at speeds of 50-60mm/s, whereas with the old setup only a tenth of this speed led to usable results, especially with very large but detailed models.

A major problem that had significantly lowered the print quality of the CR10 Max was stringing. This also caused the printer to stop printing due to collision when printing for long periods of time. In Figure 34 you can see two overall test prints which include various disciplines such as bridging, holes, walls, and overhangs. The left side shows a test print before the modifications, in which the stringing is particularly evident in the area of the cylinders. This problem could no longer be found in any of the tests nor in the right-hand test print of the same image. Special mention should be made of the overhangs, which achieved a perfect result even at an angle of 80°, which is very difficult even for high-quality and expensive printers.

Figure 34. CR10 Max Overall printing test before (left) and after (right) modifications

Another problem was the accuracy of large-area prints, where height differences in the layer were particularly noticeable in the first layer and thus led to different extrusion thicknesses, as can be seen in Figure 35. In the next layers, this caused the material to scrape up and collect at certain points, which was followed by another collision error stop. In addition, different extrusion thicknesses in the same layer lower the print quality. After the rebuild, this problem also disappeared and consistent printing results could be achieved.

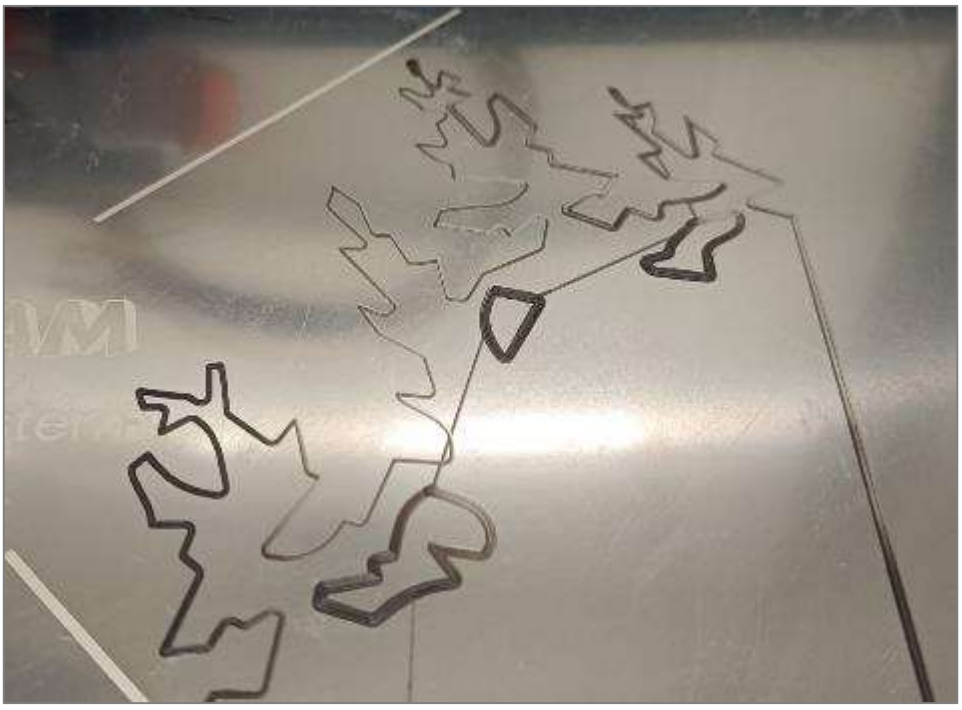

Figure 35. CR10 Max Extrusion issues

4 FOURTH AXIS IMPLEMENTATION OF A CREALITY ENDER 3

The original idea for this conversion came from a master's thesis at the Zurich University of Applied Sciences (Wüthrich, Elspass, Bos & Holdener 2021). There, a fourth rotatable axis was integrated into a Prusa i3 Mk3S+ to implement conical cutting. This approach was adopted and adapted to a Creality Ender 3. A sectional view of the assembled rotary axis can be seen in Appendix 1. Furthermore, the production drawings of the individual components, which will be discussed in more detail in chapter 4.12, can also be found in the appendix. Apart from the slicer itself and the component drawings, nothing was made available by this work, which is why the implementation of the rotation axis in the firmware was one of the essential elements.

4.1 Disassembly

In the first step, the existing Ender 3 had to be dismantled into individual parts, the hotend section was removed from the carriage and all motor cables were disconnected. The aluminium profiles were cleaned of small aluminium chips and dirt to prevent damage to the belt after installing everything back together. The cover of the motherboard housing on the underside of the printer was removed and the fan hanging from it was unplugged in order to put the cover aside and gain access to the motherboard. This is shown in Figure 36. The connectors for the motors, sensors and heater rods were disconnected and the motherboard unscrewed from its anchorage and removed. The individual components and the associated screws were named and sorted in a separation box so that the corresponding parts could be found more quickly during the later assembly.

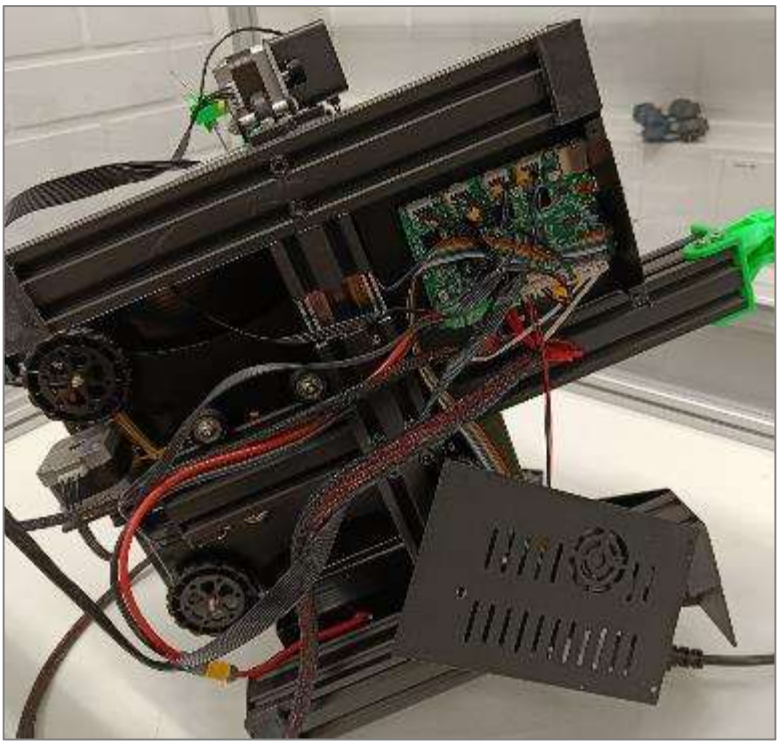

Figure 36. Bottom view of a Creality Ender 3

4.2 Duet 2 Motherboard

4.2.1 Driver

To realise a 3D printer with four moving axes, five different outputs for motors, also called drivers, are required. The corresponding drivers are X, Y, Z axis and E0 or E1 which stand for the extruder motors. Since the original motherboard of the Creality Ender 3 only has 4 drivers, a suitable device had to be selected here. The most common model for such an application is the Duet 2. In addition to the required number of drivers, it also has good computing power, does not require external cooling, and can be connected directly to an inhouse touch panel. A large documentation database with commands, configurations and entire projects provided by Duet as well. In addition, an active forum helps with more in-depth questions. For these reasons, the Duet 2 board was the ideal solution for this thesis, which was purchased with the Wi-Fi module instead of the Ethernet version for easier handling.

4.2.2 Wiring

Duet also provides the pinout diagram of each motherboard in their portfolio, which played a crucial role in the subsequent wiring process later in the project. Figure 37 already shows the five different drivers in the upper tray, which were mentioned in chapter 4.2. The motherboard has a voltage input (VIN) of 24V, which is also output in the case of the heating elements. The fans can be operated both with VIN (24V) and throttled to a 5V output voltage. Furthermore, it can be seen that in addition to the print bed heater, there are two other slots for heaters and the corresponding temperature sensors. However, since only one is needed for the hotend, an upgrade in the form of a heated chamber would be possible.

Also, important here are the phase assignments of the motor outputs, which always have to be compared in combination with the motor inputs in order to avoid short circuits or other damage, which also applies to the fans. The orientation for heaters and thermistors is not relevant.

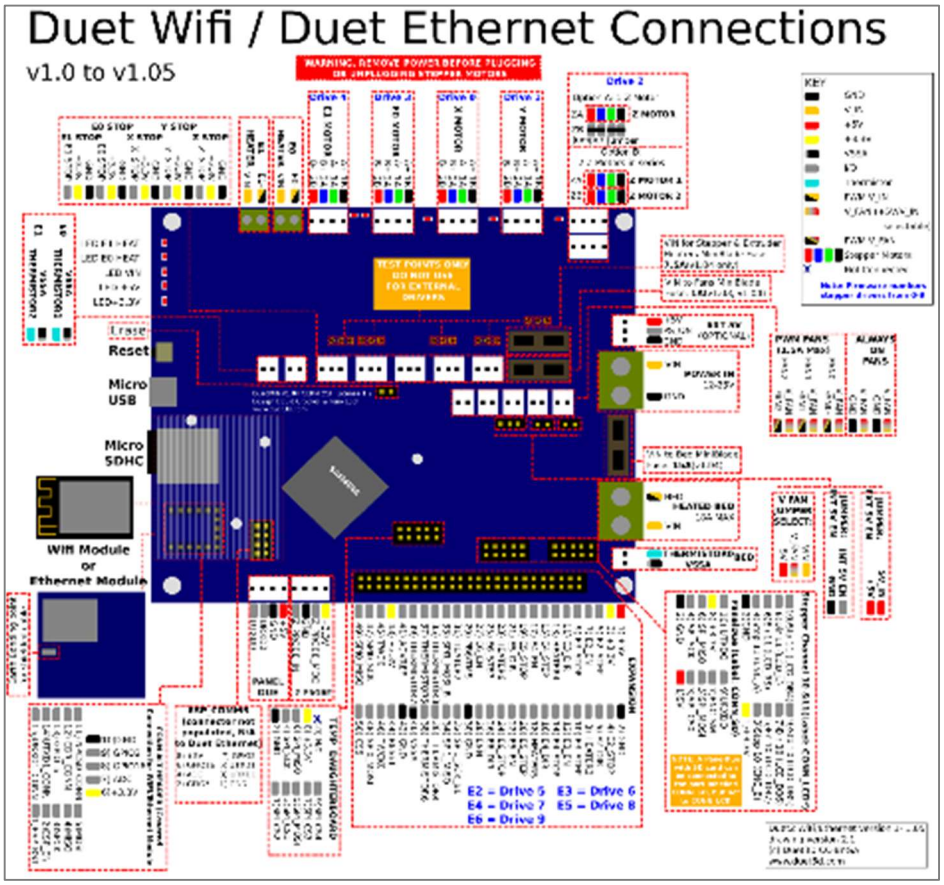

Figure 37. Duet 2 Wi-Fi Connections (Duet3D Documentation 2022)

4.3 Yet Another Terminal (YAT) serial communication

4.3.1 Duet Board connection

To establish the first contact to the motherboard, a communication terminal was needed. For this the Yet Another Terminal (YAT) was used, which is a freely accessible terminal.

After the installation the driver for Duet had to be installed to be able to communicate with it and connected via a USB cable. Then it could be started, whereupon a new terminal was created. For this, the serial port is queried, which represents the individual outputs of the computer or laptop. The terminal type, the port and the transmission speed can be defined here as well. YAT automatically detects the occupied and accessible ports and preselects them for connection.

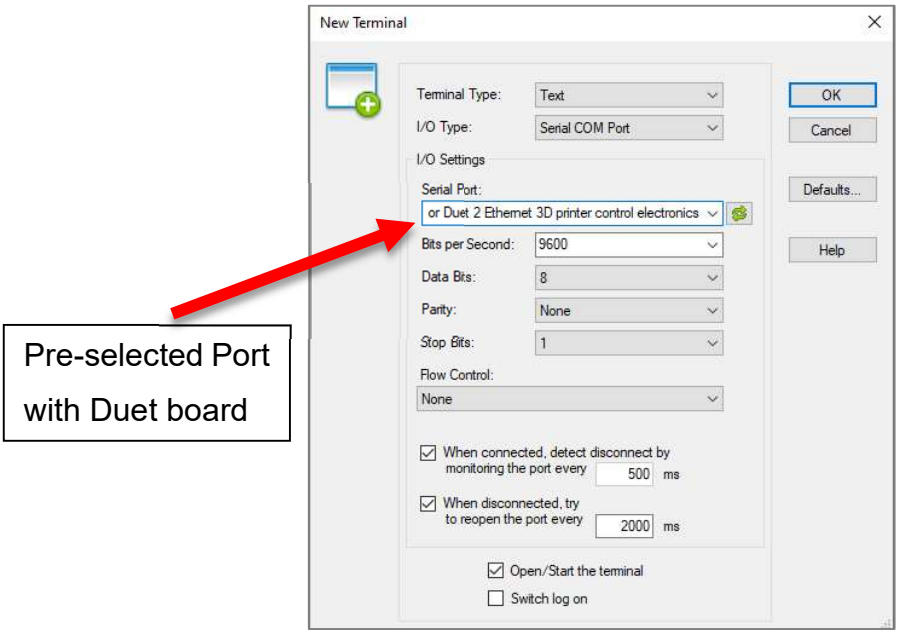

Figure 38. YAT New Terminal window

After the successful connection of the terminal to the motherboard, the language called End-Of-Line (EOL) had to be changed to <LF> under Terminal -> Settings -> Text Settings.

In the main window of the terminal the command bar is now visible in the lower area in Figure 39, over which the commands can be transferred. The white

window describes the console history, in which the previously entered commands are recorded with a timestamp or requested information is displayed.

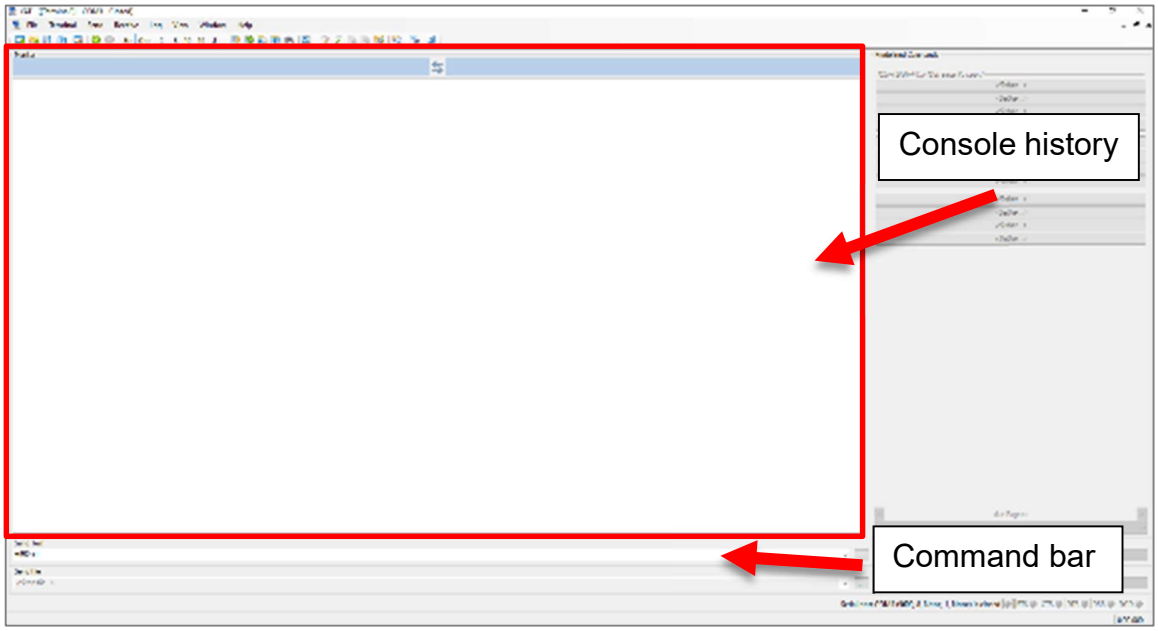

Figure 39. YAT Terminal

4.3.2 Firmware Version

To connect the motherboard to the internet and later access it via the Duet Web Server, the file DuetWifiServer.bin is needed to establish the connection. This file is not always pre-installed by default and therefore it was necessary to check which firmware version is currently installed on the board. This can be done with the following command:

```
M115 *check Firmware Version
```

This was necessary as the latest version cannot be simply upgraded immediately, but always needs a step in between at the next larger integer and then to the latest version. In this case the version 2.2.8 had to be upgrade to 3.0.0 first and then to the latest one 3.4.5, while also installing the WebServer.bin file.

4.3.3 Connecting to Network

In this step the network module was switched off, then the module status was checked and at last it was put back into idle mode and queried once more. The corresponding commands are listed as follows:

```
M552 S-1      ;disable WiFi
M552          ;check WiFi status
M552 S0       ;put WiFi into idle
M552          ;check WiFi status
```

Furthermore, the network and the corresponding password could be saved in order to connect to it (no network and password entered for data protection reasons):

```
M587 S"network-ssid" P"network-password"
```

After that the module was switched on and connected to the local WiFi network automatically:

```
M552 S1       ;connect WiFi
M552          ;check WiFi status
```

With the successful connection, the IP address of the motherboard was confirmed, which could now be copied directly into the browser and the DuetWebServer opened. The commands mentioned and the corresponding console replies can be seen in the following Figure 40.

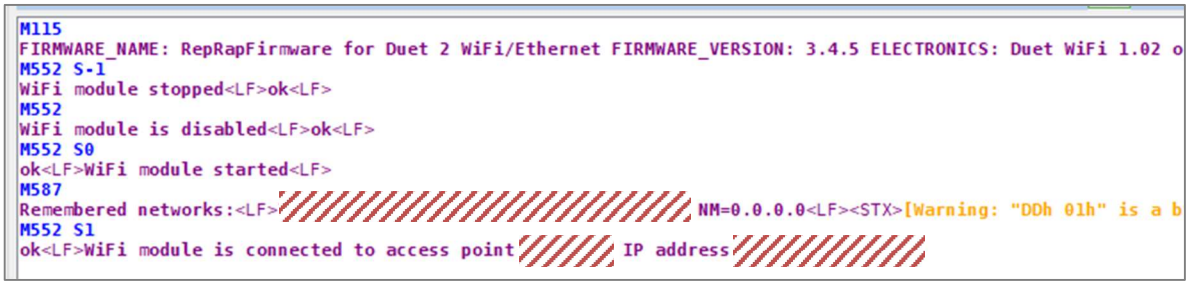

Figure 40. YAT WiFi connection

4.4 Duet Web Server (DWS)

The DWS serves as a browser-based interface for Duet products running on a RepRap operating system. This allows remote access to the printer, as well as print monitoring and other tasks that no longer need to be done on the printer itself. In addition, individual axes can be moved and homed, the heater can be heated, and print jobs can be uploaded and started.

4.4.1 Dashboard

Figure 41 shows the dashboard of the DWS, which appears automatically after every start. On the left-hand side of the screen there are further menus in the form of a folder structure. In the dashboard window itself, the positions of the individual axis motors, as well as the supply voltage (VIN) and the temperature of the motor control unit (MCU) can be seen in the upper, middle area. In the area to the right, the current temperatures of the heater, as well as the desired active and standby temperature can be found here. The chronological progression of these values is shown in the temperature chart in the upper right corner. In the lower half of the display board, you can now see the individual axes that can be used with predefined values. The extruder can also be retracted and extruded at different speeds below. The last control area is the fan control area at the bottom of the screen, in which the construction fan can be operated manually.

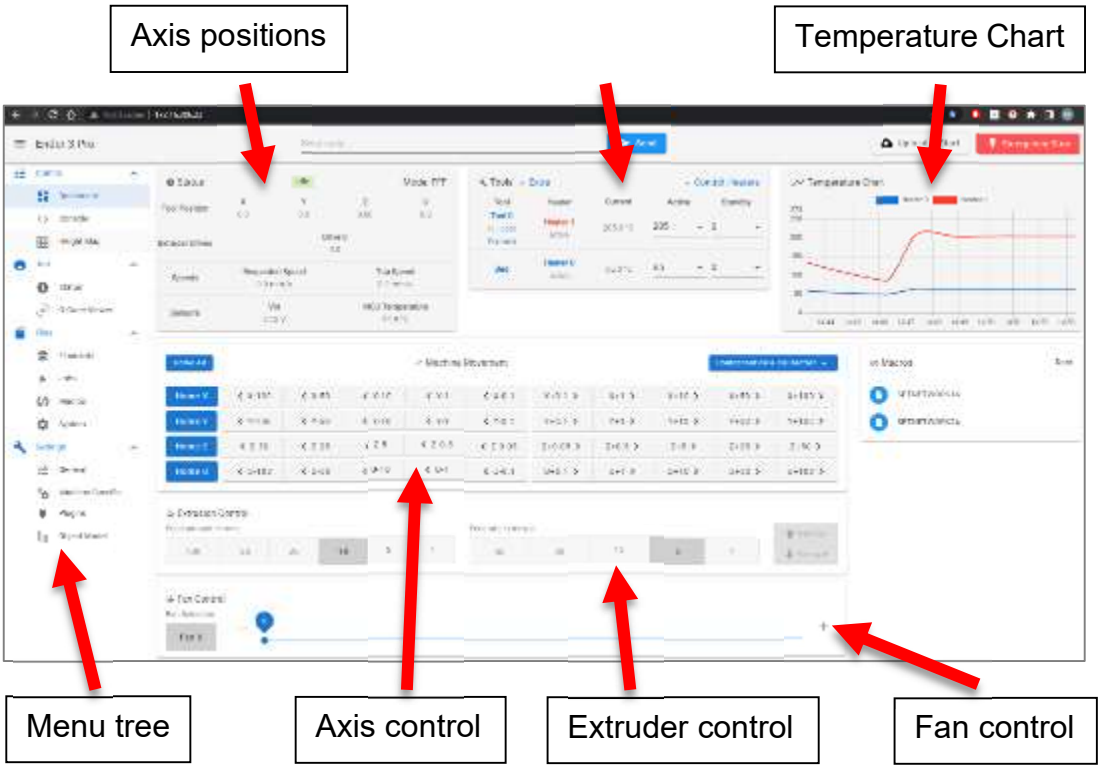

Figure 41. DWS Dashboard

4.4.2 Firmware Update

To update the firmware, the current RepRap version had to be downloaded from GitHub and saved as a ZIP file. This then had to be uploaded in the DWS in the System menu. As can be seen in Figure 42, the individual files of the firmware are already stored here. In order to overwrite the old firmware, the ZIP file only had to be uploaded via Upload System Files, which was automatically installed, and the motherboard restarted.

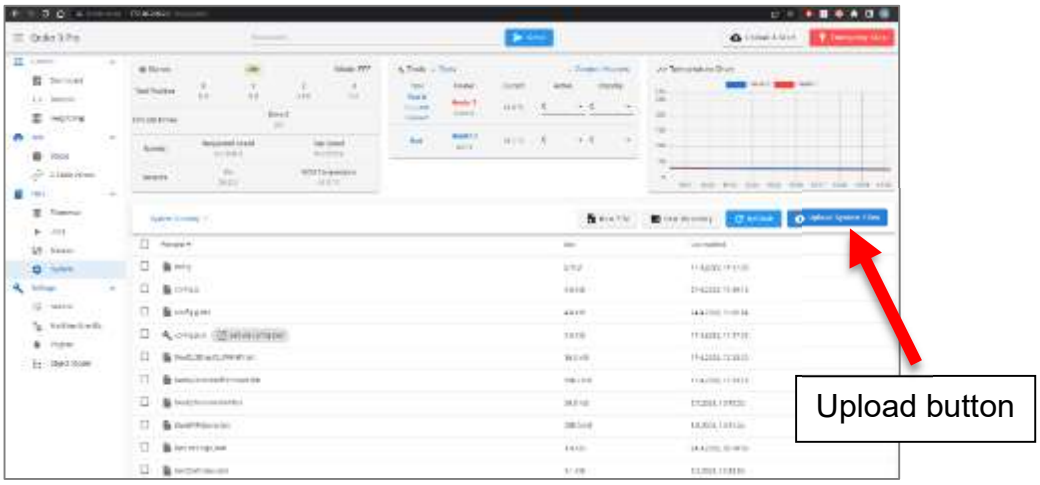

Figure 42. DWS System menu

4.4.3 Duet 2 Clone

As economic resources were limited in this project, a clone of the Duet 2 motherboard was purchased at the beginning. The communication with YAT and the internet connection had worked flawlessly at the time. However, as this was not an original Duet product, the DWS could be called up via the IP address, but everything was greyed out and entries were not accepted.

Therefore, the firmware update had to be done manually via YAT and the micro-SD card. The config.g file and the Web Server driver were copied from the ZIP file onto the card. The motherboard was able to access these and theoretically install them. This is done with the following command where module 0 is the main firmware and module 1 the web server firmware:

```
M997 S0:1    ;update firmware modules 0 and 1
```

Despite confirmed correct entry and a reboot after the update, no change could be detected after querying the firmware version. Even extensive troubleshooting could not solve this problem.

As a last resort, the motherboard was therefore cleared and all installations and files were deleted, so that the new firmware could be reinstalled later via remote access. In the case of duet, this is done via an application called Bossac. After execution, this application searches the different ports on a computer for assignments and, after selecting the corresponding port with the motherboard, it then installs the new firmware externally.

However, according to the application, no occupied output could be found here, although the corresponding port was provided with the name Bossac in the device manager of windows, in other words, the application was passively aware of this output, but could not actively use it for installation. Since the motherboard was unusable from this moment on, a new, original Duet board had to be purchased via E3D.

4.5 RepRap Firmware (RRF) Config Tool

As explained in chapter 4.2, the motherboard of the Creality Ender 3 only has 4 drivers, so not only the hardware but also the software had to be reconfigured. Since a RepRap operating system is required for the duet, a firmware generator is available from the same manufacturer. The RepRap Firmware (RRF) config tool allows you to create your own firmware, defining axes, end stops, step widths and much more.

In order to integrate the fourth movement axis, a presetup was first selected that was already stored for the Ender 3, which was why no motor-, fan data nor end stops had to be configured. Only the additional driver E1 was added under the I/O Mapping tab, which is actually intended for extruders by default and therefore does not have an end stop. This had to be implemented manually in the firmware in later steps of the project.

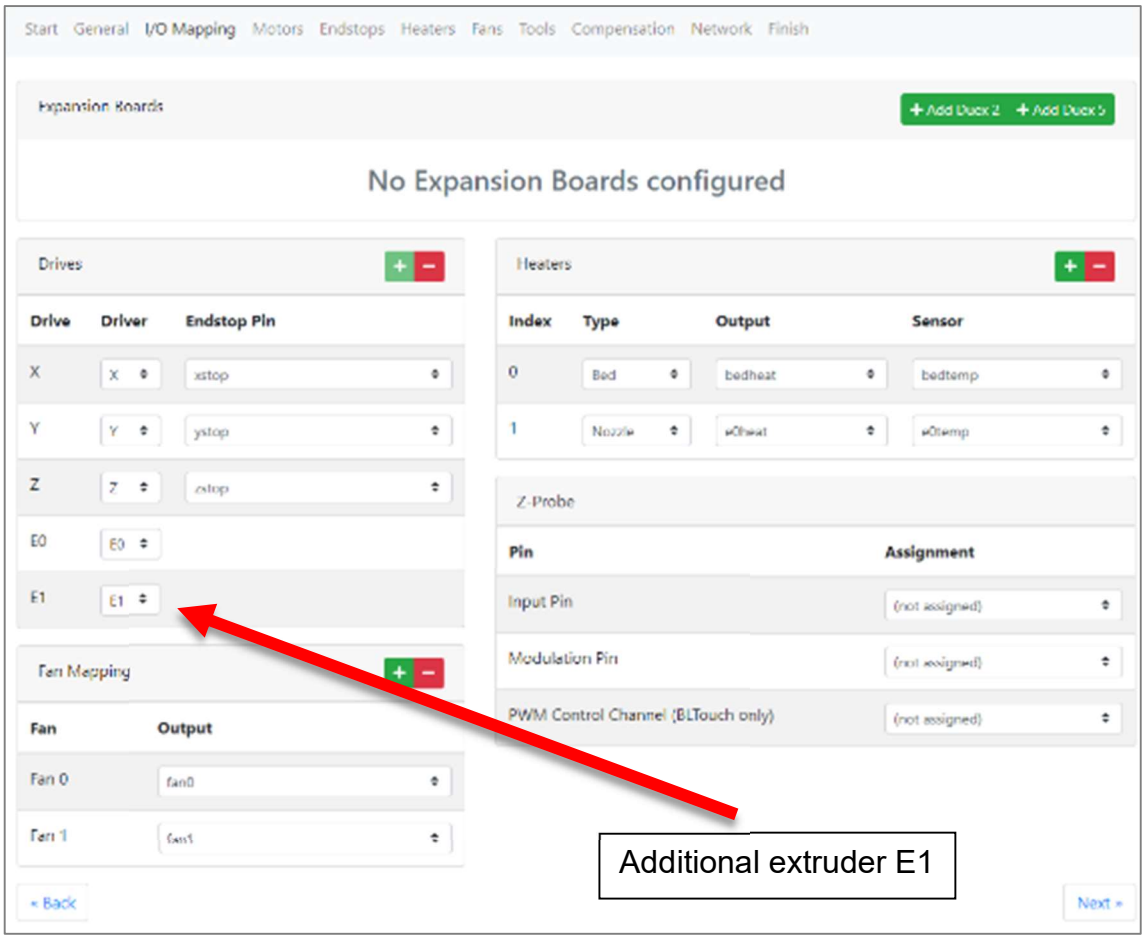

Figure 43. RRF Motor Mapping

4.6 Modify the Firmware for the fourth Axis

After uploading and installing the customised firmware, fine tuning and finalisation of the U axis implementation had to be done manually in the config.g file. The axis limits, maximum currents, speeds, and accelerations as well as the pin assignment had to be defined. This is explained in more detail in the following chapters 4.6.1 to 4.6.3.

4.6.1 Implementation of the U axis into the config.g file

In the firmware already created, the additional axis was defined as an extruder, which is why it was also titled E1. However, since this is later called up in the G code, which is created by the python scrip, with the name U, it had to be renamed. To do this, the slot on the motherboard is defined with the following command:

```
M569 P4 S1   ;P pin definition, rotation direction
```

The motor output with the corresponding variable U can now be defined to this slot like this:

```
M584 X0 Y1 Z2 E3 U4    ;defines pin 4 as U
```

The assignment of all drivers as well as the name assignment can be seen in the following Figure 44. These are listed in the config file under the designation driver. Several outputs can also be defined here for a common variable, which would look as follows:

```
M584 U4:5     ; U declared for pin 4 and 5
```

```
19 ; Driver
20 M569 P0 S1                                  ; physical drive 0 goes backwards
21 M569 P1 S0                                  ; physical drive 1 goes forwards
22 M569 P2 S1                                  ; physical drive 2 goes backwards
23 M569 P3 S1                                  ; physical drive 3 goes backwards
24 M569 P4 S1                                  ; physical drive 4 goes backwards
25 M584 X0 Y1 Z2 E3 U4                         ; set drive mapping
```

Figure 44. Config.g file driver configuration

4.6.2 Implementation of the U axis homeu.g file

In order to home the newly defined axis, another file had to be created for it in the firmware folder structure. To do this, the homex.g file was duplicated and renamed to homeu.g instead of creating the file itself. This had the advantage that the process was already stored and only the names of the axes had to be changed in the file. In the process, the process command G1 was renamed from X to U, which can be seen in Figure 45 in row seven.

A value of 400° was assumed here, so that a complete rotation of 360° was guaranteed. To prevent collisions with the print bed, the Z axis is raised by 5 mm beforehand and then lowered again, which was also adopted here. Finally, the current position was zeroed with the command G90 in line nine. This value was changed after assembly later on so that the print head is straight, as the sensor could not be mounted in such a way that it zeroes at a 90° angle.

```
5 G91                ; relative positioning
6 G1 H2 Z5 F6000     ; lift Z relative to current position
7 G1 H1 U400 F6000   ; turn to U axis sensor and stop there
8 G1 H2 Z-5 F6000    ; lower Z relative to current position
9 G90                ; absolute positioning
```

Figure 45. homeu.g file

4.6.3 U axis speed and limit modification

Since the speeds were still specified for an extruder motor, they had to be increased, but the acceleration had to be significantly reduced. Due to the inertia of the entire axis, care had to be taken to ensure that the motor or the axis did not spin on the other components and thus become loose, leading to collisions later on. The following values were assumed for the time being:

```
M566 U5000   ; max. instantaneous speed changes (mm/min)

M203 U6000   ; max. speeds (mm/min)

M201 U400    ; accelerations (mm/s^2)
```

The axle limits also had to be defined. Although it was possible to define this axis as a rotation axis, it could not be used for this application. On the one hand, rotary axes cannot be homed, as these are spindle axes, as in CNC milling, for example, and on the other hand, they would have had to be declared with the letters A, B or C instead of U, which was not possible due to the G code. Originally, it was assumed that since no value is stored for extruders, they do not have any limits.

After initial tests, however, the rotation stopped at around 200°, which was also confirmed by research in the Duet Documentary forum. For the reasons mentioned, a very high value had to be assumed, so that the axis does not move up to the limit in the course of a G-code. This can be seen in Figure 46. An additional possibility would be to home the U axis several times during the code manually with G92 and thus reset the position.

```
34 ; Axis Limits
35 M208 X0 Y-25 Z0 U-9999999999999999999 S1                    ; set axis minima
36 M208 X210 Y215 Z260 U9999999999999999999 S0                 ; set axis maxima
```

Figure 46. Config.g file axis limits

4.7 Fan voltage compatibility

Since a Prusa was used as the conversion model in the Robot master's thesis, it was initially assumed that the fans would be operated with 5V voltage. By default, however, the Duet board outputs 24V, but this can be changed with a switch next to the outputs. This was not considered during the first test runs, and when the fan started running at 45°C, it immediately burnt down.

In addition to the 40x40x10mm (Declaration 4010) axial fan, the Ender 3 also has a 40x40x10 (Declaration 4010) radial fan. This was used when modifying the CR10 Max, which was also explained in chapter 3.3.2, but it was also too large and had the wrong flow orientation. Therefore, another 30x30x10mm (Declaration 3010) axial fan had to be purchased, as there was not enough space to fit a larger model to the assembly of the U-axis.

4.8 Duet 2 motherboard with old hardware setup

In order to check the correctness of the new firmware, the hardware of the ender 3 was restored to its original state before the first attempts were made with the U axis. This should also determine the print quality and the correct control of all components. The assembly and wiring are explained in the following chapters 4.8.1 below.

4.8.1 Motherboard enclosure

In order to save space and to reuse the existing components, the Duet motherboard was placed in the same position as the old motherboard. However, since it was larger than the old one, the housing had to be modified accordingly.

For this purpose, a spacer block was 3D printed for the end of the aluminium frame profile, so that the cover plate could be positioned further forward. For the

rear area of the sheet metal, clamping plates were printed, which were fixed to the aluminium profile with a screw and t nut, which can be seen in Figure 47.

Since the cables of the print bed heater were on the side of the wall, an outlet was cut, and the edge was covered with a rubber hose to prevent injury to the cable. The cables for the touch panel were threaded through the ventilation outlets and were thus also fixed.

Figure 47. Motherboard enclosure

4.8.2 Motherboard mounting

To attach the board to the housing, the dimensions of the attachment holes were taken, and the corresponding holes drilled in the sheet metal. Since the soldering points on the back of the board allow it to be laid flat, spacer sleeves were printed out of PLA through which the M3 screws could be inserted.

To fix the motherboard, TPU sleeves were printed on the front side, with a diameter of 2.8 mm, so that the screw would cut its own thread. Due to the soft material, however, the screw starts to spin in the sleeve when it reaches a certain strength, which means that it is squeezed and fixes the board but cannot damage motherboard.

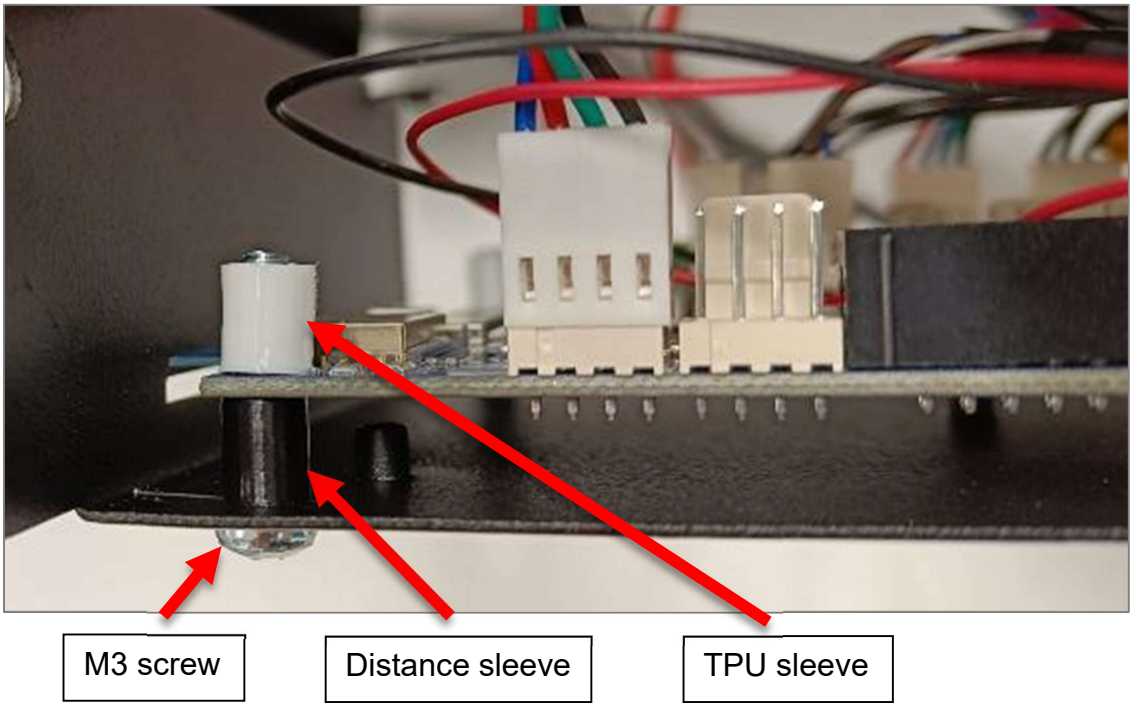

Figure 48. Motherboard mounting

4.8.3 Duet Panel housing

Since the downloaded model of the Duet Panel housing was intended for the 7-inch model and should have been mounted on a Prusa I3 MK3s+, this had to be redesigned. The panel was not attached to the side as with the RotBot, but to the place where the old control panel of the Ender 3 was located.

The corresponding dimensions were taken from the panel again, and a new housing was designed with SolidWorks. The corresponding cable outlets were placed between the base and the cover so that they could be removed at any time. In addition, a holder was constructed, which could first be screwed to the aluminium profile, and on which the housing could then be mounted, which can be seen in the following Figure 49.

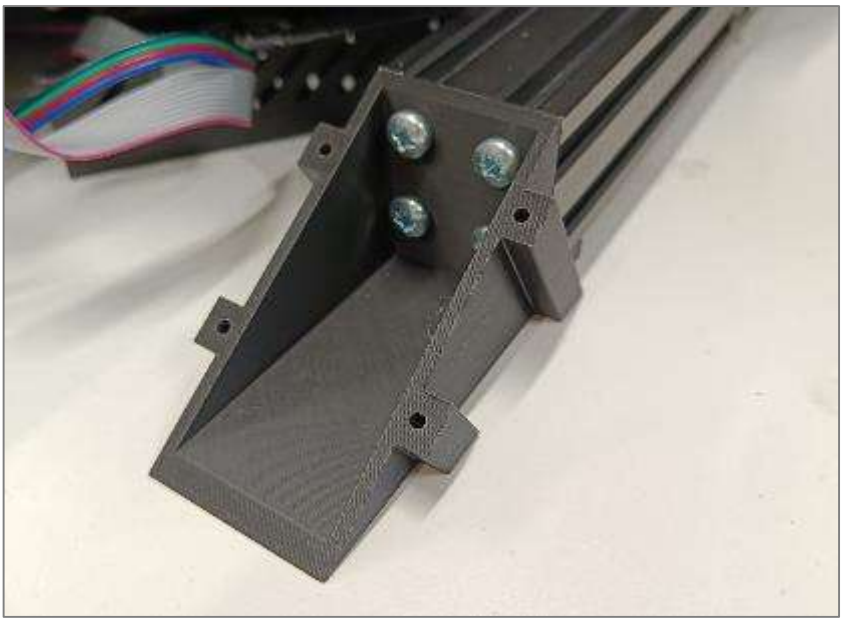

Figure 49. Duet Panel housing bracket

It was important that the lower edge of the housing rests on the floor and does not float, as this would be unpleasant to operate if the panel were to give way to the rear. Care was taken to create a comfortable angle between the display and the operator without colliding with the print bed later on due to the steep angle. The components were then 3D printed with PLA using the FDM process. This can be seen in Figure 50.

The panel itself, like the motherboard, was attached to the lid of the case using spacer sleeves between the case and the panel and soft TPU sleeves on the back. In addition, an outlet for the SD card was integrated, via which the G-code files can be transferred. The cables of the panel run directly to the motherboard, as they were too short to be integrated in the aluminium frame.

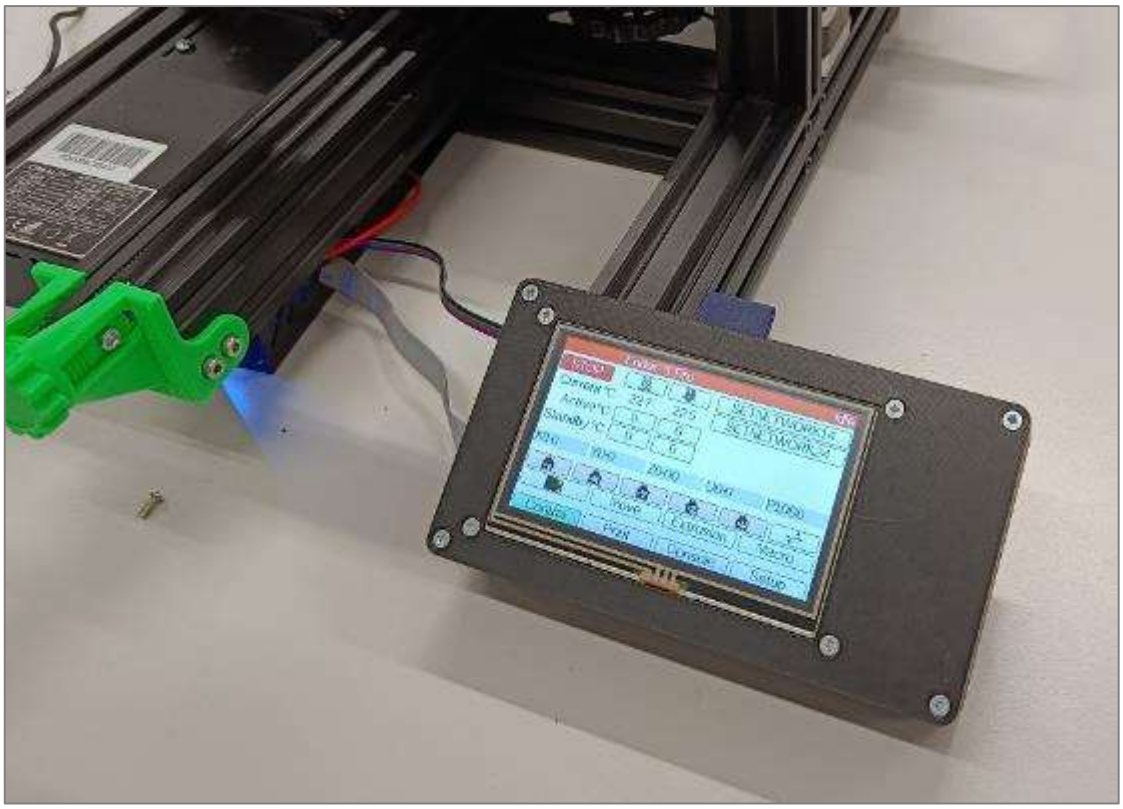

Figure 50. Duet Panel housing

4.8.4 Connecting motors and end stop switches

Since the connectors of the Creality motherboard do not fit on the Duet board, they had to be cut off and the new connectors had to be reconnected. However, the polarity of the motors had to be checked and aligned with the outputs of the motherboard.

As shown in Figure 51, the two adjacent pins on the Duet connector correspond to one pole pair. This means that pin 1 and 3 are positive poles and pins 2 and 4 are negative poles. As can be seen at the motor connector in this illustration, this sequence no longer applies. Here the two middle pins 2 and 3 are swapped because they represent the second side of the coil in the motor. This was checked with a multimeter for each motor in order to avoid short circuits and the resulting damage.

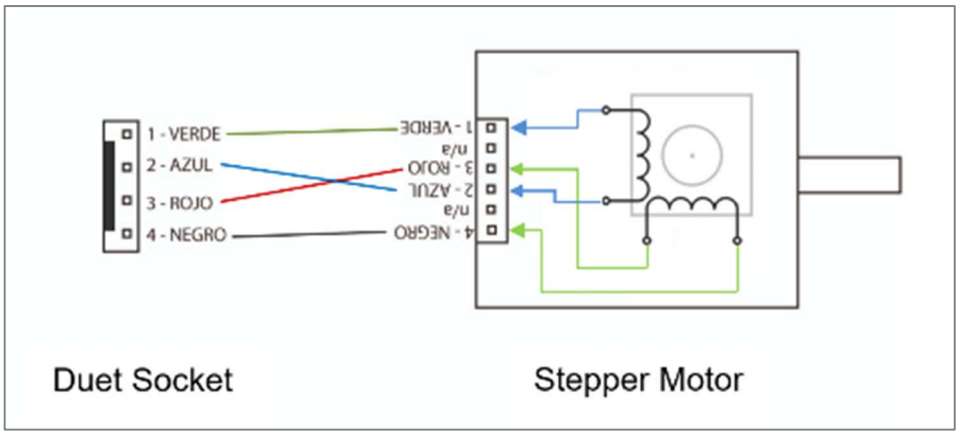

Figure 51. Motor wiring

The end switches on Creality products have two pins. This means that the motherboard checks whether the circuit is closed or not. In the case of the Duet board, however, switches with three pins were required. Here, an independent circuit is run, and as soon as the button is triggered, a separate signal is sent via the third cable, which is read by the motherboard. Therefore, all sensors had to be replaced for the time being. However, the sockets of the old switches were smaller than those of the new ones, which is why new brackets would have had to be printed, which is why the buttons were triggered manually for the home command during the first test print.

The heaters and thermistors could be connected without any further modifications, and there was no need to pay attention to the pin assignment, as only a closed circuit is required here.

4.8.5 Testing the homing command

With the motors and end switches now connected, the homing commands of the individual axes could be tested. As already mentioned, the buttons were triggered by hand, which had the advantage of being able to stop the axis early and thus avoid the motor being damaged if the button did not trigger a movement stop at the end of the axis.

After the first tests and corrections of the motor values, each of the axes could be zeroed at the corresponding end points in order to imitate the correct operation with the corresponding pressure volume. At this point, the axis limits could also be checked for correctness and the travel speeds adjusted.

4.8.6 Heater testing

After the heaters and thermistors were connected, they could also be put into operation for the first time. However, ten seconds after the first heat-up, the following error message appeared and stopped the heating process:

```
Error: Heating fault on heater 1, temperature rising much
       more slowly than expected 3.2°C/sec
```

Help was found in the Duet Documentation database. There it was described that a calibration of the heating curve is necessary for the first operation. The actual heating curve is constantly compared with the calculated heating curve. if the two values differ too much, an error message is displayed, and the heating process is stopped. Before the first calibration, this calculated heating curve is usually not correct because it is referenced to the room temperature and not to the maximum temperature of the nozzle, at which a high heating rate cannot be achieved as at room temperature. This calibration is done completely automatically with the following command:

```
M303 H1 P1 S230 ;H heater, P power, S temperature
```

This heats the corresponding heater to the defined temperature and oscillates around this value. This process can be seen in the temperature graph in Figure 52 and the individual sections of the cycle are documented in the console at the bottom of the image. The heating and cooling behaviour is recorded, and a new heating curve is calculated. In this case, the calibration of heater1 (Nozzle heater) was run through at an operating temperature of 230°C and the result was as follows:

```
Auto tuning heater 1 completed after 3 idle and 5 tuning
cycles in 655 seconds. This heater needs the following
M307 command:

 M307 H1 R2.119 K0.285:0.000 D14.13 E1.35 S1.00 B0 V24.1
```

There were no complications when heating the print bed, so calibration was not performed for this heater. The thermistor was squeezed so hard with the clamping screw during installation that the maximum value of 2000°C was output, but this was remedied after loosening the screw.

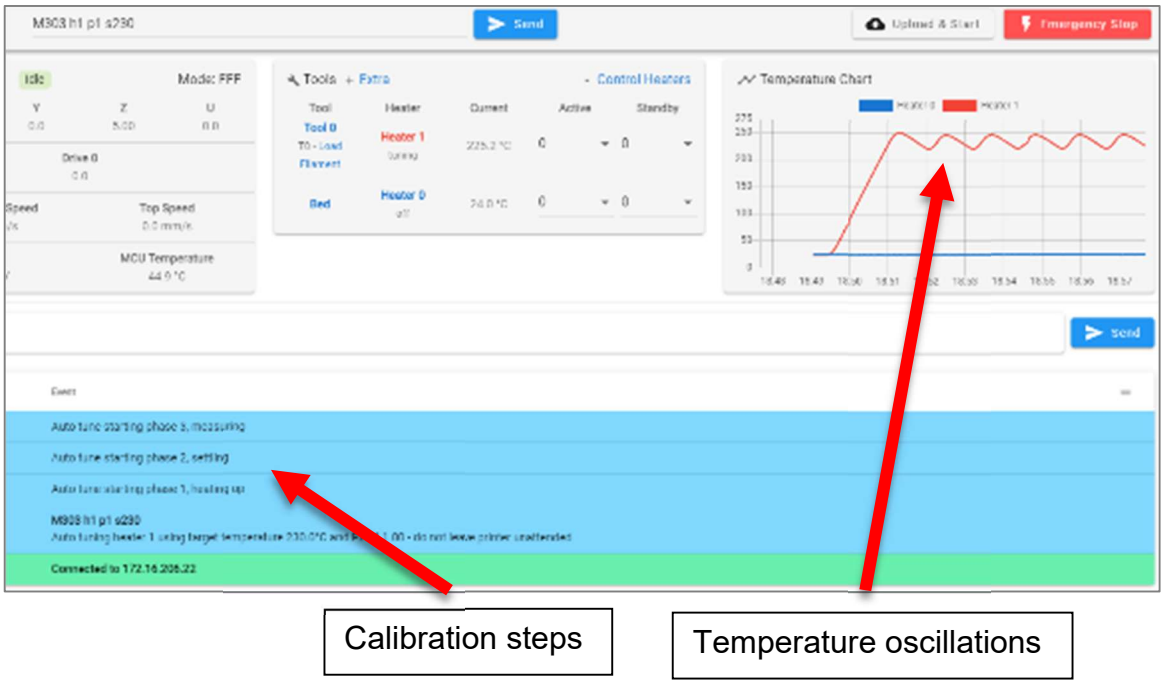

Figure 52. Heater calibration M303

4.8.7 Test print

After the first tests of all components, a first planar test print was started. This was to check the interaction of all axes, as well as the temperature of the nozzle and the extrusion movement. Without any further adjustments, a good result was achieved straight away.

Both the extrusion and the adhesion to the print bed met the expectations. As can be seen in Figure 53, the accuracy of the letters was also achieved on all axes, only the orientation of the individual layers to each other was somewhat inaccurate, which could have been eliminated by fine-tuning.

Since this test only focused on the function and not on the quality of the print itself, any unattractive features did not play a decisive role and the conversion to a non-planar setup could be started.

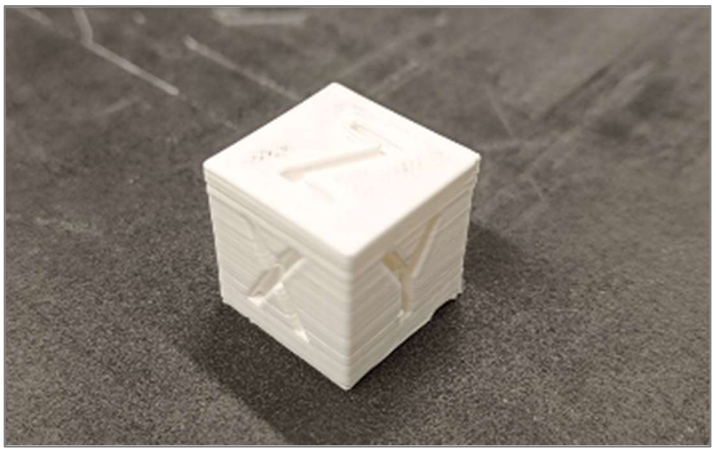

Figure 53. Planar test print with the Duet motherboard

4.9 Trinamic motion control (TMC) sensor less homing

Before the U-axis could be implemented, the endstop switches were replaced by the so-called sensor less homing. The respective axis is zeroed via the motor currents. When the respective axis arrives at the end of the travel path, the load of the motor increases, which also increases the motor current. If a value is defined that may not be exceeded, the end position can be defined without a sensor.

This type of homing has the advantage that no sensor is required, which is why, on the one hand, no extra sensor holders had to be printed and, on the other hand, no attention had to be paid to the geometries of the installed parts, which could otherwise trigger the sensor prematurely.

This could only be implemented for the X and Y axis. On the Z axis, the nozzle would press in the print bed if you moved in the negative direction. If the homing command were to be executed in the positive direction, for example upwards, the spindle would cause the frame profile of the X axis to be misaligned. In the long run, this would lead to inaccuracies or even a collision with the print bed.

4.10 U axis test run

In this section, the implementation of the u axis hardware is described in more detail. The software for this has already been stored as explained in chapter 4.6 and has now been adjusted to interact with the motor and sensor accordingly. Again, dry tests were carried out in the individual intermediate steps to prevent damage to the motor or sensor.

4.10.1 Define steps per unit

To control a stepper motor correctly, the steps per unit must first be defined. As shown in Figure 41, no units are specified for moving the individual axes, as these only represent the defined conversion value.

In the case of the linear axes X, Y and Z, one unit corresponds to one mm of travel. This can be calculated via the linear movement of the belt to the required angle of rotation of the deflection roller, which results from the diameter. The required angle of rotation is calculated with the following formula, in which the arc length is assumed to be 1 mm (travel length of the axis) and the radius of the deflection roller is 6.3 mm:

$$\varphi = \frac{s}{r} \rightarrow \varphi = \frac{1[mm]}{6.3[mm]} = 9{,}09[°] \equiv 1\ [mm] \qquad (1)$$

If you now know the angle of a single step, you can calculate back to the value step/mm. With a number of 200 steps per complete revolution and 16 micro steps per complete step, the following total number of steps per revolution is calculated:

$$200\ \left[\frac{steps}{360°}\right] * 16\left[\frac{micro\ steps}{steps}\right] = 3200\left[\frac{microsteps}{360°}\right] \qquad (2)$$

$$3200\left[\frac{microsteps}{360°}\right] = 8,\dot{8}\left[\frac{microsteps}{°}\right] \qquad (3)$$

If you multiply the two values, you get the number of steps per millimetre travelled:

$$9{,}09[°] * 8,\dot{8}\left[\frac{microsteps}{°}\right] = 80\ \left[\frac{microsteps}{mm}\right] \qquad (4)$$

This value can also be seen in Figure 54 for the X, Y and Z axes. Since only the number of steps per one degree of rotation angle is required for the U axis, this could be taken directly from formula 3. This results in a value of 8.8 steps/degree, which was also entered in the config file, as can be seen in Figure 54.

```
26 M350 X16 Y16 Z16 E16 U16 I1                          ; configure microstepping with interpolation
27 M92 X80.00 Y80.00 Z400.00 E93.00 U8.88888888888888   ; set steps per mm or steps/turn
```

Figure 54. config.g steps per unit definition

4.10.2 Inductive Ranging (IR) sensor implementation

Since the U-axis had to be able to rotate completely freely, no limit switch could be installed here, as this would otherwise engage with every rotation. Instead, an inductive sensor, which is used in the Prusa i3 MkS3+ for axis homing, was used.

To do this, the sensor slot for the U-axis on the Duet board first had to be enabled. In addition, the type of sensor had to be stored here, as it would otherwise be stored as a limit switch. The activation is again done via the config.g file, in which the pin is activated with the following command:

```
M574 U1 S1 P”e1stop” ;U axis, S sensor type, P pin name
```

You can see that the pin here is named e1, which can still be traced back to the original naming of the Duet board. In addition, the Z end stop was defined at the same time, as this was not yet enabled at that time, which can be seen in line 43 of Figure 55. The same scheme was used as for the U axis.

```
41 M574 U1 S1 P"e1stop"                 ; configure endstop for U via pin e1stop
42 M915 X Y S3 R0 F0                    ; configure stall detection
43 M574 Z1 S1 P"!zstop"                 ; configure endstop for low end on Z via pin zstop
```

Figure 55. Enable U and Z endstop pin

In order to check the pin and the sensor itself for correct operation, the Object Models menu was made visible in the DWS under Plugins. In this menu, all components and connections and their respective states are visible. In Figure XX, the end stop of the U axis is defined under sensors → endstops → 3. The number three results from Z=0, Y=1, X=2 and U=E1=3, whereby U was defined as extruder 1 and thus takes its place. In the following illustration Figure 56, under

sensor 3 is the point trigger listed, which by default has a false value. In order to test whether the end stop really worked, the sensor was held against a metallic object, whereupon this value changed to true and thus confirmed the correct functioning.

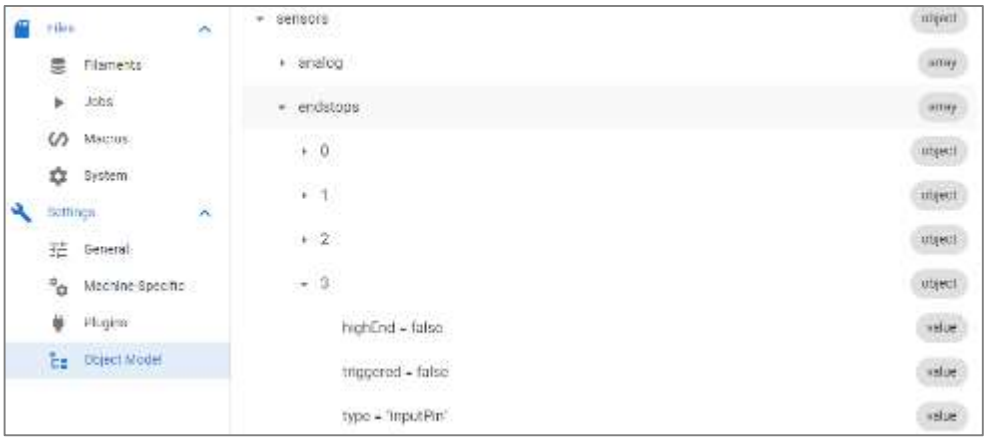

Figure 56. DWS Object Model endstop 3

4.10.3 Testing the homing command

After the dry tests, the interaction between the individual components as well as between the hard and software was checked again in the form of the homing command. On the one hand, attention was paid to whether the 400° angle of rotation was being travelled as specified in the homeu.g file, and thus whether the steps per angle corresponded to the correct value, as well as the motor stop when the sensor was triggered.
In order to be able to determine the angle precisely, a flag was mounted on the axis of the motor with adhesive tape to obtain a better overview of the movements, which can also be seen in Figure 57.
In addition to the homing command, a 360° angle was also entered via the dashboard, as this is easier to read than the 400° angle, in order to obtain final certainty about the correctness.

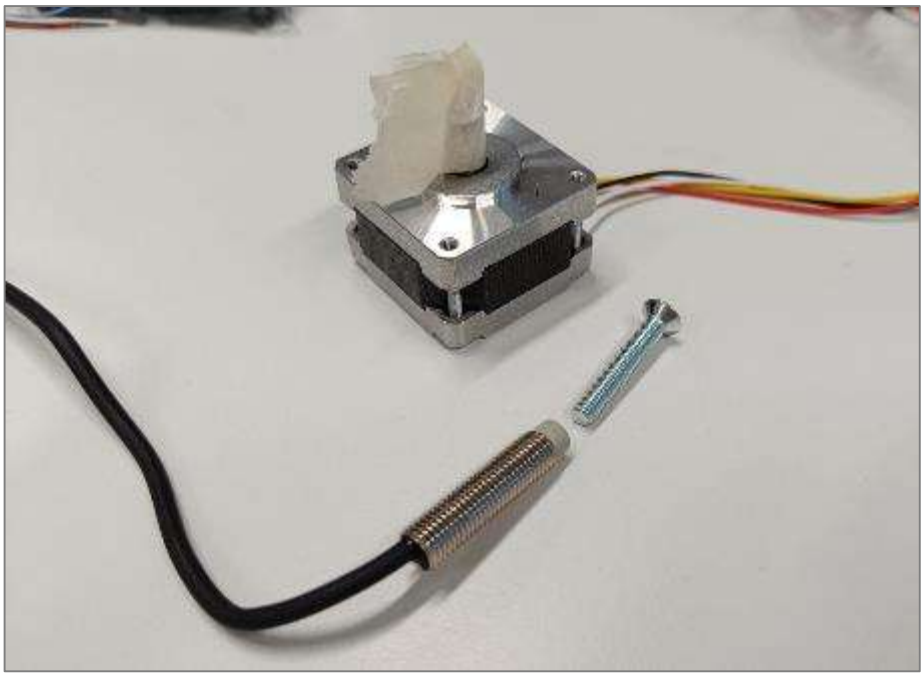

Figure 57. U axis test

4.11 Second Z axis drive

It became clear very early on in the project that the construction of the rotation axis would be very heavy. The Ender 3, on the other hand, has a Bowden kit as standard, which is why the weight of the carriage on the X-axis is very low. For this reason, only a single driven Z-axis is installed in this model and not two, as is the case with the Prusa i3 MkS3+.

The combination of high weight and one-sided drive was therefore considered very critical, which is why an upgrade kit was purchased for the Ender 3. This implements a second Z motor with spindle without much effort, so that heavier weights and inaccuracies due to the connection of the X axis profile were no longer a problem.

To achieve this, the power supply unit first had to be repositioned, as shown in Figure 58, as it is bolted directly to the vertical frame profile in the original. The motor with the spindle was then placed and fixed in this position. In principle, the duet board has the option of connecting the two Z motors separately to the motherboard, as can be seen in Figure 37, but since this would not be possible with an Ender 3 motherboard, an additional cable is included that connects both Z axis motors to a common plug.

Since this cable saves further wiring work, the old Creality connector was simply cut off and a new Duet connector was crimped onto the end of the cable and plugged back into the same place. The power supply unit was moved further back with the sheet metal supplied, so that it does not collide with the X-axis profile.

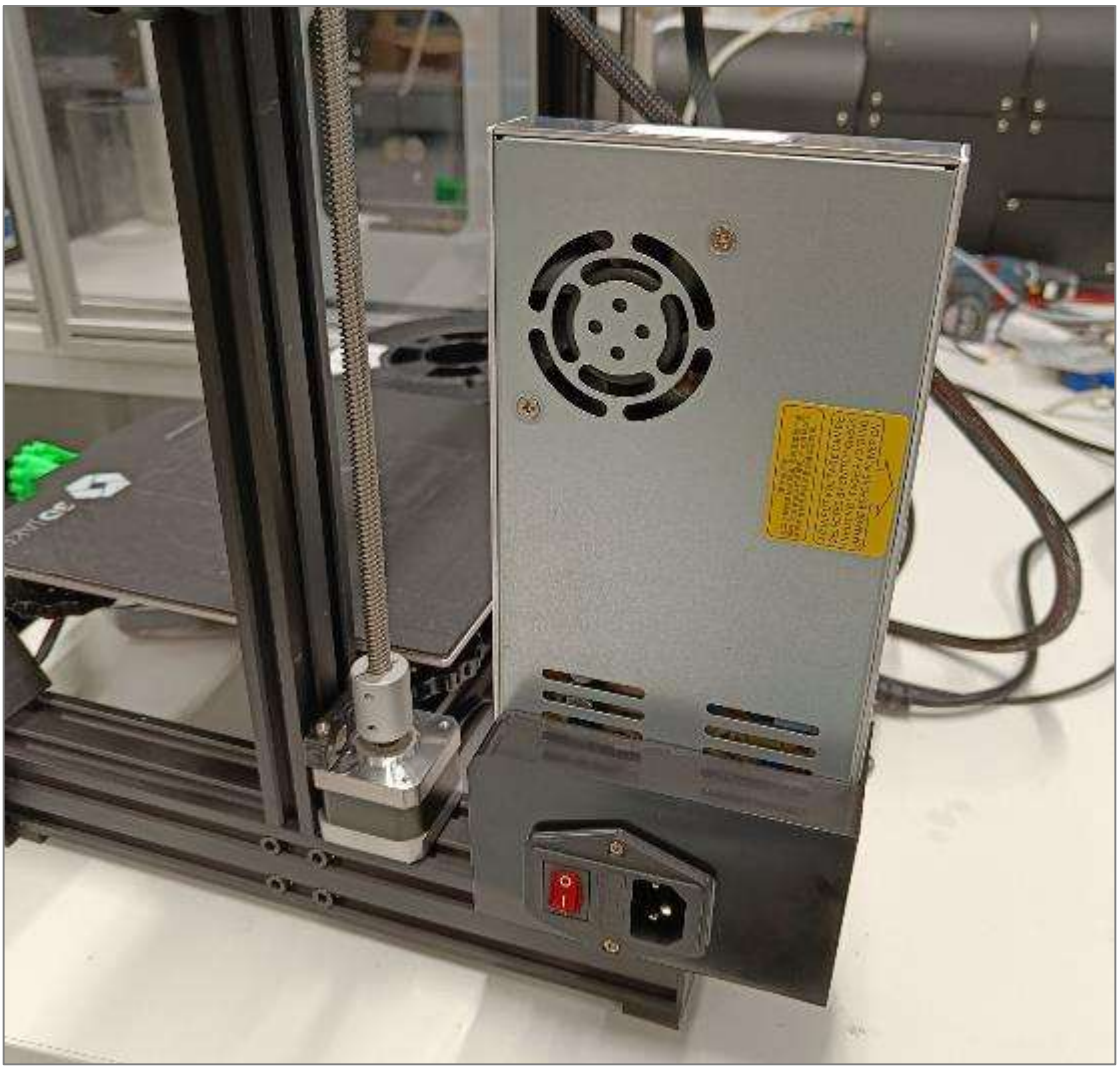

Figure 58. Implementation of a second Z axis motor

4.12 U axis components and assembly

This section deals with the components of the rotating axis and how they work together. The production methods and the individual assembly steps are discussed, as well as the changes that had to be made during the installation.

4.12.1 3D print brackets and fan shrouds

The models from the RotBot master's thesis could not be taken over directly. The main part, on which all components are screwed, is basically intended to hold the Prusa, which does not have a carriage with V rollers but with two sliding rods. Therefore, the mounting points had to be redesigned, taking into account that the entire axle can still be removed after assembly. This component was printed from PETG to achieve high strength and to prevent bending in the component due to the high weight.

The fan brackets, which are clamped directly to the heatsink, were printed using the SLS process. This was necessary because these components come into contact with the high temperatures at the heatsink itself and, above all, the mounting of the component fan, whose ducts run around the hotend, is exposed to the highest temperatures. Since in principle ASA could also be printed with this printer, this would mean that the hotend would be heated up to almost 300°C, and there would only be around 2-3mm of air in between for insulation, whereupon the shroud would either soften or even melt. The corresponding components and their composition are shown in Figure 59.

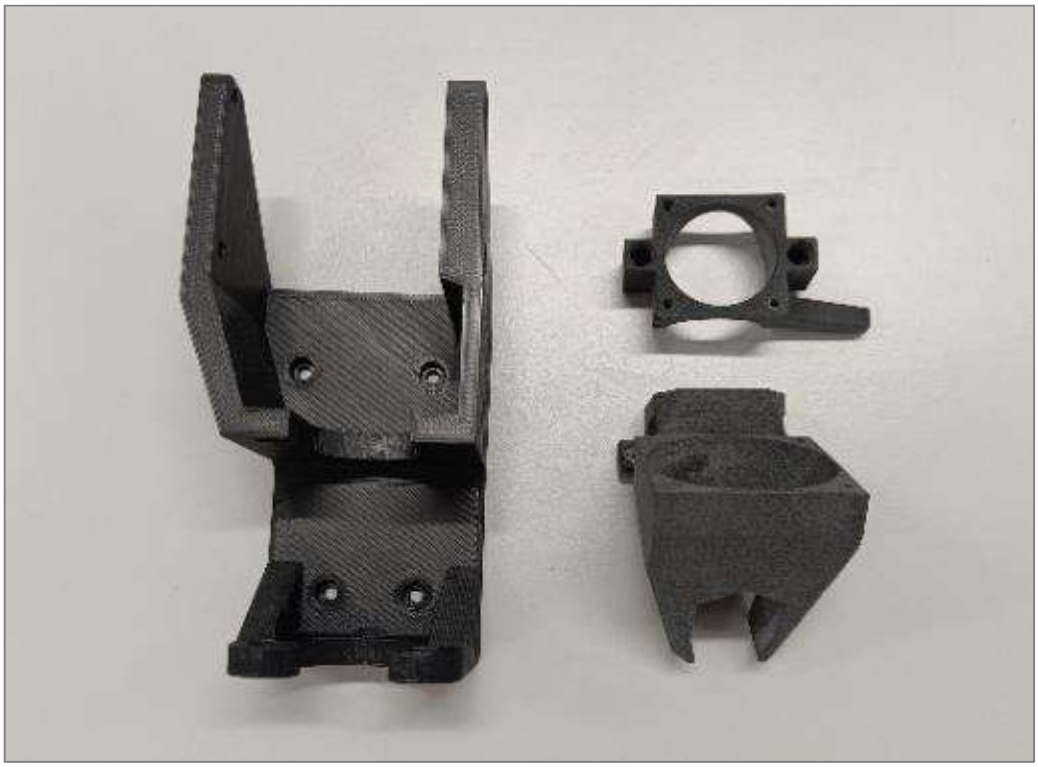

Figure 59. 3D printed U axis parts

4.12.2 Tube reaming and folding

The hollow shaft was manufactured on a lathe. A tube with an outer diameter of Ø5 mm and an inner diameter of Ø4.5 mm was purchased in advance. The outer diameter is determined by the coupling that connects the shaft and the motor. The inner diameter, however, had to be expanded to Ø4.75 mm.

To do this, the tube was first cut to the required length of 105 mm and then reamed with a reamer with a diameter of Ø4.7. This accuracy was sufficient for this value, as only the PTFE hose must be able to be pushed through. These dimensions can also be found in the drawing in appendix 5.

Furthermore, however, a deviation from the original was made in that a rebate was added to the lower end of the tube. This allowed the tube to be clamped together in the heatsink with the heat break and thus made twist-proof. The following Figure 60 shows how the rebate was made with the tailstock.

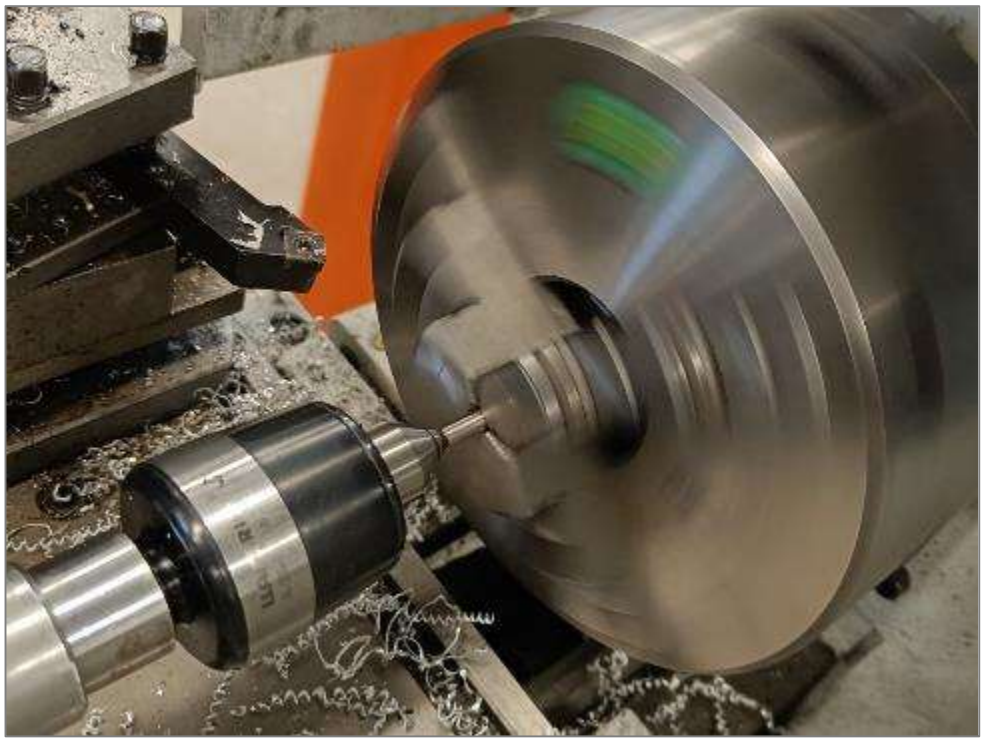

Figure 60. Manufacturing the rebate of the U axis pipe

4.12.3 Nozzle and heatsink modification

Both the nozzle and the heatsink had to be individually adapted; the corresponding production drawings are also provided in appendix 3 for the heatsink and appendix 4 for the nozzle. The differences between the original components and the modified ones are shown in the picture, with the original part on the left and the modified part on the right.

The heatsink was first cut off directly at the shoulder with a metal saw and then turned planar with the lathe. After that, layer by layer was removed in tenths of a millimetre steps, thus slowly approaching the total length of 32 mm. In addition, the hole along the axis of rotation was drilled out to 5mm so that the hollow shaft could be inserted through it.

Since the university's lathe was defective at this point in the project, the nozzle could no longer be manufactured on it. Therefore, as an emergency solution, the nozzle was first cut off with a metal saw and then clamped in a drill press. There, the tip was ground off with a file at high speed, which was possible due to the soft composition of the brass. The rear side and the rearmost part of the thread were also ground off, as there was no thread run out in the hole provided in the hotend and it could therefore not be cut to its full depth. This method of finishing led to inaccuracies, which negatively affected the result.

Figure 61. Modified nozzle (left) and heatsink (right)

4.12.4 Hotend CNC milling

The nozzle of this printer is at an angle of 45°, which made the use of a standard nozzle simply impossible and had to be specially manufactured. Since the hotend is a component with very small but deep holes, and the corresponding tolerances are very precise here, this component had to be CNC milled. Since this was not possible in-house, contact was made with the neighbouring vocational school, which agreed to manufacture it. Again, the production drawing can be seen in appendix 2.

The main problem with this part was the 1.7 mm hole, which was 25 mm deep. This ratio of diameter to depth makes accurate drilling very difficult, as such a drill quickly runs out of true. This should also have coincided well with the second hole from the back of the hotend, as the molten filament is pushed through this, and any inaccuracy is a problem point in the flow. However, the result was not entirely satisfactory and extrusion problems were to follow later. The finished part is shown in Figure 62.

Figure 62. CNC milled hotend

4.12.5 U axis assembly

At this point, the U axis could be assembled. This was also done according to the RotBot diagram, the drawing of which can be found in the appendix 1. The assembly of the entire axis and the individual components are labelled in Figure 63.

First the rotation motor was screwed into the anchorage, as it is located in the middle of the axis and cannot be reassembled later. The next component was the Hemera extruder, which is screwed into the top of the bracket over the sides. It was always important to shorten the screws so that they would not damage the housing, which was also marked with stickers.

The rotating part, consisting of the hollow shaft, PTFE hose, slipring, heatsink and heartbreak, was assembled in advance and inserted from below together with the coupling. The slipring had to be fixed to the 3D housing and the coupling had to be butt clamped to both the shaft and the motor. Finally, only the fan shroud duo had to be mounted.

The hotend was not installed at this stage because of the thermistor and the heating rod, nor were the fans themselves. These first had to be soldered to the cables of the slipring and for this reason were not fixed for easier handling.

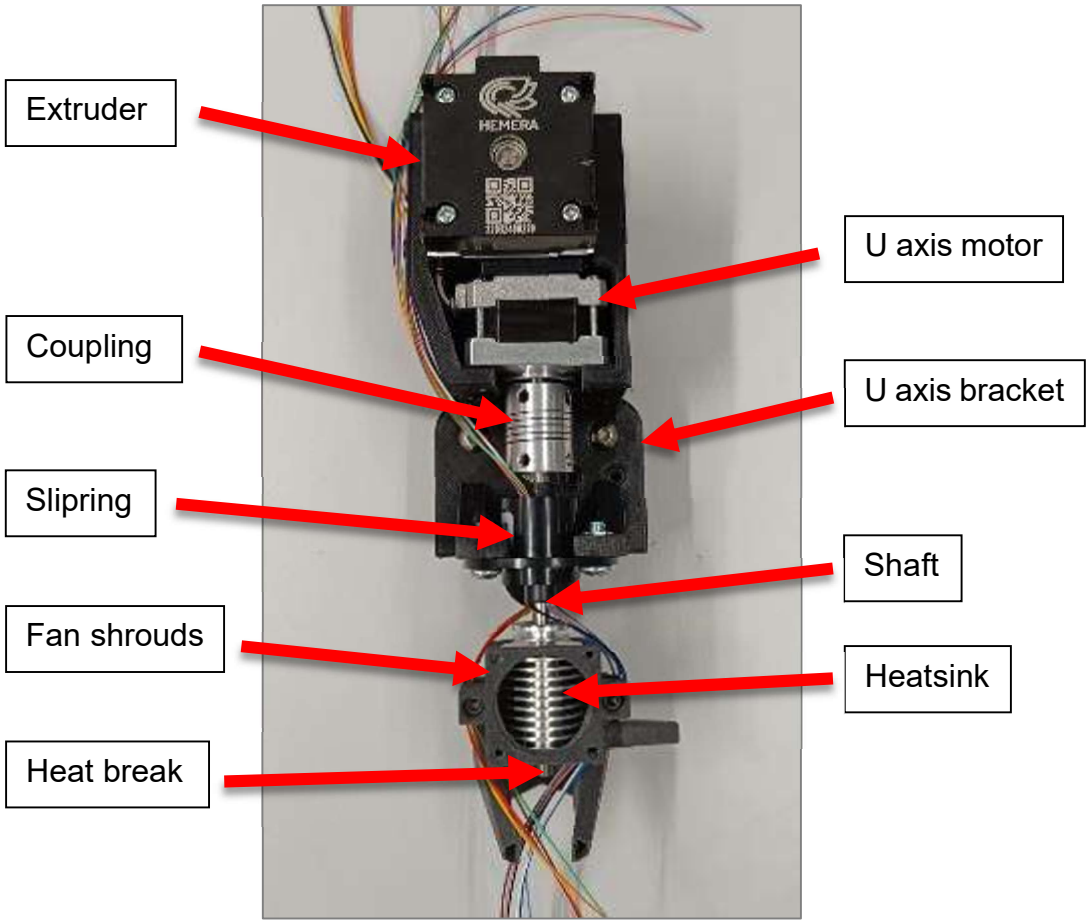

Figure 63. U axis assembly

4.12.6 Wiring

In the last step, all electrical components had to be soldered to the cables of the slipring so that they could pass on the signal without twisting. To do this, each component was held at the corresponding position and the length of the cable was marked to ensure that as little excess cable as possible was left. This can be seen in Figure 64. This could otherwise get caught on the frame or even with the 3D print during the rotational movement and tear out later. In addition, care was taken to ensure that several connection points were not directly next to each other. In order to be able to assign the colour coding to the respective components during the wiring on the back, a list was created in which it was documented which phase was soldered to which cable of the slipring.

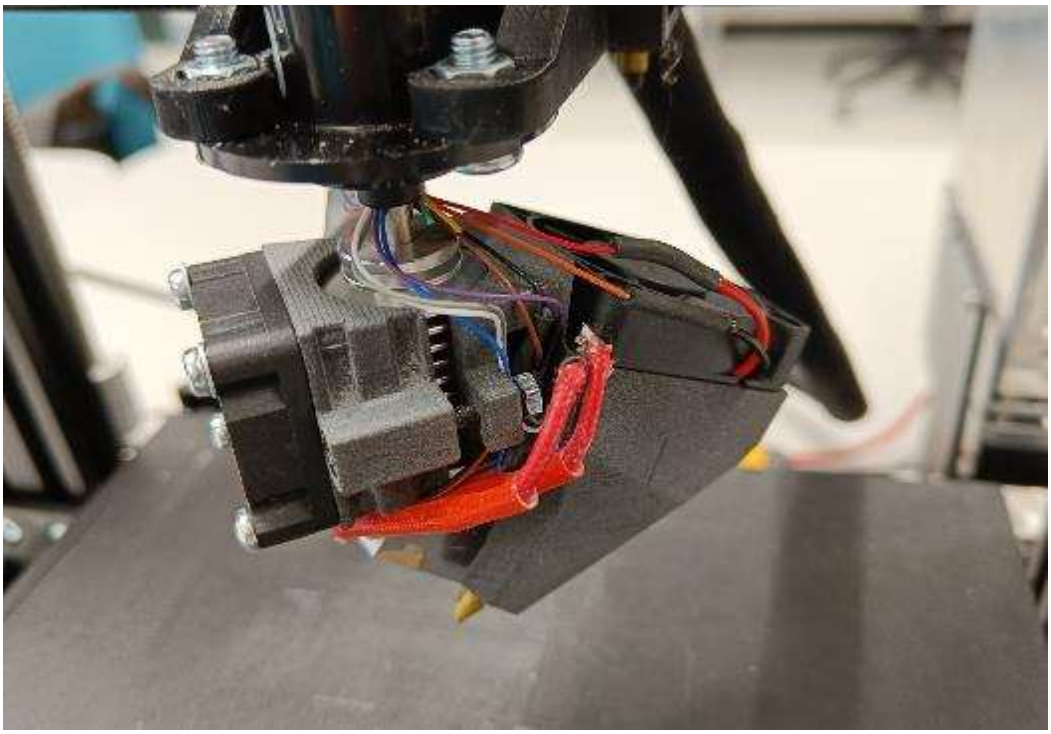

Figure 64. Printhead wiring

On the other side of the slipring, the cables that run directly to the motherboard were only connected via clamps and not soldered. This meant that the entire print head could still be removed and disconnected from the printer as soon as the clamps were removed, which would not have been possible with soldered connections.

The cables, together with the extruder and u axis motor cable, were then wrapped in a hose to bind them together and therefore prevent them from tangling up with the print bed. In addition, the entire strand is stiffened by the bundling and thus has more stability and also looks more visually appealing, which can be seen in Figure 65. The cables of the Z-axis motors and those of the U and Z-axis end stops were routed separately, as they could not travel alongside the X-axis carriage.

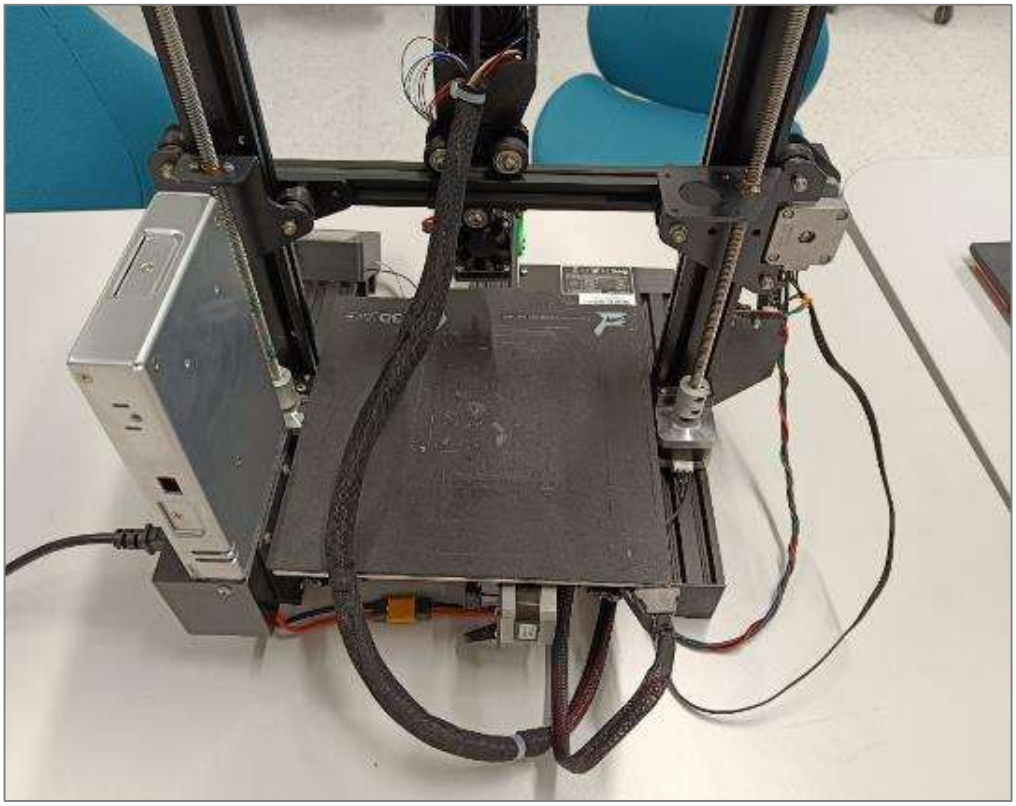

Figure 65. Cable hose on the printer backside

4.12.7 Z and U axis endstop repositioning

Due to the geometry of the printhead, the end stop of the Z axis had to be adapted. For this purpose, the dimensions resulting from the zeroing of the X and Z axes were taken and a corresponding holder for the sensors was constructed.

The design for the U-axis sensor was originally intended for the Prusa i3 and could therefore not be used on the Ender 3, as there is no space on the back of the trolley on this model. This meant that the sensor could not move flexibly with the X axis but had to be fixed to the frame of the printer. Additionally, it had to be taken into account that the part fan is further away from the axis of rotation than

the metal pin that triggers the sensor. Therefore, the sensor had to be directed parallel to the U axis in order to prevent a collision with the fan, which made the design more difficult. The described mounting for the sensors can be seen in Figure 66.

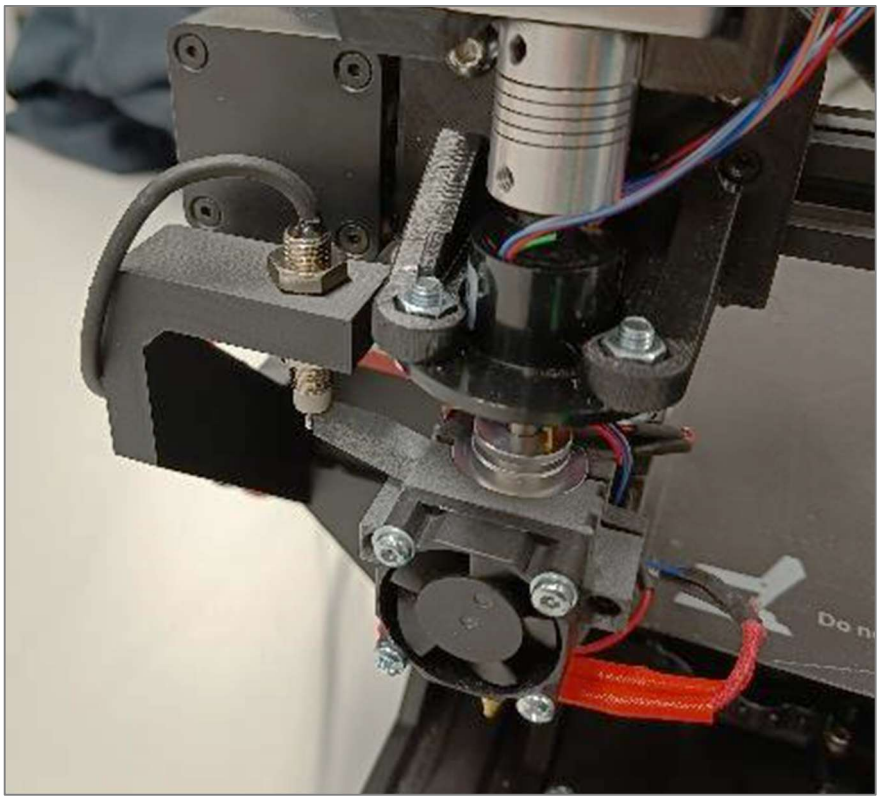

Figure 66. U axis home sensor

4.13 Homing rework

Due to the repositioning of the Z and U sensors, the corresponding homing commands also had to be adapted. For this purpose, a new receptacle was constructed, which was screwed onto the holes of the old axle sensor. This meant that further work on the frame itself could be avoided. The corresponding component was 3D printed using the FDM process.

4.13.1 Z axis homing

To avoid later collisions with the print bed, the Z axis sensor was placed below the print bed level. This required that the print bed was not in that position at the time of the homing command. To guarantee this, a sequence of home commands was implemented in the homez.g file. The sequence is as follows :

```
1) Y axis home

2) Y axis moves all the way back

3) Z axis home

4) Z axis moves up again

5) Y axis moves forward again.
```

Because the Y axis first zeroes and then moves backwards, enough space is freed up at the front for the entire extruder head to move below the printing plane, where the Z axis gets homed. Then the Z axis moves back above the print bed, whereupon the Y axis can move back to its original position. The corresponding sequence is shown in the homez.g file in the appendix.

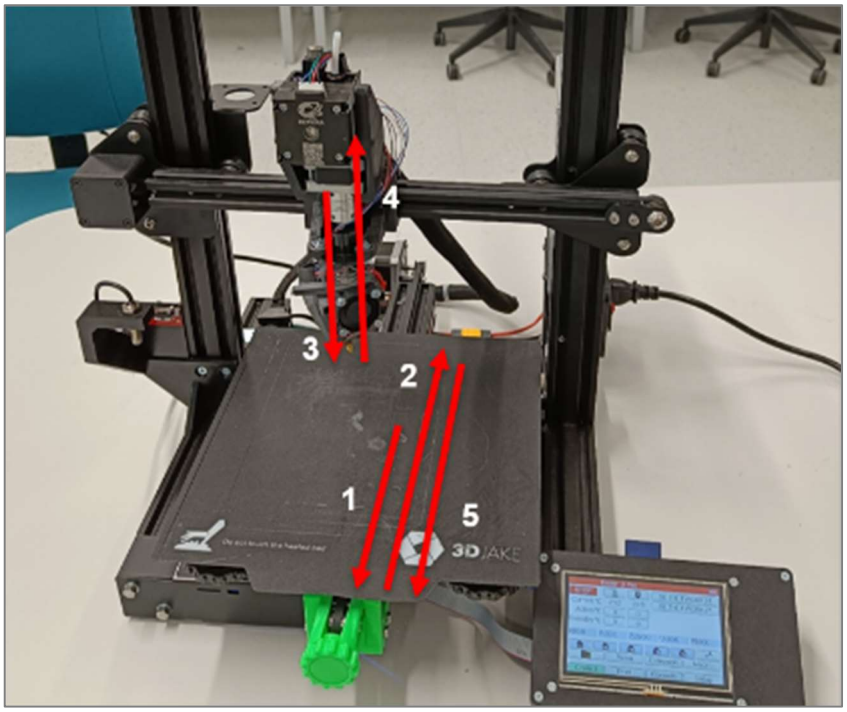

Figure 67. Z axis homing sequence

4.13.2 U axis homing

For the U-axis, the sensor was placed in such a way that the same sequence could be adopted and only the homing of the X and U axes were added at the end, which were already explained in chapter 584.6.2 and in Figure 45 in more detail. This results in the following workflow:

1) Y axis home

2) Y axis moves all the way back

3) Z axis home

4) X axis home

5) U axis home

6) X axis moves back to the middle

7) Z axis moves up again

8) Y axis moves forward again.

The corresponding sequence is again shown in Figure 68, and the corresponding code of the homeu.g file can be found in the appendix.

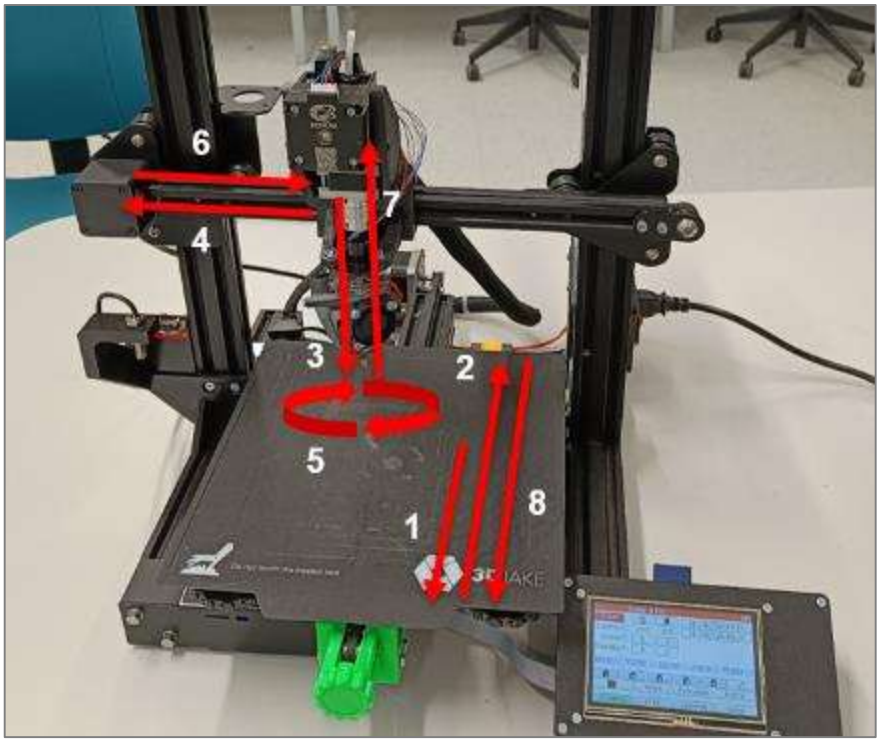

Figure 68. U axis homing sequence

Since all four movable axes were already homed in one run in this workflow, this sequence could also be used for the homeall.g file. This is usually retrieved before each print and checks the position of all the axes.

4.14 Conical slicing process

The function of the slicing process has already been explained in the theoretical section of this paper, so in this chapter only the individual steps have been gone through, which are also given in the slicer manual.

In the first step, a CAD test object was created which was to be both cylindrical and have an overhang in order to test the functionality of supportless printing. For this purpose, only a smaller and a larger cylinder were placed on top of each other in order to keep the model as simple as possible despite these requirements. The CAD model is shown in Figure 69. The STL file was saved in the project folder specified by the Python script so that it could access the file without any problems.

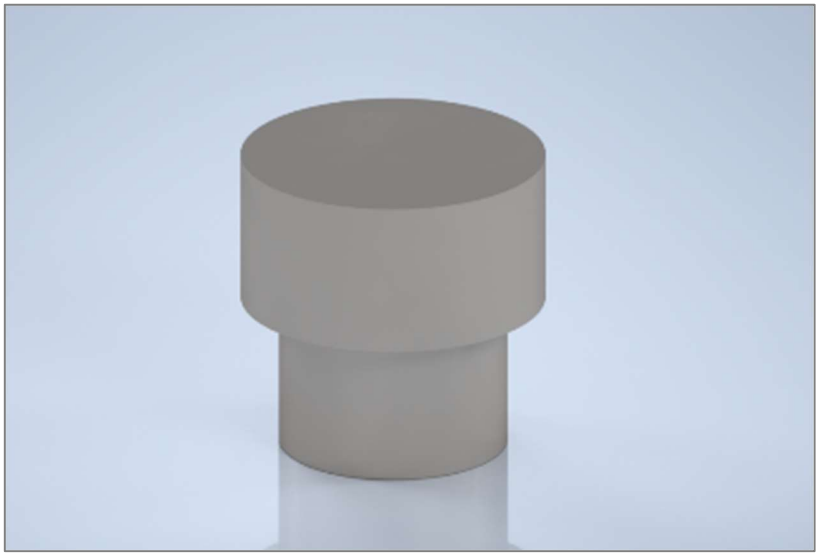

Figure 69. Conical slicing CAD model

This was warped along the axis in the first step, the transformation step, with the first Python script. Figure 70 already shows that the model was not deformed around the axis of rotation, but this axis was placed at the imaginary corner of a cube surrounding the cylinder. This meant that the model was not rotationally symmetrically deformed, which led to an error in the slicing process. This error could only be corrected to a limited extent. Since this offset error of the axis did not occur with every STL model, it was difficult to identify the problem, which would also have required in-depth Python knowledge.

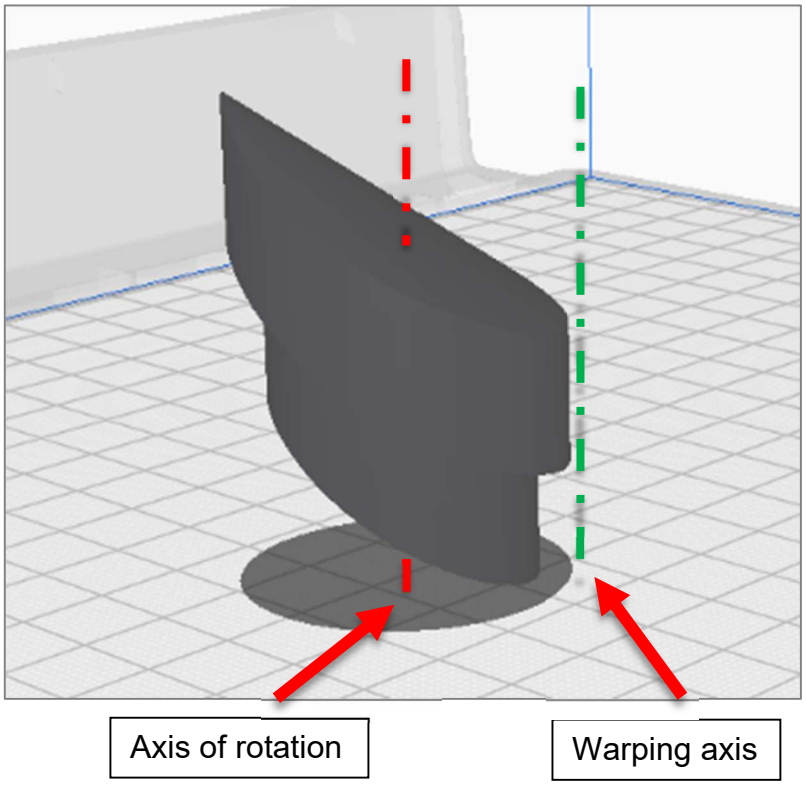

Figure 70. Conical slicing warping step

For the reasons just mentioned, only the testing process was continued in order to also test the reverse transformation of the G-code. For this purpose, the model that had just been deformed was sliced with the open-source slicer Ultimaker Cura 5.1.1. An infill of 100% was assumed, as hollow spaces would otherwise be reproduced in the form of empty layers, and this would have posed a problem during extrusion. Furthermore, the thickness of the top and bottom layers was set to 0mm, and the option of a support construction and print bed adhesion was deselected.

This slice was then saved again in the form of a G-code in the corresponding project folder. In the last step, the reverse transformation python code accessed this. In the input area of the code, small changes such as the positioning of the model could be specified before it transformed the paths of the G-code back into the form of the original model.

The result could be loaded into Cura in the form of another G-code and thus evaluated. As can be seen in Figure 71, the appropriate axis was not selected for the second transformation. As a result, the component was curved in two

dimensions at this point. Although the shape is similar to that of the initial model, the paths do not give the desired result. In this application, this should be seen in the form of horizontal rings that run at a 45° angle in the inner direction of the axis.

The G-code was transferred to the printer for the first tests and the first few movements were checked. However, in order to test the correctness of the interaction of all axes, a simple and short G-code was written in the form of a spiral, in which the X and Y axes perform a circular movement, and the U axis simultaneously adjusts the angle, which gave the final confirmation of the functionality of the setup.

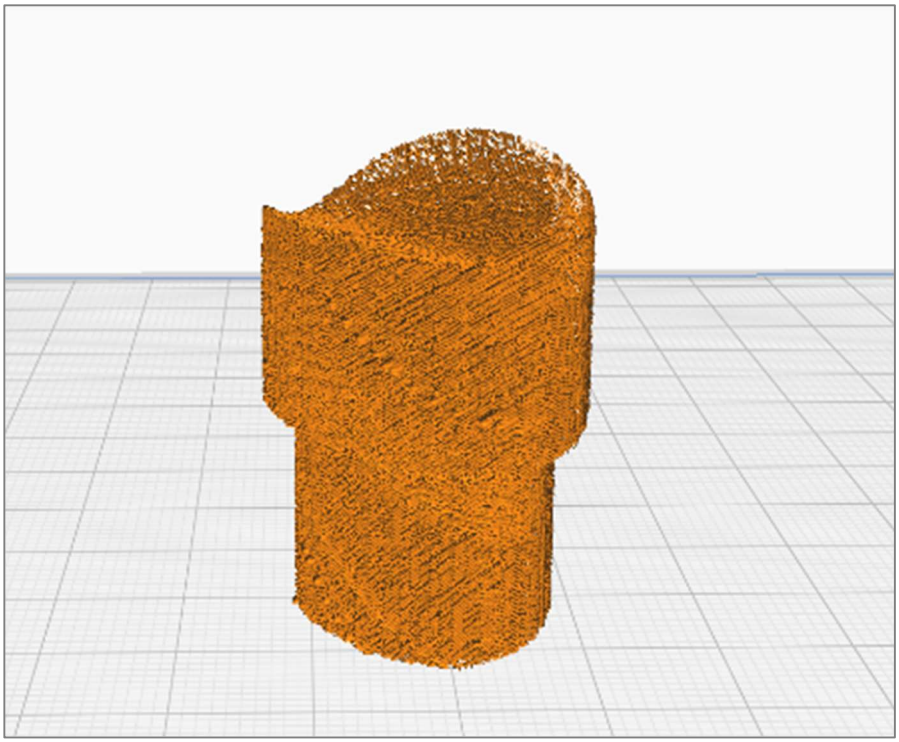

Figure 71. Conically cut G-code

5 NON-PLANAR PRINTING WITH STOCKNOZZLE

5.1 Set up Windows Subsystem Linux (WSL)

The open-source slicer software Slic3r is a Linux-based application. It is necessary to integrate Linux into Windows in the form of a subsystem. In principle, there are two ways of doing this: on the one hand, a virtual box can be created which simulates another operating system on a computer, and on the other hand, there is the option of enabling this in the form of a subsystem as a separate drive. Since Windows 10 version 19041 and higher, such a subsystem is already stored under the name Ubuntu and can be installed and executed via the Windows PowerShell. The following command was used for this:

```
wsl --install
```

Thus, in addition to the standardised drives, an additional drive "Linux" is created with the folder "Ubuntu", which has the Linux folder structure and no longer that of Windows. Again, note that data and folders cannot simply be moved between this drive and all other Windows drives; this topic is discussed in more detail in Chapter 5.3. The folder path for this drive and the folders it contains is as follows:

```
\\wsl.localhost\Ubuntu
```

Detailed installation instructions and further information can be found on the following Microsoft Learn page:

```
https://learn.microsoft.com/en-us/windows/wsl/install
```

5.2 Install and start Slic3r

The next step is to install the slicer software with the following instructions given by the GitHub installation guide:

```
https://github.com/Zip-o-mat/Slic3r/tree/Non-planar
```

Before installing the slicer software, the Linux installation commands needed by the slicer software have to be updated. These can be done with the following APT-get (Advanced Package Tool) command which is shown here:

```
sudo apt-get install build-essential libgtk2.0-dev lib-
wxgtk3.0-gtk3-dev libwx-perl libmodule-build-perl git
cpanminus libextutils-cppguess-perl libboost-all-dev
libxmu-dev liblocal-lib-perl wx-common libopengl-perl
libwx-glcanvas-perl libtbb-dev libxmu-dev freeglut3-dev
libwxgtk-media3.0-gtk3-dev libboost-thread-dev libboost-
system-dev libboost-filesystem-dev libcurl4-openssl-dev
libextutils-makemaker-cpanfile-perl
```

Afterwards, the data package on GitHub can be accessed:

```
https://github.com/Zip-o-mat/Slic3r.git
```

The folder was changed with the command change directory (cd):

```
cd Slic3r
```

The correct download and localisation can be checked at last:

```
git checkout Non-planar
```

In the next step, the downloaded perl files are executed in order to install the slicer. First, a data package is exported:

```
export LDLOADLIBS=-lstdc++
```

In this step, the perl file is executed and the first installation step is completed:

```
perl Build.PL
```

The second step is to install the graphical user interface (GUI):

```
perl Build.PL --gui
```

Now the Slic3r software can be started:

```
perl slic3r.pl
```

In some cases, it can happen that an environment variable cannot be found or has an incorrect value:

```
*Fatal Error: wxGLCanvas is only supported on X11 cur-
rently.  You may be able to work around this by setting
environment variable GDK_BACKEND=x11 before starting your
program. Segmentation fault
```

This environment variable can either be set permanently in the system or worked around within the session using the export command:

```
export GDK_BACKEND=x11
```

5.3 Copy data from Windows to Linux

Since in most cases the STL files needed for slicing are created with Windows-compatible programs, they are not compatible with the Linux drive. This means that data cannot simply be copied and moved between the Linux and Windows operating systems. However, it is possible to use the mount (mnt) command to convert files and move them between the two drives with the given origin path and the file name:

```
sudo cp /mnt/c/Users/kyle/Documents/linuxtest.txt .
```

This works in both directions, from Windows to Linux and vice versa. However, since the resulting G-code of the slicer is often copied to a USB stick or SD card that is inserted into a 3D printer, conversion is no longer necessary. This is because USB sticks are FAT32 (File Allocation Table 32GB) formatted and thus make it possible to exchange data between different operating systems. This is a hardware alternative to the mount command just mentioned.

5.4 Store printer dimensions and geometries

When the application is started for the first time, the user will be asked to enter the dimensions of the nozzle and the printhead. This is due to the fact, already explained in chapter 2.5.4, that the distances limit the maximum print angle. Furthermore, standard dimensions such as print bed size and filament diameter are also requested.

After the initial input window, the STL file can now be imported and aligned via the main menu. By default, the model is positioned at the coordinate origin. Under the Settings tab, print, filament, and printer settings can be selected to define more precise properties.

The "Non-planar layers" settings menu played a particularly important role in this project, as it allows the Non-planar option to be activated and the frame conditions such as maximum angle and minimum Non-planar area to be defined, thus having a significant influence on the slice result. This menu can be seen in Figure 72. Non-planar layers settingsFigure 72. Under "Horizontal layers", the number of top layers can be determined in order to find the appropriate number of top layers for the respective surface. There is also the possibility of implementing planar adaptive slicing, but this only led to minor changes and errors in the slicing process, so further attempts were left out.

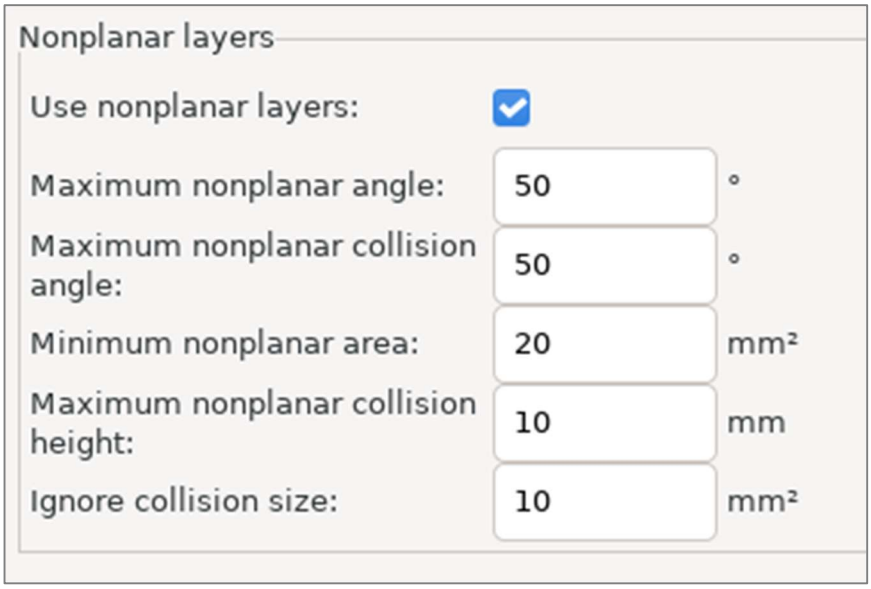

Figure 72. Non-planar layers settings

5.5 Non-planar slicing

Within the framework of this project, the "Non-planar 3D printing Test" model published by TeachingTech on Thingiverse was used as the test model, which has a low crash potential due to its low gradients and was therefore ideally suited for the first test. The model can be found under the following link:

https://www.thingiverse.com/thing:3842477

In order to obtain comparable results, several tests were printed with a different number of non-planar top layers in order to determine how the number of layers affects the print quality, the lowest value being 3 layers. During slicing, the outer wall layers are printed with the previously set thickness before the Non-planar layers are inserted as a kind of infill into this layer. This can be seen in Figure 73, where the vertical shell is shown in yellow and the non-planar top layers in red.

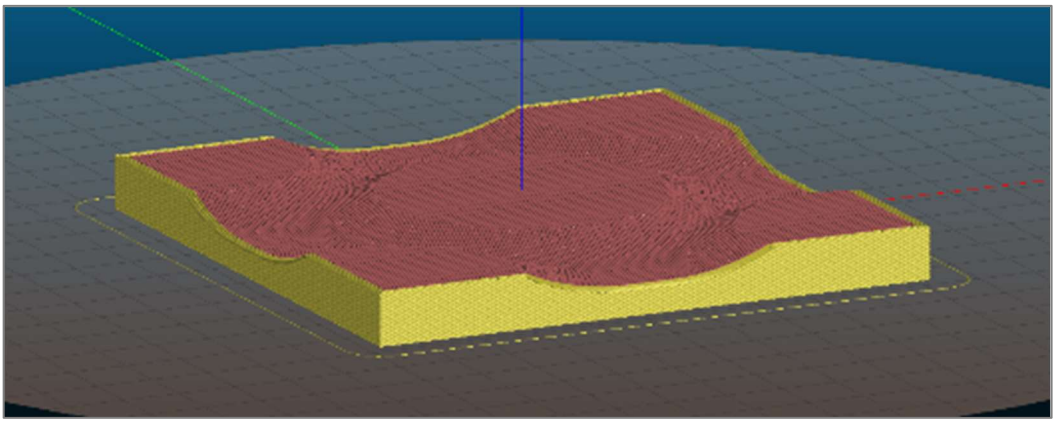

Figure 73. Test model sliced with Slic3r software

Other main print settings have been defined as:

- Layer height: 0,15mm
- Vertical shells perimeters: 3 (minimum)
- Horizontal shell: Top: 3,7 & 12 / Bottom 3
- Infill density: 20%
- Fill pattern: Stars

5.6 Print result

Figure 74 shows the print results with the different numbers of topcoats. All tests were printed on a Creality Ender 3 in order to minimise the risk of potential external errors and to obtain comparable results. The filament used here was PLA in Silver from Extrudr.

Test A is an ordinary planar print, therefore the stepping effect is visible especially in the plateau intermediate areas and are visible in this model in the form of rings. The planar plateaus itself are completely smooth. The positive and negative quality aspects of this printing process are clearly visible here.

Test B shows the first print with non-planar top layers, where only three top layers were chosen. It is obvious here that due to the low infill density and the low number of top layers, the bridged cavities resulted in a very low surface quality, which led to a very unclean result overall. In addition, the roll layers broke out or were not properly connected to the top layers.

Test C now shows the variant with 7 top players. The indentations between the cavities have completely disappeared here and the planar surfaces are also completely flat. It is evident that the surface itself is very rough, which is probably due to a lower extrusion in these layers. This serves to prevent over-extrusion on steeper surfaces and collisions later on.

Test D is the last attempt in the series with 12 top layers. No significant quality improvements are apparent. It can therefore be concluded that too many top layers have already been chosen, as they take up more time and material and therefore become inefficient.

In general, it can be said that the optimal number of final layers depends on the infill density and the infill pattern. These two factors determine the cavities that have to be bridged and can lead to an undesirable result. In order to make a more precise statement about this relationship and the influence of the individual aspects, further experiments would be necessary, but are not within the scope of this work.

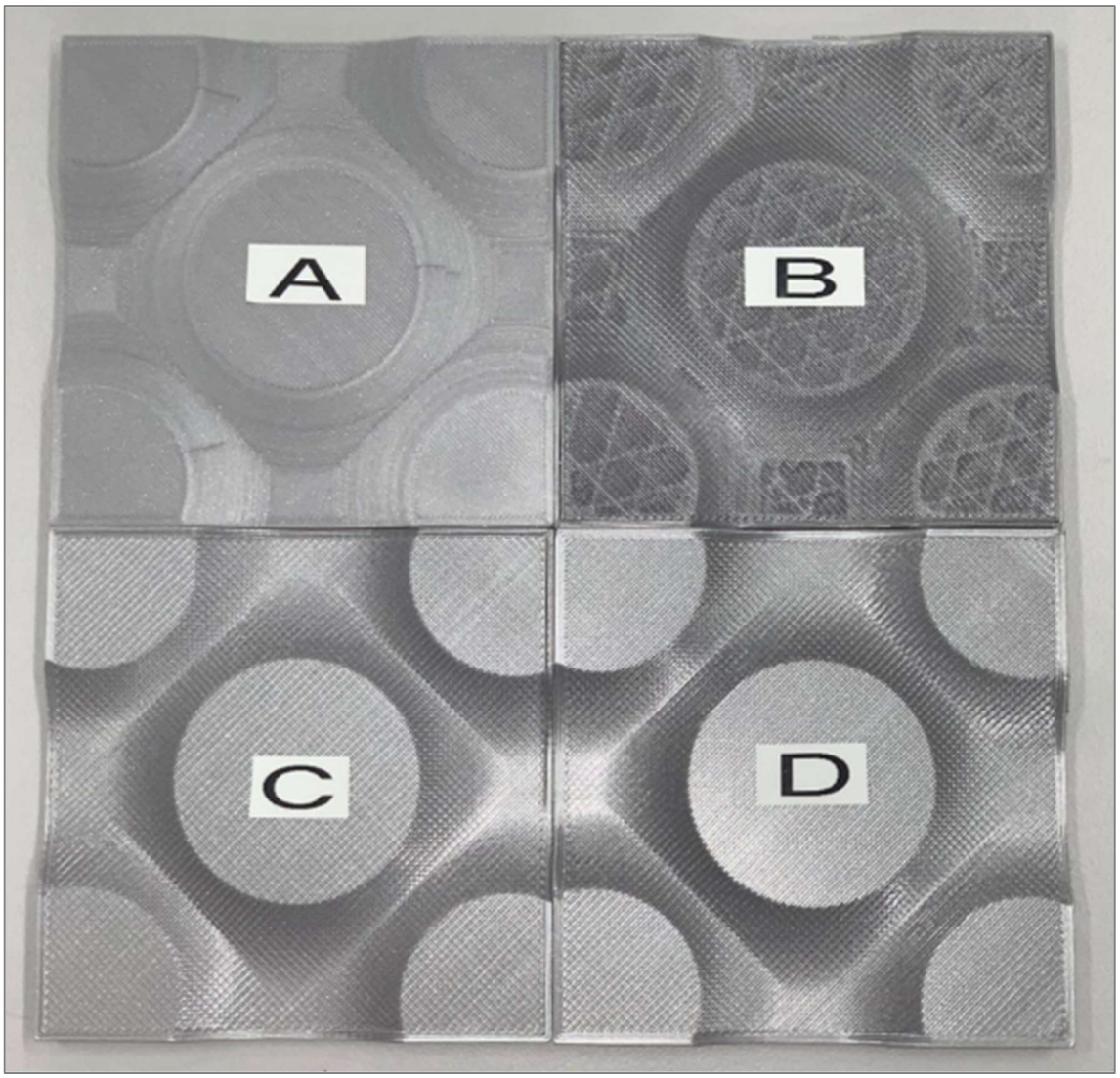

Figure 74. Printing results of a standart planar print (A), with 3 non-planar top layers (B), with 7 non-planar top layers (C) and with 12 non-planar top layers (D)

6 CONCLUSION

6.1 Creality CR10 Max modification

As already briefly mentioned in chapter 3.4, significant improvements were achieved in the subsequent test prints after the modification. A clear improvement in the accuracy of long travels was achieved, which confirms the functionality of the linear rails. In addition, these also increased the stiffness, especially in the area of the X axis, which was not as distinctive in the old setup. Due to the soft composition of the V rollers and the hard aluminium base on which they run, abrasion could be detected quite clearly.

On the one hand, this contaminates the V slot, in which the belt also runs, which absorbs the plastic particles and wears it out more quickly together with the pulley. On the other hand, this abrasion on the rollers means that the entire carriage sinks in the Z direction, which had to be compensated for by regular calibration. This is no longer the case with the rail system and therefore represents a very low-maintenance and long-lasting solution.

The direct extruder enables results with more quality than before even at high speeds of 60 mm/s. However, large-area or very small, detailed objects are often very unclean and look fused. Another problem was the adhesion to the print bed, which could not be consistently achieved at higher speeds. This was particularly evident in the form of warping. However, it may be said that improvements could be achieved throughout all disciplines.

6.2 Fourth axis implementation

Generating the G-code to move the four-axis printer proved to be very difficult and the corresponding problems could not be completely solved within the scope of this work. However, initial tests with self-generated sequences delivered correct motion sequences. The construction and implementation of the axis can therefore be considered successful both in the area of software and in the interaction with motors, heating elements and sensors.

The extrusion of the melted filament caused difficulties. On the one hand, the holes in the hotend were not precise enough, and on the other hand, the self-made nozzle did not meet the required tolerances. As a result, the filament not only oozed through the nozzle tip, but also through the thread of the nozzle and also that of the heat break. This led to a pressure loss which is why no correct strand could be extruded due to under extrusion.

In addition, the alignment of the PTFE hose in the area of the extruder proved to be difficult. This was due to the inaccuracy of the individual components, which meant that they were not exactly aligned with each other, and the fact that the filament is supplied on rolls, which means that it has a corresponding curvature. The combination of a straight filament guide and curved filament often led to the filament getting stuck at the transition from the extruder to the PTFE and having to be helped by hand.

For the reasons mentioned above, it was not possible to start a complete test print, but the motion sequences reflect the correct functioning of the system.

6.3 Non-planar printing with stock nozzle

The method of non-planar printing with a standard nozzle could be implemented with very little effort. The software effort was manageable and delivered convincing results.

The test prints showed that the surface quality is mainly dependent on the combination of surface inclination, infill density and the number of top layers. Therefore, a higher infill density had to be selected on average than would have been the case with normal planar prints.

Due to the surface inclination, under-extrusion is necessary in the non-planar region, which leads to the fact that the top layer is not consistently connected to the outer wall and has led to separation in this area.

Despite the poorly developed process, no problems were detected during the slicing process itself. Only the slicer itself crashed from time to time, but this had no influence on the print result itself.

7 DISCUSSION

7.1 Creality CR10 Max modification

After the conversion, it can be clearly stated that clear improvements can be achieved through appropriate modifications. Since the CR10 Max is a large-area FDM printer and therefore objects with large dimensions are printed that are not feasible on other printers, the axis accuracy over long distances plays a major role here.

This was ensured by the linear rails and is therefore a key component. In addition, the associated rigidity makes it possible to mount a direct extruder, as this would have been a problem for the old roller system due to the increased weight. The direct extruder itself solved the stringing problem, which is often the cause of component collisions, as poor extrusion often leads to lumping.

The problem of component overheating is probably due to the smaller component fan. This does not manage to supply sufficient air via the flow channels and ensure the associated cooling effect. One possibility would be to install the same fan with a larger thickness or a second small fan on the opposite side of the print head to increase the cooling capacity.

Such conversion kits must also always be considered from an economic point of view. In the case of the CR10 Max conversion, the costs amounted to around 40% of the purchase price of the printer. As this represents a significant portion of the total price, such modifications should always be considered when purchasing the printer, as a model with a higher initial price and no modifications can still save costs in the long run due to durability.

7.2 Fourth axis implementation

The implementation of a rotating axle in an existing three-axle system requires a lot of resources, on the one hand a broad knowledge pool and the corresponding time are essential components to achieve such a conversion, on the other hand financial as well as technical and software skills are not irrelevant.

The existing advantage of such a set-up is, as already explained, support-free printing, but this is not universally applicable. In addition, such a rotary axis cannot be installed on every printer without further modification, since, as with an Ender 3, the one-sided drive of the Z-axis is not sufficient to perform precise movements. Furthermore, due to the construction volume of the print head, printing volume is also lost. Although this is only the case in the Z direction with the Ender 3 model, it is also limited in the X direction with other printers such as the Prusa i3 Mk3S+.

The design of the conical slice process is also not user-friendly, as it was developed as part of a research project and is therefore not easy to use. In addition, there are no detailed instructions or manuals that could help.

The components needed to realise an unlimited rotary axis are also difficult to obtain and often involve long shipping times, which should be taken into account in projects with time constraints.

7.3 Non-planar printing with stock nozzle

Non-planar slicing with a standard nozzle offers the possibility of sealing flat surfaces for a low effort. In addition, it is possible to switch between planar FDM printing and non-planar printing without any conversions, as the only difference here is the slicing process.

it is important to differentiate between two aspects. If a smooth, closed surface is desired, then the usual planar printing is still suitable. If, however, more value is placed on the contour of the top layer, this process offers the optimal possibility to implement this. Since the non-planar layers have to be printed with under extrusion, the result is a rough surface that resembles that of a textile fabric. Thus, not only the composition of the top layer is different, but also its structure. This process can be implemented by any user and thus offers an optimal solution with which 3D printing stands out.

8 REFERENCES

Ahlers, D. 2018. 3D Printing of Nonplanar Layers for Smooth Surface Generation. Accessed on 20 March 2023 https://tams.informatik.uni-hamburg.de/publications/2018/MSc_Daniel_Ahlers.pdf.

Ahmed, W., Alabdouli, H., Alqaydi, H., Mansour Aya, Khawaha, H. A. & Jassmi, H. A. 2020. Open Source 3D Printer: A Case Study. Accessed on 8 March 2023 http://www.ieomsociety.org/ieom2020/papers/865.pdf.

Alexandra, 2021. 3D printer parts: Understanding the purpose of each component. Accessed on 31 March 2023 https://www.bcn3d.com/3d-printer-parts-understanding-the-purpose-of-each-component/.

Learn Circuit Rocks, 2021. Auto Bed Level Sensors for FDM Printers. Accessed on 20 March 2023 https://learn.circuit.rocks/auto-bed-level-sensors-for-fdm-printers.

Birail Motors, 2021. Linear Rails and Linear Rods: Which One Is Better? - Birail Motors. Accessed on 20 March 2023 https://birailmotors.com/linear-rails-and-linear-rods-which-one-is-better/.

Braam, D. 2017. Understanding firmware. Accessed on 16 April 2023 https://ultimaker.com/learn/understanding-firmware.

Bruère, V. M., Lion, A., Holtmannspötter, J. & Johlitz, M. 2022. Under-extrusion challenges for elastic filaments: the influence of moisture on additive manufacturing, pp. 445–452. DOI: 10.1007/s40964-022-00300-y.

Carolo, L., 2020. The Best 3D Printer Nozzle Types, Sizes & Materials. Accessed on 31 March 2023 https://all3dp.com/2/3d-printer-nozzle-size-material-what-to-know-which-to-buy/.

Carrier, P., 2016. Comparison between temperature sensors used in 3D printers – Part 1. Accessed on 31 March 2023 https://dyzedesign.com/2016/06/temperature-sensors-used-3d-printers-part-1/.

Duet3D Documentation Duet3D, 2022. Wiring your Duet 2 mainboard. Accessed on 29 April 2023 https://docs.duet3d.com/en/How_to_guides/Wiring_your_Duet_2.

Dwamena, M., 2023. How to Flash & Upgrade 3D Printer Firmware – Simple Guide. Accessed on 16 April 2023 https://3dprinterly.com/how-to-flash-3d-printer-firmware/.

Etienne, J., Ray, N., Panozzo, D., Hornus, S., Wang & C. L. Charlie, Martinez, Jonas. CurviSlicer: slightly curved slicing for 3-axis printers: ACM Transactions on Graphics: Vol 38, No 4. Accessed on 19 March 2023 https://dl-acm-org.ez.lapinamk.fi/doi/10.1145/3306346.3323022.

Florian, D., 2023. How to Build a 3D Printer: Firmwares. Accessed on 16 April 2023 https://www.drdflo.com/pages/Guides/How-to-Build-a-3D-Printer/Firmware.html.

Inther Software Development, 2020. “Oh, we have a 3D printer in the office” or FDM printing basics. Accessed on 17 March 2023 https://isd-soft.com/tech_blog/oh-3d-printer-office-fdm-printing-basics/.

Introduction to Fused Filament Fabrication (FFF) 3D printing technology. Accessed on 18 March 2023 https://www.bcn3d.com/documents/White_Paper_BCN3D-Introduction_to_Fused_Filament_Fabrication_FFF_3D_Printing_technology.pdf.

Jess Koeniguer, 2023. How Stepper Motors Provide Precision Control | Clippard Knowledgebase. Accessed on 17 March 2023 https://www.clippard.com/cms/wiki/how-stepper-motors-provide-precision-control.

Kalpesh, T., Nihal, P., Sanket Patole, Sanket Ruikar, Mr. A.B. Sutar & Ms. Sudeshana Sawrate. 2021. 915_47.Fabrication_of_3D_component_manufacturing_system_based_on_FDM_Technique. Accessed on 20 March 2023 http://www.ijasret.com/VolumeArticles/FullTextPDF/915_47.Fabrication_of_3D_component_manufacturing_system_based_on_FDM_Technique.pdf.

Kywoo, 3. 2021. V slot Wheels VS Linear Rails, Which one is a better option. Accessed on 16 April 2023 https://www.kywoo3d.com/blogs/3d-printer-news/v-slot-wheels-vs-linear-rails.

Leapfrog 3D Printers, 2019. 3D Printing Concepts and 3D Printer Parts - Leapfrog 3D Printers. Accessed on 30 March 2023 https://www.lpfrg.com/guides/3d-printing-concepts-and-3d-printer-parts/.

Lim, S., Buswell, R. A., Valentine, P. J., Piker, D., Austin, S. A. K. & Xavier de. 2016. Modelling curved-layered printing paths for fabricating large-scale construction components. DOI: 10.1016/j.addma.2016.06.004.

Liu, J., Gaynor, A. T., Chen, S., Kang, Z., Suresh, K., Takezawa, A., Li, L., Kato, J., Tang, J., Wang, C. C. L., Cheng, L., Liang, X. & To, A. C. 2018. Current and

future trends in topology optimization for additive manufacturing, pp. 2457–2483. DOI: 10.1007/s00158-018-1994-3.

Marlatt, S., 2022. Bowden Tube: Pros & Cons, Best Options, and More. Accessed on 31 March 2023 https://all3dp.com/2/bowden-tube-all-you-need-to-know/.

Mwema, Fredrick, Madaraka Akinlabi & Esther Titilayo. Basics of Fused Deposition Modelling (FDM), pp. 1–15. DOI: 10.1007/978-3-030-48259-6_1.

Nayyeri, P., Zareinia, K. & Bougherara, H. 2022. Planar and nonplanar slicing algorithms for fused deposition modeling technology: a critical review, pp. 2785–2810. DOI: 10.1007/s00170-021-08347-x.

Nisja, G. A., Cao, A. & Gao, C. 2021. Short review of nonplanar fused deposition modeling printing, e221. DOI: 10.1002/mdp2.221.

O'connell, J. 2021. Non-Planar 3D Printing: All You Need to Know, *All3DP*, 31 January [Online] https://all3dp.com/2/non-planar-3d-printing-simply-explained/. Accessed on 16 April 2023.

Ömer, E. & Mehmet, A. 2021. Non-Planar Toolpath for large scale additive manufacturing. Accessed on 21 March 2023. DOI: 10.46519/ij3dptdi.956313.

Peko, I., Špar, I. & Basic, A. 2016. Rapid Prototyping of Mechanical Measurement Level Device https://www.researchgate.net/publication/308367161_Rapid_Prototyping_of_Mechanical_Measurement_Level_Device.

Printables.com, 2023. 4-axis modification for MK3s with rotational printing head von Mich | Kostenloses STL-Modell herunterladen | Printables.com. Accessed on 3 May 2023 https://www.printables.com/de/model/288723-4-axis-modification-for-mk3s-with-rotational-print/files.

Richter, A., 2023. The Anatomy of a 3D Printer: Screens | MatterHackers. Accessed on 16 April 2023 https://www.matterhackers.com/articles/3d-printer-anatomy-screens.

S. Bedi. 2016. Image Processing (IP) Assisted Tools for Pre- and Post-Processing Operation in Additive Manufacturing (AM) https://www.semanticscholar.org/paper/Image-Processing-(IP)-Assisted-Tools-for-Pre-and-in/0c3f386db9aded3549d48d1913754161f0e9de69.

2023. Sensors used in 3D Printers | FUTEK. Accessed on 20 March 2023 https://www.futek.com/applications/Sensors-Used-in-3D-Printers.

Tarun Agarwal, 2020. Stepper Motor Driver : Working Principle, Types and Its Applications. Accessed on 1 April 2023 https://www.elprocus.com/what-is-a-stepper-motor-driver-types-and-its-applications/.

Tiny Machines 3D, 2023. Linear Rail Upgrade for Creality CR-10 Max. Accessed on 1 May 2023 https://www.tinymachines3d.com/products/linear-rail-upgrade-for-creality-cr-10-max-3d-printers.

Wüthrich, M., Gubser, M., Elspass, W. J. & Jaeger, C. 2021. A Novel Slicing Strategy to Print Overhangs without Support Material, p. 8760. DOI: 10.3390/app11188760.

Wüthrich, M., Elspass, W. J., Bos, P. & Holdener, S. 2021. Novel 4-Axis 3D Printing Process to Print Overhangs Without Support Material, pp. 130–145. DOI: 10.1007/978-3-030-54334-1_10.

Appendix A - 1/3

Print head: sectional view

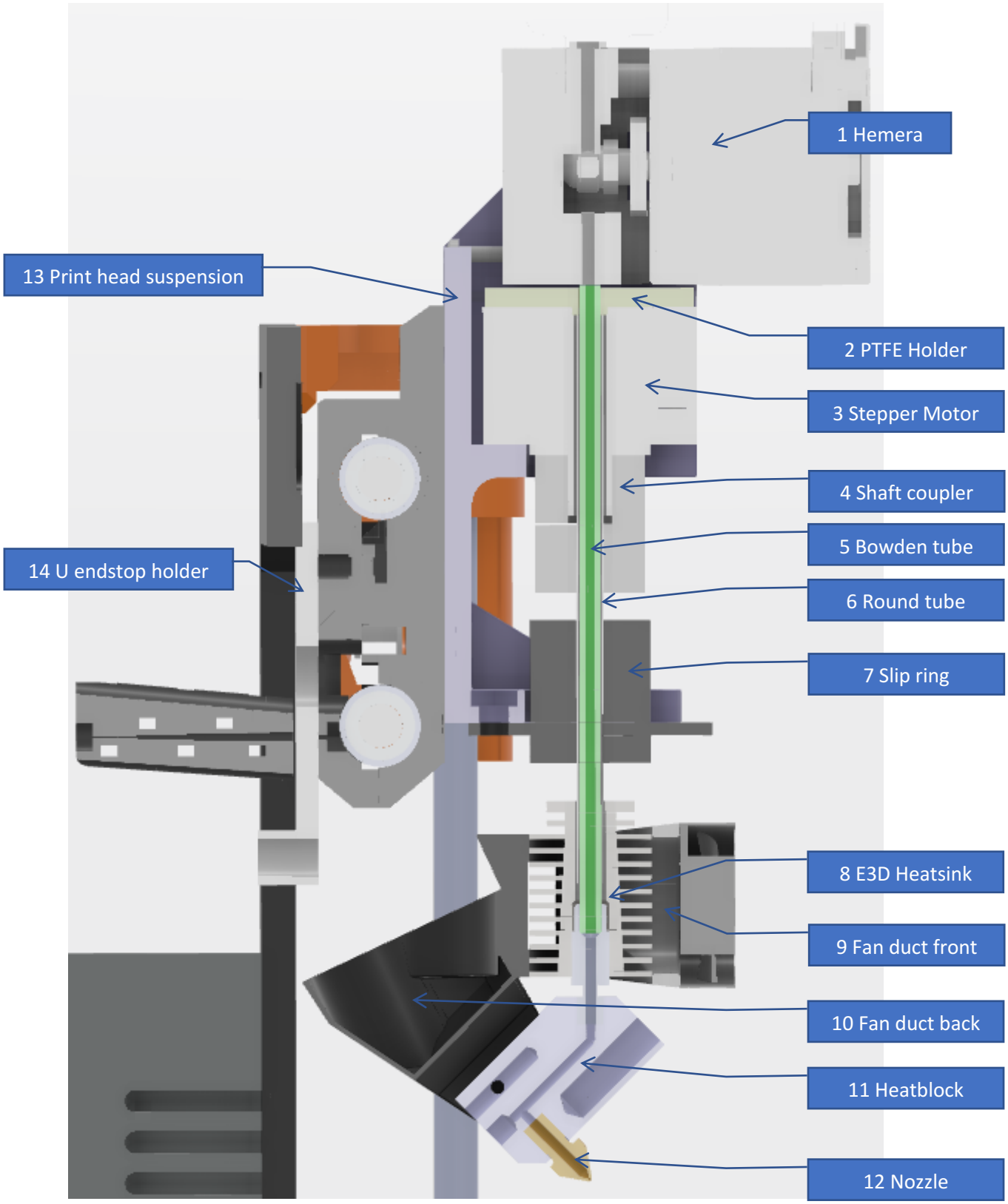

Appendix A - 2/3

Rotbot: Front view

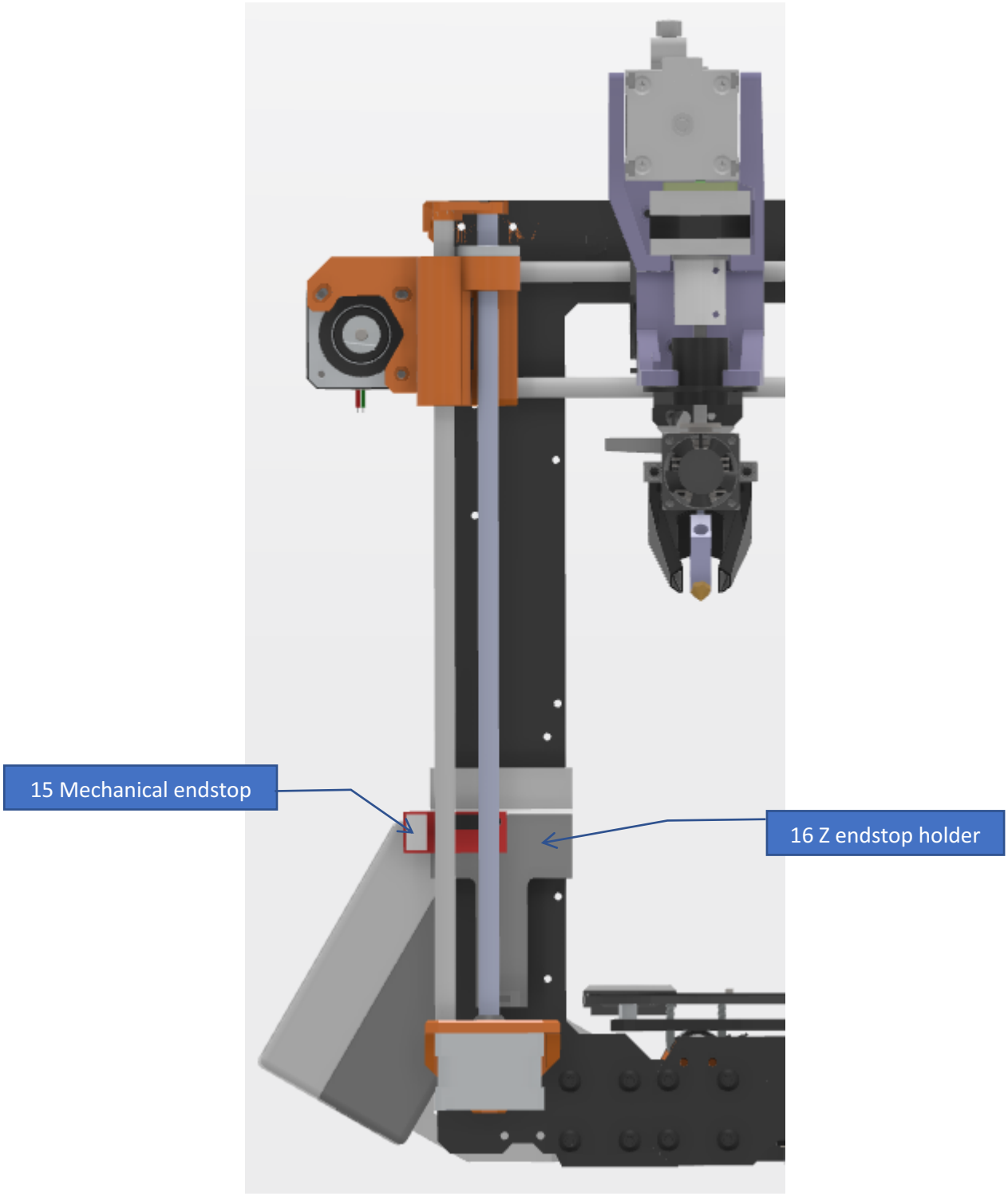

Appendix A - 3/3

RotBot: Rear view

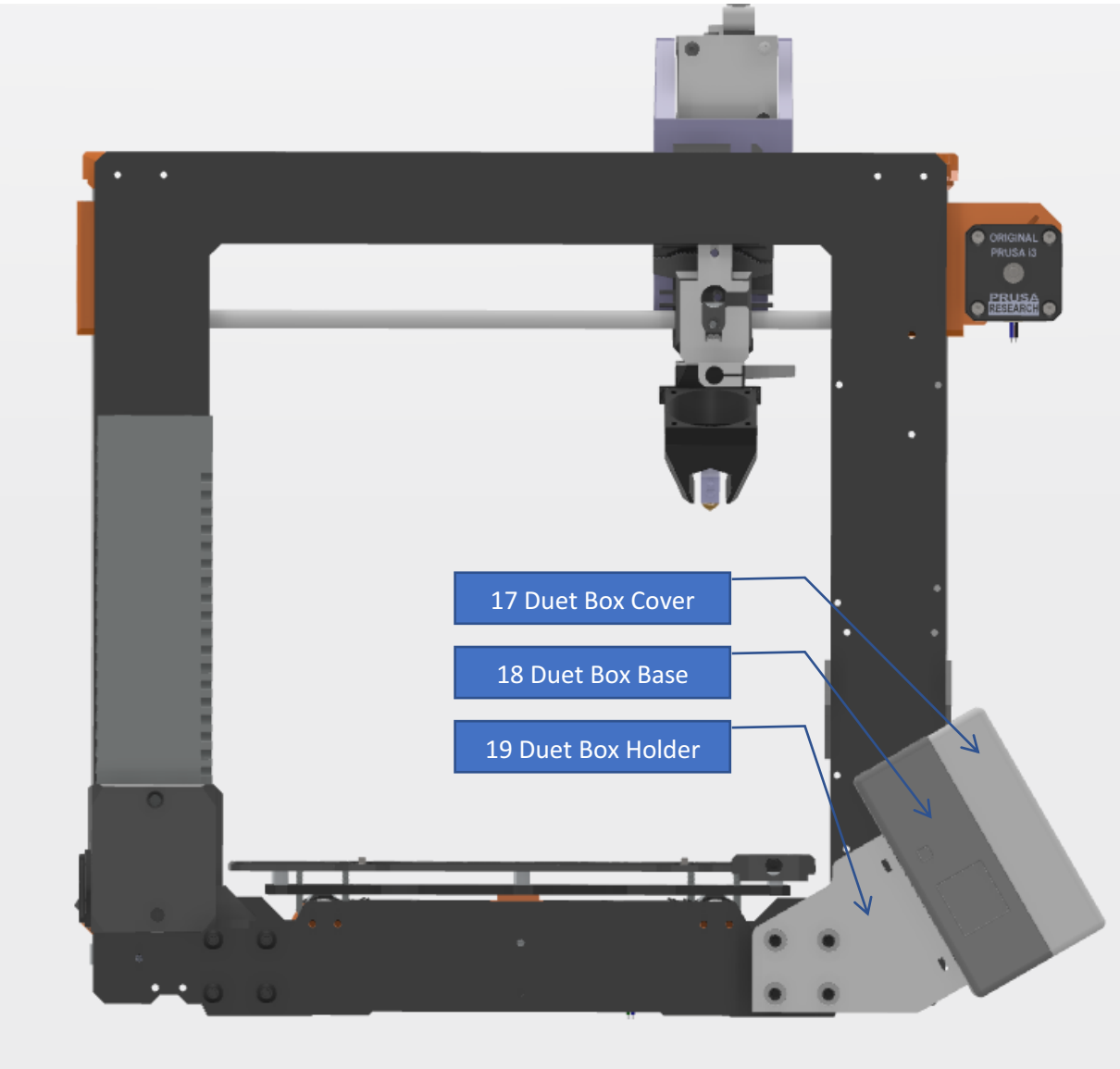

Appendix B

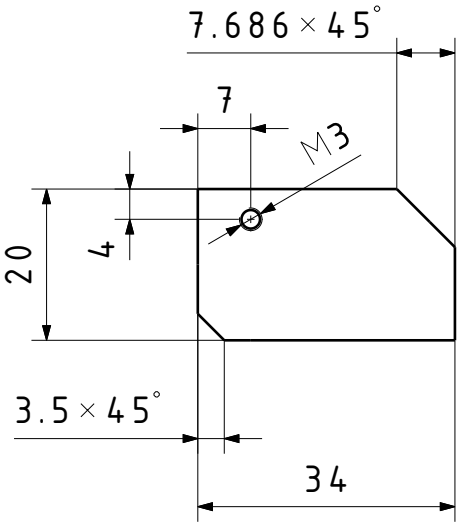

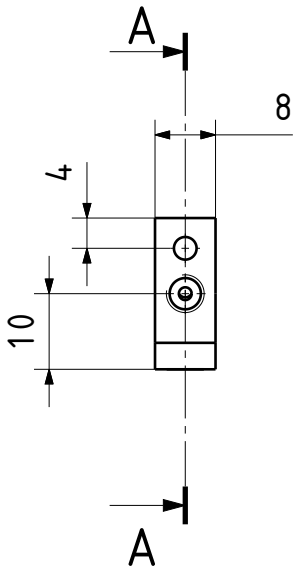

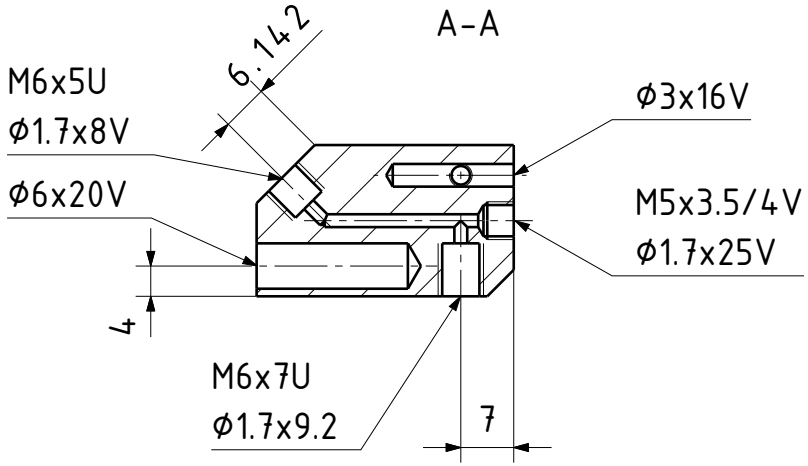

Allgemeintoleranzen ISO 2768-mK

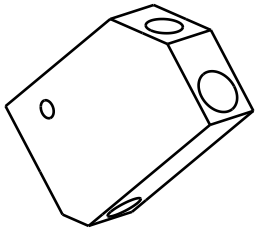

Pos.	Menge	Einheit	Sachnummer	Benennung / Merkmale

Änd.			Änd.			Erstellt	cren	30.09.2022	Massstab 1:1
						Geprüft			
						Normgeprüft			
						Freigeben			

Ohne sep. Stückliste ☐		Auftrags-Nr.			
Sep. Stückliste gleicher Nr. ☐		Ursprung	3D Experience	Anz. Blatt 1	Blatt-Nr. 1
Sep. Stückliste anderer Nr. ☐	Sach-Nr.	Ersatz für			

School of Engineering
IMS Institut für Mechatronische Systeme

Benennung: Heaterblock

Zeichnungs-Nr.

Appendix C

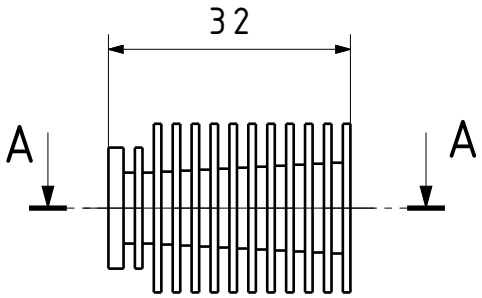

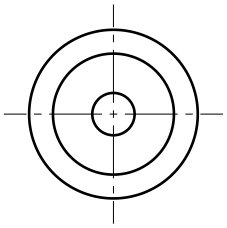

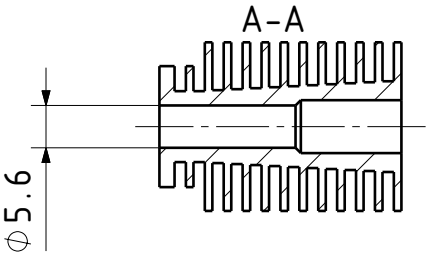

Allgemeintoleranzen ISO 2768-mK
Kanten gebrochen 0.2 ... 0.4

Pos.	Menge	Einheit	Sachnummer	Benennung / Merkmale

Änd.	Änd.	Erstellt	cren	19.07.2022	Massstab 1:1
		Geprüft			
		Normgeprüft			
		Freigeben			
Ohne sep. Stückliste ☐		Auftrags-Nr.			
Sep. Stückliste gleicher Nr. ☐		Ursprung	3D Experience	Anz. Blatt 1	Blatt-Nr. 1
Sep. Stückliste anderer Nr. ☐	Sach-Nr.	Ersatz für			

School of Engineering
IMS Institut für Mechatronische Systeme

Benennung: Heatsink_v2

Zeichnungs-Nr.

Appendix D

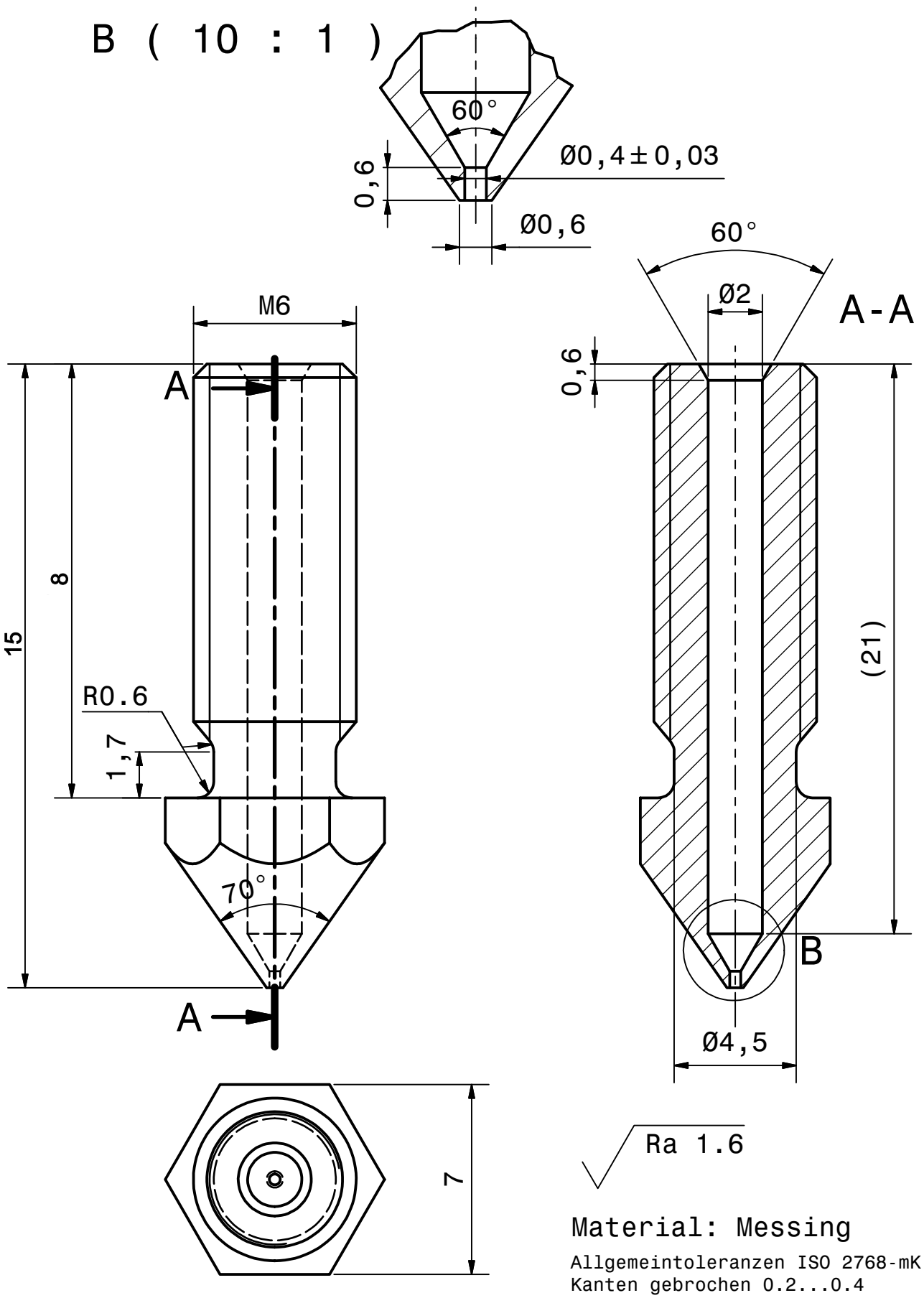

Material: Messing

Allgemeintoleranzen ISO 2768-mK
Kanten gebrochen 0.2...0.4

Düse	**Gezeichnet**	**bosphi01**	
	Datum	**02.12.2018**	
Zürcher Hochschule für Angewandte Wissenschaften	**Massstab**	**5 : 1**	**A4**

Appendix E

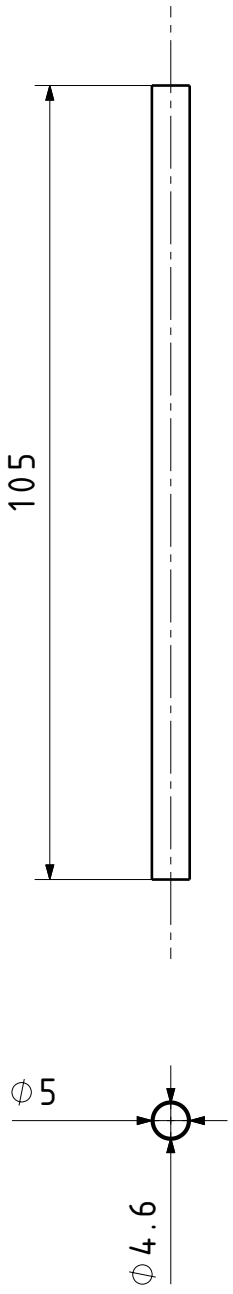

Allgemeintoleranzen ISO 2768-mK
Kanten gebrochen 0.2 ... 0.4

Pos.	Menge	Einheit	Sachnummer	Benennung / Merkmale

Änd.	Änd.	Erstellt	cren	19.07.2022	Massstab 1:1
		Geprüft			
		Normgeprüft			
		Freigeben			
Ohne sep. Stückliste ☐		Auftrags-Nr.			
Sep. Stückliste gleicher Nr. ☐		Ursprung	3D Experience	Anz. Blatt 1	Blatt-Nr. 1
Sep. Stückliste anderer Nr. ☐	Sach-Nr.	Ersatz für			

zhaw School of Engineering
IMS Institut für Mechatronische Systeme

Benennung: Rundrohr_5x105

Zeichnungs-Nr.

Appendix F - 1/2

```
; Configuration file for Duet WiFi (firmware version 3.3)
; executed by the firmware on start-up
;
; generated by RepRapFirmware Configuration Tool v3.3.16 on Mon Apr 17 2023
12:22:26 GMT+0300 (Osteuropäische Sommerzeit)

; General preferences
M575 P1 S1 B57600                                ; enable support for PanelDue
G90                                              ; send absolute coordinates...
M83                                              ; ...but relative extruder moves
M550 P"Ender 3 Pro"                              ; set printer name
M918 P1 E4 F2000000                              ; configure direct-connect
display

; Network
M552 S1                                          ; enable network
M586 P0 S1                                       ; enable HTTP
M586 P1 S0                                       ; disable FTP
M586 P2 S0                                       ; disable Telnet

; Driver
M569 P0 S1                                       ; physical drive 0 goes
backwards
M569 P1 S0                                       ; physical drive 1 goes
backwards
M569 P2 S1                                       ; physical drive 2 goes forwards
M569 P3 S1                                       ; physical drive 3 goes
backwards
M569 P4 S1                                       ; physical drive 4 goes
backwards
M584 X0 Y1 Z2 E3 U4                              ; set drive mapping
M350 X16 Y16 Z16 E16 U16 I1                       ; configure microstepping with
interpolation
M92 X80.00 Y80.00 Z400.00 E93.00 U8.88888888888888          ; set steps per mm
or steps/turn
M566 X1200.00 Y1200.00 Z24.00 E300.00 U500.00    ; set maximum instantaneous
speed changes (mm/min)
M203 X9000.00 Y9000.00 Z700.00 E6000.00 U6000.00 ; set maximum speeds (mm/min)
M201 X500.00 Y500.00 Z200.00 E5000.00 U400.00   ; set accelerations (mm/s^2)
M906 X800 Y800 Z800 E1000 U500 I50               ; set motor currents (mA) and
motor idle factor in per cent
M84 S30                                          ; Set idle timeout

; Axis Limits
M208 X15 Y-33 Z0 U-99999999999999999999 S1     ; set axis minima
M208 X210 Y215 Z260 U99999999999999999999 S0  ; set axis maxima

; Endstops
M574 X1 S3                                      ; configure sensorless endstop
for low end on X
M574 Y2 S3                                      ; configure sensorless endstop
for low end on Y
M574 U1 S1 P"e1stop"                                      ; configure endstop for
U
```

Appendix F - 2/2

```
M915 X Y S3 R0 F0
M574 Z1 S1 P"!zstop"                              ; configure switch-type (e.g.
microswitch) endstop for low end on Z via pin zstop
;M574 X1 S1 P"xstop"                              ; configure switch-type (e.g.
microswitch) endstop for low end on X via pin xstop
;M574 Y1 S1 P"ystop"                              ; configure switch-type (e.g.
microswitch) endstop for low end on Y via pin ystop

; Z-Probe
M558 P0 H5 F120 T6000                             ; disable Z probe but set dive
height, probe speed and travel speed
M557 X15:215 Y15:195 S20                          ; define mesh grid

; Heaters
M308 S0 P"bedtemp" Y"thermistor" T100000 B4092  ; configure sensor 0 as
thermistor on pin bedtemp
M950 H0 C"bedheat" T0                             ; create bed heater output on
bedheat and map it to sensor 0
M307 H0 R0.301 K0.459:0.000 D4.37 E1.35 S1.00 B0
; enable bang-bang mode for the bed heater and set PWM limit
M140 H0                                           ; map heated bed to heater 0
M143 H0 S150                                      ; set temperature limit for
heater 0 to 150C
M308 S1 P"e0temp" Y"thermistor" T100000 B4092   ; configure sensor 1 as
thermistor on pin e0temp
M950 H1 C"e0heat" T1                              ; create nozzle heater output on
e0heat and map it to sensor 1
M307 H1 R2.207 K0.451:0.000 D14.39 E1.35 S1.00 B0 V24.1
      ; disable bang-bang mode for heater  and set PWM limit
M143 H1 S275                                      ; set temperature limit for
heater 1 to 275C

; Fans
M950 F0 C"fan0" Q500                              ; create fan 0 on pin fan0 and
set its frequency
M106 P0 S0 H-1                                    ; set fan 0 value. Thermostatic
control is turned off
M950 F1 C"fan1" Q500                              ; create fan 1 on pin fan1 and
set its frequency
M106 P1 S1 H1 T45                                 ; set fan 1 value. Thermostatic
control is turned on

; Tools
M563 P0 D0 H1 F0                                  ; define tool 0
G10 P0 X0 Y0 Z0                                   ; set tool 0 axis offsets
G10 P0 R0 S0                                      ; set initial tool 0 active and
standby temperatures to 0C

; Custom settings are not defined
```

Appendix G - 1/2

```
; homeall.g
; called to home all axes


;Y home
M400                    ; Y homing
M913 X40 Y40            ; Y homing
M400                    ; Y homing
G91                     ; Y homing
G1 H2 Z10 F6000         ; Y homing
G1 H1 Y220 F6000        ; Y homing
G1 H2 Y-10 F4000        ; Y homing
G1 H1 Y220 F4000        ; Y homing
G92 Y230                ; Y homing
M400                    ; Y homing
M913 X100 Y100 Z100     ; Y homing
G90                     ; change to absolute values
G0 Y-33                 ; move Y to -33 (backend)
M400                    ; wait until all moves are finished

;Z home
G91                     ; Z homing
G1 H1 Z-265 F3000       ; z homing
G92 Z0                  ; z homing

;X home
M400                    ; X homing
M913 X40 Y40 Z40        ; X homing
M400                    ; X homing
G91                     ; X homing
G1 H1 X-255 F5000       ; X homing
G1 H2 X5 F6000          ; X homing
G1 H1 X-255 F4000       ; X homing
G90                     ; X homing
M400                    ; X homing
M913 X100 Y100 Z100     ; X homing
M400                    ; X homing

;U home
G91                     ; U homing
G1 Z4,3                 ; U homing
M400                    ; U homing
G1 H1 U400 F2000        ; U homing
M400                    ; U homing
G1 U2                   ; U homing
G90                     ; U homing
M400

;going back into resting position
G91                     ; relative positioning
G1 X50                  ; go back into the X axis middle
G1 Z8,5                 ; go up to printbed hight
G92 Z0                  ; set Z position to axis minimum (you may want to adjust
this)
```

Appendix G - 2/2

```
G1 Z20                  ; lift Z relative to current position
G90                     ; absolute positioning
G0 Y215                 ; move printbed backwards
```

Appendix H - 1/2

```
; homeu.g
; called to home the U axis


;Y home
M400                    ; Y homing
M913 X40 Y40            ; Y homing
M400                    ; Y homing
G91                     ; Y homing
G1 H2 Z10 F6000         ; Y homing
G1 H1 Y220 F6000        ; Y homing
G1 H2 Y-10 F4000        ; Y homing
G1 H1 Y220 F4000        ; Y homing
G92 Y230                ; Y homing
M400                    ; Y homing
M913 X100 Y100 Z100     ; Y homing
G90                     ; change to absolute values
G0 Y-33                 ; move Y to -33 (backend)
M400                    ; wait until all moves are finished

;Z home
G91                     ; Y homing
G1 H1 Z-265 F3000       ; Y homing
G92 Z0                  ; Y homing

;X home
M400                    ; X homing
M913 X40 Y40 Z40        ; X homing
M400                    ; X homing
G91                     ; X homing
G1 H1 X-255 F5000       ; X homing
G1 H2 X5 F6000          ; X homing
G1 H1 X-255 F4000       ; X homing
G90                     ; X homing
M400                    ; X homing
M913 X100 Y100 Z100     ; X homing
M400                    ; X homing

;U home
G91                     ; relative positioning
G1 Z4,3
M400
G1 H1 U400 F2000        ; turn to U axis sensor and stop there
M400
G1 U2
G90                     ; absolute positioning
M400

;going back into resting position
G91                     ; relative positioning
G1 X50                  ; go back into the X axis middle
G1 Z8,5                 ; go up to printbed hight
G92 Z0                  ; set Z position to axis minimum (you may want to adjust
this)
```

Appendix H - 2/2

```
G1 Z20                  ; lift Z relative to current position
G90                     ; absolute positioning
G0 Y215                 ; move printbed backwards
```

Appendix I

```
; homex.g
; called to home the X axis
;
; generated by RepRapFirmware Configuration Tool v3.3.16 on Tue Apr 18 2023
14:34:44 GMT+0200 (Mitteleuropäische Sommerzeit)
;Y home
M400                    ; Y homing
M913 X40 Y40            ; Y homing
M400                    ; Y homing
G91                     ; Y homing
G1 H2 Z10 F6000         ; Y homing
G1 H1 Y220 F6000        ; Y homing
G1 H2 Y-10 F4000        ; Y homing
G1 H1 Y220 F4000        ; Y homing
G92 Y230                ; Y homing
M400                    ; Y homing
M913 X100 Y100 Z100     ; Y homing
G90                     ; change to absolute values
G0 Y-33                 ; move Y to -33 (backend)
M400                    ; wait until all moves are finished

;Z home
G91                     ; relative positioning
G1 H1 Z-265 F3000       ; move Z down until the endstop is triggered
G92 Z0                  ; set Z position to axis minimum (you may want to adjust
this)

M400 ; Wait for current moves to finish
M913 X40 Y40 Z40        ; drop motor current to 70%
M400
G91                     ; relative positioning
G1 H1 X-255 F5000       ; move quickly to X axis endstop and stop there (first
pass)
G1 H2 X5 F6000          ; go back a few mm
G1 H1 X-255 F4000       ; move slowly to X axis endstop once more (second pass)
G90                     ; absolute positioning
M400
M913 X100 Y100 Z100     ; return current to 100%
M400

;going back into resting position
G91                     ; relative positioning
G1 X50
G1 Z20                  ; lift Z relative to current position
G90
G0 Y215
```

Appendix J

```
; homey.g
; called to home the Y axis
;
; generated by RepRapFirmware Configuration Tool v3.3.16 on Tue Apr 18 2023
14:34:44 GMT+0200 (Mitteleuropäische Sommerzeit)
M400                    ; Wait for current moves to finish
M913 X40 Y40 ; drop motor current to 70%
M400
G91                     ; relative positioning
G1 H2 Z5 F6000          ; lift Z relative to current position
G1 H1 Y220 F6000        ; move quickly to Y axis endstop and stop there (first
pass)
G1 H2 Y-5 F4000         ; go back a few mm
G1 H1 Y220 F4000        ; move slowly to Y axis endstop once more (second pass)
G1 H2 Z-5 F4000         ; lower Z again
G92 Y230                ; absolute positioning
M400
M913 X100 Y100 Z100     ; return current to 100%
M400
```

Appendix K

```
; homez.g
; called to home the Z axis
;
; generated by RepRapFirmware Configuration Tool v3.3.16 on Mon Apr 17 2023
12:22:26 GMT+0300 (Osteuropäische Sommerzeit)
G91                     ; relative positioning
G1 H2 Z10 F6000         ; lift Z relative to current position

;Y home
M400                    ; Y homing
M913 X40 Y40            ; Y homing
M400                    ; Y homing
G91                     ; Y homing
G1 H1 Y220 F6000        ; Y homing
G1 H2 Y-10 F4000        ; Y homing
G1 H1 Y220 F4000        ; Y homing
G92 Y230                ; Y homing
M400                    ; Y homing
M913 X100 Y100 Z100     ; Y homing
G90                     ; change to absolute values
G0 Y-33                 ; move Y to -33 (backend)
M400                    ; wait until all moves are finished

G91                     ; relative positioning
G1 H1 Z-265 F3000       ; move Z down until the endstop is triggered
G1 Z13,5
G92 Z0                  ; set Z position to axis minimum (you may want to adjust
this)

; Uncomment the following lines to lift Z after probing
G91                     ; relative positioning
G1 Z20                  ; lift Z relative to current position
G90
```